PadR-like transcription factors of *Listeria monocytogenes* EGD-e

Von der Fakultät für Lebenswissenschaften

der Technischen Universität Carolo-Wilhelmina zu Braunschweig

zur Erlangung des Grades

eines Doktors der Naturwissenschaften

(Dr. rer. nat.)

genehmigte

D i s s e r t a t i o n

von Samuel Hauf
aus Rostock

1. Referentin: Professorin Dr. Antje Flieger
2. Referentin: Professorin Dr. Susanne Engelmann
eingereicht am: 07.08.2019
mündliche Prüfung (Disputation) am: 13.12.2019
Druckjahr 2020

Vorveröffentlichungen der Dissertation

Teilergebnisse aus dieser Arbeit wurden mit Genehmigung der Fakultät für Lebenswissenschaften, vertreten durch die Mentorin der Arbeit, in folgenden Beiträgen vorab veröffentlicht:

Publikationen

Hauf S, Möller L, Fuchs S, and Halbedel S. **PadR-type repressors controlling production of a non-canonical FtsW/RodA homologue and other trans-membrane proteins in *Listeria monocytogenes***. Sci Rep. 2019 Jul 11;9(1):10023. doi: 10.1038/s41598-019-46347-w.

Hauf S, Herrmann J, Miethke M, Gibhardt J, Commichau FM, Müller R, Fuchs S, Halbedel S. **Aurantimycin resistance genes contribute to survival of *Listeria monocytogenes* during life in the environment**. Mol Microbiol. 2019 Apr;111(4):1009-1024. doi: 10.1111/mmi.14205.

Tagungsbeiträge

Hauf S, Herrmann J, Miethke M, Gibhardt J, Commichau FM, Müller R, Fuchs S, Halbedel S. **Aurantimycin resistance genes found in *Listeria monocytogenes* are widespread in the Firmicutes phylum**. Presented at: Bacell meeting; April 2019; Ljubljana, Slovenia

Hauf S, Gibhardt J, Commichau FM, Fuchs S, Halbedel S. **Characterization of LftR, a PadR-like transcription factor in *Listeria monocytogenes***. Presented at: VAAM annual meeting; April 2018; Wolfsburg, Germany

Posterbeiträge

Hauf S, Herrmann J, Miethke M, Gibhardt J, Commichau FM, Müller R, Fuchs S, Halbedel S. **Aurantimycin resistance genes contribute to survival of *Listeria monocytogenes* during life in the environment**. Presented at: 20th International Conference on Bacilli and Gram-Positive Bacteria; July 2019; University of Maryland, USA

Hauf S, Herrmann J, Miethke M, Gibhardt J, Commichau FM, Müller R, Fuchs S, Halbedel S. **Aurantimycin resistance genes contribute to survival of *Listeria monocytogenes* during life in the environment**. Presented at: VAAM annual meeting; March 2019; Mainz, Germany

Hauf S and Halbedel S. **Control of an FtsW/RodA homolog by a PadR-like stress regulator in *Listeria monocytogenes***. Presented at: VAAM - 3rd Discussion Meeting Microbial Cell Biology; November 2018; Rauischholzhausen, Germany

Summary

Transcriptional regulators belonging to the PadR family contribute to resistance against antibiotics and small toxic compounds in many bacteria. The genome of the Gram-positive human pathogen *Listeria monocytogenes* contains 5 genes encoding proteins belonging to the PadR family. The exact regulons and biological functions of these PadR-like transcription factors remained elusive.

Four genes encoding PadR-like transcription factors were inactivated in *L. monocytogenes* EGD-e in order to compare the transcriptome of the resulting strains to the wild type using RNA-sequencing. The RNA-sequencing data revealed that all four PadR-like transcription factors strongly repress a small set of genes comprising one or two transcriptional units. In most cases the repressors could be shown to be autoregulatory. When the PadR-like proteins are inactivated, the transcription of the target genes increases between 100- and 500-fold. The strong repression under standard conditions suggests that it is beneficial for the bacteria to inactivate the target genes under most conditions, while increased transcription occurs only under very specific conditions.

In order to identify conditions leading to the expression of genes controlled by PadR-like transcription factors, promoter-*lacZ* fusions were constructed using the most strongly repressed promoters. Using these reporters, a natural compound collection was screened for substances inducing transcription. This screen identified aurantimycin A as an inducer of LftR-controlled gene expression. The depsipeptide antibiotic aurantimycin A, produced by the soil bacterium *Streptomyces aurantiacus*, is very toxic for Gram-positive bacteria. Surprisingly, the MIC of aurantimycin against *L. monocytogenes* is much higher compared to other Gram-positive bacteria. The resistance depended on expression of the *lieAB* genes which is tightly regulated by LftR in interplay with LftS. The LieAB transporter was shown to protect *L. monocytogenes* from aurantimycin induced lysis. This is the first description of an aurantimycin resistance mechanism. The system discovered may play a vital role for the survival, spread and persistence of *L. monocytogenes* in the soil, where it may come into contact with the antibiotic producing bacterium *S. aurantiacus*.

Genes controlled by another PadR-type transcription factor, LstR, were shown to be induced by the 16-membered macrolide antibiotic josamycin, but they were not involved in resistance against this antibiotic. One of the genes controlled by LstR, *lmo0421*, encodes a homolog to RodA or FtsW, which are involved in cell wall biosynthesis. Still, under the conditions investigated, Lmo0421 did not possess RodA or FtsW functionality, so its biological function remained unclear.

The *padR*-like gene *lmo0599* (*lltR*) was important for growth of *L. monocytogenes* at low temperatures. The inactivation of *lmo0599* impaired the growth of *L. monocytogenes* at 6°C. It was also shown that this phenotype depended on the overexpression of the gene *lmo0600* in the absence of *lltR*.

Taken together, the results suggest that the PadR-like transcription factors in *L. monocytogenes* act as repressors to control the expression of a very specific set of genes. These genes are mostly surface associated and become active under defined conditions only. They may play an important role in response to certain environmental stimuli and for survival in the environment.

Zusammenfassung

In vielen Bakterien regulieren PadR-typ Transkriptionsfaktoren Resistenz-mechanismen gegen toxische Substanzen oder Antibiotika. Im Genom des Gram-positiven Listeriose Erregers *Listeria monocytogenes* sind insgesamt fünf Gene enthalten, welche Proteine aus der PadR Proteinfamilie codieren. Die genauen Regulons, sowie die biologische Funktion dieser Transkriptionsfaktoren waren großteils unbekannt.

Vier der fünf Gene, welche für Transkriptionsfaktoren vom PadR-Typ kodieren, wurden inaktiviert und die Transkriptome der entsprechenden Stämme mit dem Wildtyp verglichen. Die Daten zeigten, dass PadR-Typ-Faktoren eine kleine Zahl an Genen stark reprimieren. In den meisten Fällen waren die Repressoren auch selbstregulierend. Die Inaktivierung der Repressoren führte zu einer 100- bis nahezu 500-fachen Induktion der jeweiligen Zielgene. Diese starke Repression unter Standardbedingungen weist darauf hin, dass es vorteilhaft sein könnte, die Zielgene nur unter sehr spezifischen Bedingungen zu exprimieren, während unter anderen Bedingungen besser ist, dass die Gene nicht exprimiert werden.

Mithilfe von Promoter-*lacZ* Fusionen der am stärksten reprimierten Gene wurde die Naturstoffsammlung des DZIF auf Substanzen, welche die Genexpression induzieren, untersucht. Diese Experimente zeigten, dass LftR-kontrollierte Gene von Aurantimycin A induziert werden. Aurantimycin A ist ein Depsipeptidantibiotikum, welches von dem Bodenbakterium *Streptomyces aurantiacus* produziert wird und welches für viele Gram-positive Bakterien sehr giftig ist. Überraschenderweise war *L. monocytogenes* deutlich resistenter gegen das Antibiotikum als andere Bakterien, wie sich in einer hohen minimalen Hemmkonzentration zeigte. Diese Resistenz basierte auf der Expression der *lieAB* Gene, welche von LftR und LftS kontrolliert wird. Es wurde gezeigt, dass der LieAB Transporter *L. monocytogenes* vor Lyse durch Aurantimycin schützt. Dies ist die erste Beschreibung eines Resistenzmechanismus gegen Aurantimycin. Der entdeckte Mechanismus könnte eine wichtige Rolle für das Überleben und die Verbreitung von *L. monocytogenes* im Boden spielen, wenn es dort mit dem Aurantimycin-produzierenden Bakterium *S. aurantiacus* zusammentrifft.

Andere Gene, welche von dem Transkriptionsfaktor LstR reguliert werden, wurden durch das Makrolidantibiotikum Josamycin induziert. Sie hatten jedoch keinen Einfluss auf die Resistenz gegenüber Josamycin. Ein von LstR kontrolliertes Gen, *lmo0421*, kodiert für ein Protein mit Homologie zu RodA oder FtsW, welche an der Zellwandbiosynthese beteiligt sind. Es konnte jedoch gezeigt werden, dass unter den getesteten Bedingungen Lmo0421 die Funktion von RodA oder FtsW nicht übernehmen konnte.

Das Gen *lmo0599* (*lltR*) war wichtig für das Wachstum von *L. monocytogenes* bei niedrigen Temperaturen. Nach Inaktivierung von *lmo0599* war Wachstum bei 6°C nur eingeschränkt möglich. Es wurde auch gezeigt, dass dieser Phänotyp von der Überexpression des Genes *lmo0600* verursacht wurde.

Zusammenfassend kann gesagt werden, dass die PadR-Typ-Transkriptionsfaktoren in *L. monocytogenes* die Expression einer kleinen Anzahl von Genen reprimieren. Diese Gene sind meinst membranassoziiert und werden nur unter bestimmten Bedingungen aktiviert. Es könnte sein, dass diese Gene eine wichtige Rolle für die Reaktion auf spezielle Umweltsignale und das Überleben in der Umwelt spielen.

Contents

1 Introduction **1**

1.1 *Listeria monocytogenes* . . . 1

1.1.1 Historic descriptions of *L. monocytogenes* . . . 1

1.1.2 Listeriosis - *L. monocytogenes* as a pathogen . . . 2

1.1.3 Morphology and physiology of *L. monocytogenes* . . . 2

1.1.4 *L. monocytogenes* in the environment - saprophyte or pathogen? . 3

1.2 Antibiotics . . . 6

1.2.1 Main target structures of antibiotics . . . 6

1.2.2 Antibiotic resistance mechanisms . . . 7

1.3 PadR-like repressors . . . 9

1.3.1 The PadR family of proteins . . . 9

1.3.2 PadR - the transcriptional regulator of phenolic acid decarboxylase 12

1.4 PadR-like transcription factors in *L. monocytogenes* . . . 13

1.4.1 LadR regulates *mdrL* expression . . . 15

1.4.2 LstR - a lineage-specific thermal regulator . . . 16

1.4.3 LftR regulates the expression of the *lieAB* transporter genes . . . 17

1.4.4 Lmo0599 and Lmo1213 - two uncharacterized PadR-like proteins 18

1.5 Aims of this study . . . 19

2 Materials and Methods **21**

2.1 Primers . . . 21

2.2 Plasmids . . . 28

2.3 Bacterial strains . . . 36

2.4 DNA based work . . . 44

2.4.1 Preparation of genomic DNA . . . 44

2.4.2 PCR . . . 45

2.4.3 Agarose gel electrophoresis . . . 47

2.4.4 DNA purification . . . 48

2.4.5 Plasmid purification . . . 48

2.4.6 Endonuclease digestion . . . 48

2.4.7 Ligation . . . 49

2.4.8 Sanger sequencing . . . 49

2.5 RNA based work . . . 50
2.5.1 Cultivation . . . 50
2.5.2 RNA extraction . . . 50
2.5.3 RNA quantification . . . 51
2.5.4 RNA gel electrophoresis . . . 51
2.5.5 Northern blotting . . . 52
2.5.6 Detection of specific mRNA transcripts . . . 53
2.5.7 RNA sequencing . . . 54
2.6 Protein based work . . . 58
2.6.1 Protein over-expression and purification . . . 58
2.6.2 Isolation of cellular proteins . . . 59
2.6.3 Quantification of protein concentrations . . . 59
2.6.4 ONPG β-galactosidase assay . . . 59
2.7 Microbiology . . . 60
2.7.1 Cultivation . . . 60
2.7.2 Genetic engineering . . . 61
2.7.3 Disc diffusion assay . . . 62
2.7.4 Growth curves . . . 63
2.7.5 Lysozyme mediated lysis . . . 63
2.7.6 Agar plate based screen for *lacZ* induction . . . 64
2.7.7 MIC determination - broth dilution . . . 64
2.7.8 Lysis by aurantimycin . . . 65
2.7.9 Selection of aurantimycin-resistant suppressors . . . 65
2.7.10 Selection of lltR* cold growth suppressors . . . 65
2.7.11 Scanning or transmission electron microscopy . . . 66

3 Results **67**
3.1 The regulons of the PadR-like repressors as determined by RNA sequencing 67
3.1.1 RNA sequencing data exploration and cut-off definition for weakly expressed genes . . . 69
3.1.2 Genes differentially expressed in the Δ*lftR* mutant . . . 73
3.1.3 Genes differentially expressed in the Δ*ladR* mutant . . . 75
3.1.4 Genes differentially expressed in the Δ*lstR* mutant . . . 76
3.1.5 Genes differentially expressed in the *lltR** mutant . . . 78
3.1.6 Confirmation of the RNA sequencing results by measuring promoter activity in a β-galactosidase assay . . . 79
3.2 Determination of conditions leading to the induction of genes controlled by PadR-like transcription factors . . . 82
3.2.1 Conditions leading to the activation of LftR-controlled genes . . . 85
3.2.2 Induction of LftR-controlled genes depends on LftS . . . 89
3.2.3 Conditions leading to the activation of LstR-controlled genes . . . 93
3.2.4 Activity of the *lstR-sigC-lmo0421* operon depends on SigC . . . 94
3.3 The genes of the LftR regulon contribute to aurantimycin-resistance . . . 96

3.3.1 Identification of spontaneous aurantimycin-resistant suppressor mutants . . . 98
3.4 Identification of the LftR operator site . . . 102
3.4.1 Determination of the minimal P_{lieA} promoter . . . 102
3.4.2 Identification of the P_{lieA} promoter region important for LftR binding . . . 104
3.4.3 Systematic mutagenesis of the 69-51 bp region of the P_{lieA} promoter to identify the LftR binding motif . . . 106
3.4.4 Confirmation of the LftR operator in P_{lftRS} . . . 108
3.5 Effect of the genes *sigC*, *lstR* and *lmo0421* on the resistance against the inducing macrolides josamycin and tylosin . . . 110
3.6 Effect of *lstR* and *lmo0421* on the resistance against cell wall targeting antibiotics . . . 111
3.7 Determining if Lmo0421 has RodA- or FtsW-like functionality . . . 113
3.8 Cold-sensitive growth phenotype of the *lltR** mutant . . . 115
3.9 Effect of the genes *lmo0600* and *lmo0601* on growth at refrigeration temperature . . . 117
3.10 Characterization of *lltR** suppressor mutants that are able to grow at 6°C . 118

4 Discussion **121**
4.1 PadR-like repressors strongly regulate a small set of genes . . . 121
4.2 Conditions leading to the activation of PadR-dependent promoters . . . 124
4.3 LftR-controlled aurantimycin-resistance genes might be important for the survival of *L. monocytogenes* in the environment . . . 126
4.4 Mutations found in aurantimycin-resistant suppressors . . . 128
4.5 The LftR operator sequence . . . 132
4.6 The function of LstR remains unclear . . . 134
4.7 LltR-controlled genes are associated with the ability of *L. monocytogenes* to grow at low temperature . . . 136

Chapter 1

Introduction

1.1 *Listeria monocytogenes*

1.1.1 Historic descriptions of *L. monocytogenes*

In the modern scientific literature, the first encounters with bacteria that were most likely *Listeria* date to the early 20th century. In 1924, Murray et al. observed a disease in rabbits in a breeding facility for laboratory animals. A characteristic feature of the disease was large mononuclear leucocytosis. They succeeded in isolating a small gram-positive bacillus from infected animals which they named *Bacterium monocytogenes* (Murray et al. 1926). Soon afterwards, infections in humans caused by similar bacteria were also reported (Nyfeldt 1929, Burn 1936). In 1933, Gill showed a connection between the fatal "circling disease" in sheep and a small gram-positive bacillus, which he named *Listerella monocytogenes* (Gill 1933). From that time on, many more cases of infection with *Listeria* were reported in different animals causing meningitis, encephalitis, septicaemia or abortion of pregnancy (Gray and Killinger 1966).

The early descriptions of *Listeria* already linked the disease now known as listeriosis to the consumption of inadequate feed (Murray et al. 1926) and even today, *L. monocytogenes* gets the most attention for outbreaks of listeriosis caused by the consumption of contaminated food (Pouillot et al. 2016, Angelo et al. 2017, Halbedel et al. 2019).

1.1.2 Listeriosis - *L. monocytogenes* as a pathogen

Listeriosis is the disease caused by infection with bacteria from the genus *Listeria*. It has been observed in a wide variety of animals for example sheep, pigs, cows, chickens, birds and even fish or crustaceans (Fenlon 1999). *L. monocytogenes* is the main causative agent of human listeriosis, while other species like *L. seeligeri*, *L. innocua*, or the animal pathogen *L. ivanovii* rarely cause human disease (Rocourt et al. 1986, Perrin et al. 2003, Guillet et al. 2010).

In healthy humans, listeriosis usually manifests in gastrointestinal symptoms like diarrhea, or flu-like symptoms such as fever and muscle aches (Ooi and Lorber 2005). However, immune suppressed persons, elderly people and pregnant woman are especially vulnerable to infections with *L. monocytogenes* (Silk et al. 2013). In these groups, the disease often manifests in more severe illnesses, for example meningitis, encephalitis, septicaemia or abortion of pregnancy and death from listeriosis is not uncommon (Slutsker and Schuchat 1999, Charlier et al. 2017).

Infection sources range from fruit and vegetables over milk, meat products and fish to soft cheeses or other ready-to-eat foods. (Schuchat et al. 1992, Dalton et al. 1997, Swaminathan and Gerner-Smidt 2007, McCollum et al. 2013, Stephan et al. 2015). Heating above 70°C has been shown to reliably inactivate *L. monocytogenes* (Mackey and Bratchell 1989), so a common characteristic of all foods often identified as infection sources is that they are usually consumed without additional heating prior to consumption. Foods that have been cooked during preparation can become re-contaminated at a later stage of processing, causing disease when the bacteria are able to grow during storage. Because of the severity of the disease in risk groups, outbreaks of *L. monocytogenes* are a major public health concern (Valk et al. 2005, Mateus et al. 2013).

1.1.3 Morphology and physiology of *L. monocytogenes*

L. monocytogenes is a small gram-positive rod of approximately 1 μm in length (about half the size of *Bacillus subtilis*, a closely related bacterium). It is motile by polar or peritrichous flagella, but loses motility at higher temperatures (not motile at 37°C) (Gray and Killinger 1966, Rocourt 1999). Its optimum growth temperature is around 37°C although it can also grow at temperatures near freezing or up to around 45°C (Junttila et al. 1988, Annous et al. 1997). The genome of the *L. monocytogenes* reference strain EGD-e is 2.944.528 base pairs in size with a GC content of 38 % (Glaser et al. 2001). *L. monocytogenes* does not form spores, but is highly resistant to physical and chemical stresses like low temperature, alkaline or acidic pH, high salt concentration and the presence of

various disinfectants (Junttila et al. 1988, George et al. 1988, Best et al. 1990, Vasseur et al. 1999).

For the role of *L. monocytogenes* as a food associated pathogen, its abilities to grow at refrigeration temperatures, to replicate at acidic and alkaline pH as well as to multiply at high salt concentrations are especially important, because such conditions are often used to treat or conserve food for longer periods of time (Bucur et al. 2018). High tolerance to adverse conditions set this pathogen apart from other bacteria. The mixture of unique properties -like its ability to grow at low temperatures, in environments high in salt or under acidic conditions- means that most methods of preservation (cooling, salting, pickling) are inadequate to protect food from spoilage by *L. monocytogenes*. The major route of infection is the ingestion of contaminated food. For this reason, it is also important to know where the *L. monocytogenes* comes from and how it gets onto food.

1.1.4 *L. monocytogenes* in the environment - saprophyte or pathogen?

Bacteria belonging to the species *L. monocytogenes* seem to be widespread in the environment, because they could be isolated from a variety of different sources like surface and ground water, decaying plant matter, silage, or soil (Fenlon 1999). Contributing to its ubiquitous occurrence in nature are its ability to utilize a variety of carbon sources (Pine et al. 1989), swimming motility below 30°C (Gründling et al. 2004), and the capacity to grow at low temperature as well as high osmolarity (Cole et al. 1990). Still, knowledge on the life cycle and persistence in natural habitats is sparse and it is uncertain in which niches *L. monocytogenes* actually replicates.

A common hypothesis is that soil and especially decaying vegetation is the primary habitat of *Listeria* species (Vivant et al. 2019). Decaying plant matter seems to be one environmental niche where *L. monocytogenes* is able to grow (Donald et al. 1995, Fenlon 1999). The widespread presence of *L. monocytogenes* in the environment is one hint that it may be a saprophytic organism. The observation that in the presence of plant sugars like cellobiose virulence genes are not activated (Milenbachs et al. 2003) is supporting this hypothesis. Additionally, *L. monocytogenes* is able to hydrolyse chitin, one of the most common polymers in natural systems (Paspaliari et al. 2015). The hydrolysis of chitin is up-regulated at low temperatures that are common in the environment while low chitinase activity is observed at 37°C (Leisner et al. 2008). There are also hints that *L. monocytogenes* might be part of the commensal microflora of the gut, because it could be carried asymptomatically in the gastrointestinal tract by up to 10 % of the human population (Farber and Peterkin 1991).

Although *L. monocytogenes* occurs ubiquitously in the environment and could be a part of

the gut microflora in healthy persons, it also has the ability to actively invade eukaryotic host cells (Pizarro-Cerdá et al. 2012). After invasion, *L. monocytogenes* does not only survive inside the host cell, but can actively replicate inside the cytoplasm (Joseph and Goebel 2007). It is therefore classified as a facultative intracellular pathogen. Phosphorylated sugars present in the cytosol of host cells can also be utilized by *L. monocytogenes* and these sugars do not repress virulence genes as is the case with plant-derived sugars such as cellobiose (Chico-Calero et al. 2002). In healthy individuals, the immune system generally limits the infection to gastrointestinal symptoms (Ooi and Lorber 2005). In contrast, in immunocompromized persons infections with *L. monocytogenes* often become systemic and lead to very serious outcomes including death. The adaptation of *L. monocytogenes* to life in the environment as well as inside eukaryotic hosts has led to the suggestion that this bacterium possesses two very different personalities (Gray et al. 2006).

The transition from saprophyte to pathogen is mainly controlled by the virulence regulator PrfA reacting to a variety of environmental signals (Freitag et al. 2009). Once contaminated food is ingested, *L. monocytogenes* enters the gut and an infection cycle starts upon contact of the bacterium with gut epithelial cells (Pentecost et al. 2006). The infection cycle of *L. monocytogenes* is shown in figure 1.1. The bacterium triggers phagocytosis by the host cell through interaction of the internalins InlA or InlB with the host cell receptors E-cadherin or Met, respectively (Mengaud et al. 1996, Shen et al. 2000). The InlA mediated interaction with E-cadherin is especially important for the ability of *L. monocytogenes* to cross the gut epithelial barrier (Lecuit et al. 2001, Ortega et al. 2017).

After entry into host cells, the resulting phagosome is lysed by the combined action of listeriolysin (LLO) and the phospholipases PlcA and PlcB (Cossart et al. 1989, Smith et al. 1995, Kanki et al. 2018). Once inside the cytoplasm, the bacterium starts to grow, replicates and then moves actively by polymerizing host actin with the help of the actin-assembly inducing protein ActA (Domann et al. 1992, Kocks et al. 1993, Southwick 2006). The active movement allows the bacterium to spread to neighbouring cells and to repeat the infection cycle. This way of moving between host cells also allows *L. monocytogenes* to breach all major anatomical infection barriers present in the human body (for example the blood-brain barrier or the placental barrier) and to infect into the brain or the foetus. (Gray and Killinger 1966, Berche 1995, Faralla et al. 2018, Ghosh et al. 2018). In this systemic stadium the disease is very difficult to treat and special antibiotic treatment regimes need to be followed depending on the manifestation observed in the patient (Jones and MacGowan 1995). An understanding of the mechanisms of antibiotic treatment and antimicrobial resistance in *Listeria* is therefore essential.

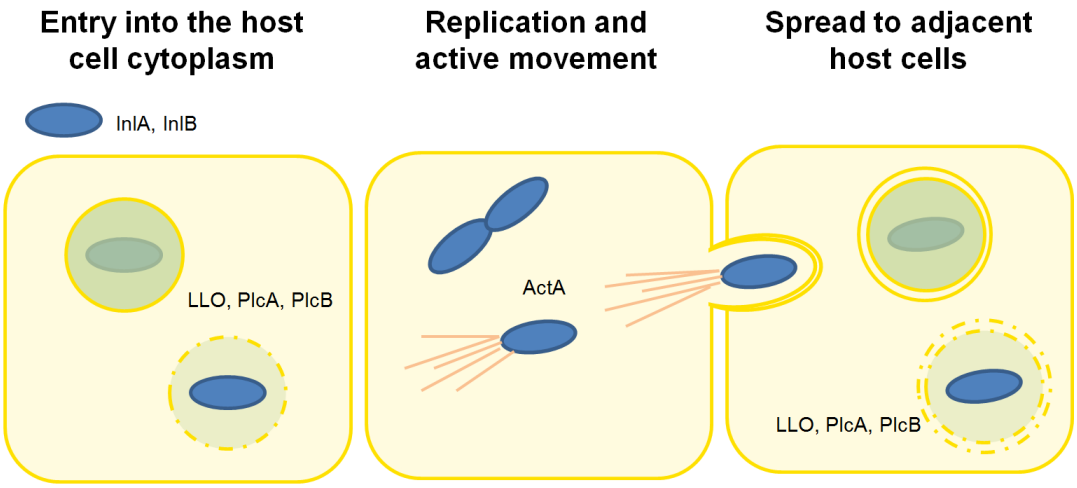

Figure 1.1: The infection cycle of *L. monocytogenes*. There are three main stages in *L. monocytogenes* infections. First, the bacterium enters the host cell cytoplasm. Initial attachment and phagocytosis are mediated by the interaction of the bacterial internalins InlA and InlB with the host cell receptors E-cadherin and Met, respectively. The phagosome is destroyed after phagocytosis by the combined action of listeriolysin O, PlcA and PlcB. In a second stage, the bacterium starts to grow and replicate inside the cytoplasm. *L. monocytogenes* can move actively inside of the host cells by polymerizing host actin molecules with ActA. The third stage of infection is the spread to adjacent host cells. Here, *L. monocytogenes* uses the energy of actin polymerization to breach the cell membranes and then re-initiates the escape from the newly formed vesicle.

1.2 Antibiotics

For people infected with bacteria, the most potent medicines that help to cure the patients are antibiotics. Usually, antibiotics are small compounds that kill the bacteria or prevent their growth without major negative impact on the patient. In order to be used in a clinical setting, *in vitro* as well as *in vivo* effectiveness, a lack of toxicity for humans, and reasonably low cost are essential factors (Moellering 1981). Substances that fulfil these criteria usually target structures that are specific for bacteria and do not occur in human cells. Often, the target structures are involved in the synthesis of DNA, RNA, proteins or the bacterial cell wall (Kohanski et al. 2010). Beginning with the famous discovery of penicillin by Alexander Fleming in 1929 (Fleming 1929), many antibiotic substances (for example gentamycin or vancomycin) have been isolated from natural sources, the most fertile of which were soil dwelling *Streptomyes* species (Clardy et al. 2009). The treatment of Listeriosis is commonly performed with penicillins in combination with gentamicin, because resistance to these antibiotics is rarely reported (Morvan et al. 2010). However, treatment with other antibiotics like vancomycin or macrolides might be necessary for particular maifestation of the disease (Jones and MacGowan 1995).

1.2.1 Main target structures of antibiotics

Antibiotics often binds and inactivate or interfere with the biological function of a main cellular target structure. Figure 1.2 shows cellular processes that are targets of different antibiotics. For example, DNA-gyrase or topoisomerase complexes, essential for prokaryotic DNA maintenance, are bound and misregulated by quinolone antibiotics (Aldred et al. 2014). The bacterial RNA polymerase is inactivated by rifamycins and the cell membrane compromised by polymyxins (Campbell et al. 2001, Trimble et al. 2016). Protein biosynthesis at the bacterial ribosome is the target of many different antibiotics such as tetracyclines and aminoglycosides, interfering with the 30S subunit, or macrolide antibiotics and chloramphenicol that target the 50S subunit of the bacterial ribosome (McCoy et al. 2011). The β-lactams, for example penicillin, bind and inactivate proteins involved in the synthesis of the cell wall, the so called penicillin binding proteins (PBPs) (Frère et al. 1992). The disruption of those important cellular processes has varying effects on the bacterial cell, but all result in the inhibition of growth. Generally, antibiotics are also classified as bacteriostatic and bactericidal, depending on whether they impact bacterial growth or kill the bacteria (Kohanski et al. 2010).

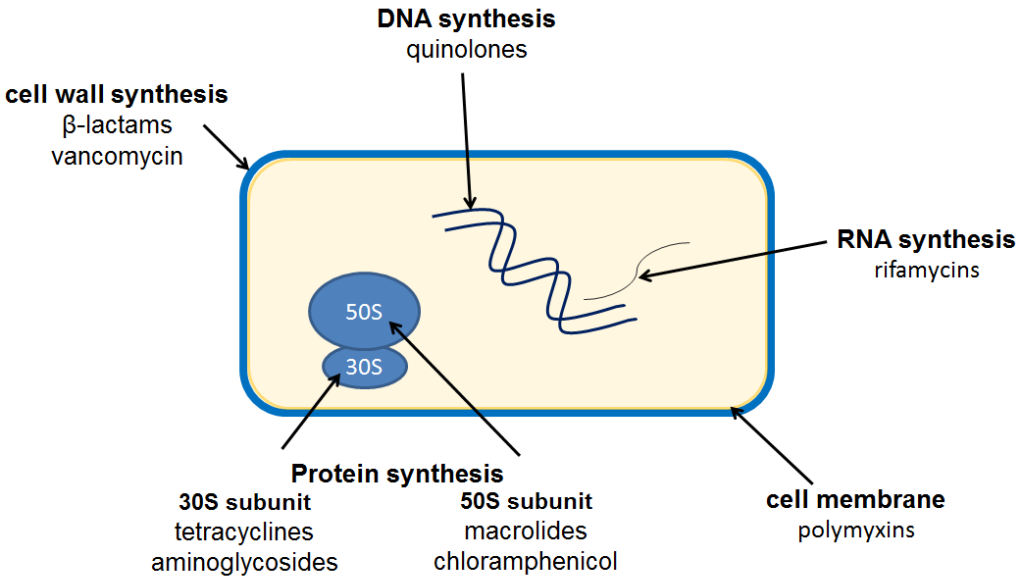

Figure 1.2: Major points of action of common antibiotics. Schematic showing structures or processes commonly targeted by antibiotics as well as some antibiotics that interfere with them. Adapted after Kapoor et al. 2017

1.2.2 Antibiotic resistance mechanisms

Many different microorganisms naturally produce antibiotics. A large variety of antibiotically active substances have been isolated from sources like fungi, plants and bacteria, but most of the active compounds were isolated from streptomycetes (Korzybski et al. 1967). It is likely that microorganisms produce antibiotics to gain an edge over competitors, but antibiotics in nature could also be important for other purposes for example as signals to communicate with other organisms (Clardy et al. 2009). Whatever their significance in nature might be, as soon as substances inhibiting growth appeared, resistance mechanisms should also have evolved. The co-evolution of antibiotic producers and their competitors may have led to the diverse set of antibiotics and resistance mechanisms that are found in nature today (Munita and Arias 2016). Some common ways to resist an antibiotic are discussed below:

1. The spatial exclusion of the antibiotics,
2. The temporal exclusion of the antibiotics,
3. The modification of the antibiotic target structure,
4. The modification of the antibiotic, and
5. The efflux of the antibiotic

An obvious way to avoid any harmful effects caused by an antibiotic is to avoid or min-

imize contact with the substance (spatial exclusion). Due to their size, microorganisms are very limited in their capacity to move over long distances, but they can avoid contact by separating themselves spatially. The most prominent examples for such behavior are the formation of biofilms or capsules. Both mechanisms rely on the production of an extracellular matrix as a barrier to prevent antibiotics from reaching the cell. The polysaccharide capsule formed by some *Klebsiella pneumoniae* strains mediates resistance to antimicrobial peptides (Campos et al. 2004) and biofilm formation is a serious problem in staphylococcal infections (Stewart 2002, Høibya et al. 2010). Biofilms of *L. monocytogenes* can also be the cause of recurrent contamination in the food industry, because of their resistance against common disinfection agents (Pan et al. 2006).

Another way to cope with an antibiotic stress is to wait until it disappears (temporal exclusion). Some bacteria are known to form dormant cell types such as persister cells and spores that are metabolically inactive and thus resistant to antibiotic treatment (Lewis 2012). Biofilms also make use of this mechanism, because the nutrient limited conditions inside of the biofilm slow bacterial growth thereby reducing the negative effects antibiotics have on the bacteria (Stewart 2002). Spores and persister cells are a major cause of chronic or recurring infections with for example *Clostridium* or *Staphylococcus* species (Wood et al. 2013, Tetz and Tetz 2017).

More direct responses that increase the resistance to an antibiotic are also possible. Most antibiotics possess a single main cellular target structure and this target can be modified in subtle ways that prevent binding of the antibiotic while retaining the biological function (target modification). Macrolides for example bind with high affinity to the bacterial ribosome and interfere with protein synthesis (Mazzei et al. 1993, Kannan et al. 2014). A commonly found macrolide resistance mechanism is the methylation of the ribosome to prevent macrolide binding (Weisblum 1995). Cell wall modifications leading to vancomycin resistance in *S. aureus* (Cui et al. 2006) and mutations in the β-subunit of the RNA polymerase leading to rifampin resistance are further examples for this mechanism (Alifano et al. 2015). Another way is to bypass the target completely by having another structure taking over its function as found for example in methicillin resistant *S. aureus* that acquired an exogenous, class B PBP (PBP2a) encoded by *mecA* (Wu et al. 2001). In *L. monocytogenes* HflXr, a ribosome-splitting factor, confers protection against lincomycin and erythromycin probably by recycling stalled ribosomes (Duval et al. 2018).

Soon after the clinical use of penicillin became a standard treatment, resistances by β-lactamase mediated cleavage of the antibiotic were described (Beigelman and Rantz 1950). Such enzymatic degradation or modification of antibiotics is a strategy used by different bacteria to inactivate a wide range of antibiotics (Wright 2005). The same strategy is also used by antibiotic producing organisms to protect themselves against the antibiotics they produce. For example the antibiotic streptomycin is phosphorylated by its producer *Streptomyces griseus* and the phosphorylated form does not interfere with protein biosynthesis (Sugiyama et al. 1981).

Antibiotic efflux is another commonly employed resistance mechanism. This type of resistance can be found in all domains of life and ranges from very specific transporters that only act on specific substances to multi-drug efflux pumps that transport a wide variety of compounds (Poole 2007, Du et al. 2018). There are five major classes of efflux pumps in bacteria. These are the ATP-binding cassette (ABC) transporters, major facilitator superfamily (MFS) transporters, multidrug and toxic compounds extrusion (MATE) transporters, small multidrug resistance (SMR) and resistance-nodulation-division (RND) transporters (Du et al. 2018). The ABC-type transporters directly use the chemical energy stored in ATP to drive conformational changes that enable transport. All the others classes use energy stored in electrochemical gradients across the membrane to power active compound transport (Blanco et al. 2016, Du et al. 2018). Efflux pumps constantly work against a gradient to keep the antibiotic concentration inside the cell low. For this reason, there is an ongoing energetic cost associated with this type of resistance, although it is not necessarily associated with a measurable fitness reduction (Alvarez-Ortega et al. 2013). As an example, the resistance against tetracycline mediated by efflux pumps is more common than other mechanisms like target modification or degradation of the antibiotic (Roberts 2005). Efflux pumps also confer fluoroquinolone resistance to *Pseudomonas aeruginosa* or macrolide resistance to *S. pneumoniae* (Mef pumps) (Ambrose et al. 2005, Aeschlimann 2012) and the MATE type transporter FepA mediates fluoroquinolone resistance in *Listeria monocytogenes* (Guérin et al. 2014).

1.3 PadR-like repressors

1.3.1 The PadR family of proteins

The family of PadR-like repressors got its name from the **p**henolic **a**cid **d**ecarboxylase **r**epressor PadR. The name PadR was initially introduced to describe a repressor protein regulating the expression of the phenolic acid decarboxylase gene *padA* in *Pediococcus pentosaceus* (Barthelmebs et al. 2000b). It was shown that the PadR protein negatively regulates the production of PadA, an enzyme that is responsible for the conversion of toxic phenolic acids into less toxic substances (Barthelmebs et al. 2000b). In the presence of phenolic acids, the repressor is inactivated and the phenolic acids are detoxified by PadA (Gury et al. 2004).

Infobox 1: PadR - PadR-like transcriptional regulator family
"Members of this family are transcriptional regulators that appear to be related to the pfam01047 family. This family includes PadR, a protein that is involved in negative regulation of phenolic acid metabolism." [a]

[a] https://www.ncbi.nlm.nih.gov/Structure/cdd/cddsrv.cgi?uid=308908

In general, the structure of PadR-like proteins places them all in the HTH (Helix-Turn-Helix) superfamily. Proteins of this superfamily are mostly transcription factors involved in nucleic acid binding and the regulation of gene expression (Aravind et al. 2005). It has been proposed that the overall length of the protein can serve to further classify PadR-like proteins into two subfamilies (Huillet et al. 2006). Subfamily I contains a long C-terminus forming a coiled coil dimerization domain separated from the DNA binding domain by a linker (Silva et al. 2005), while subfamily II has a short C-terminal domain containing only one dimerization helix (Fibriansah et al. 2012).

Infobox 2: HTH Superfamily - Helix-turn-helix domain proteins
"A large family of mostly alpha-helical protein domains with a characteristic fold; most members function as sequence-specific DNA binding domains, such as in transcription regulators. This superfamily also includes the winged helix-turn-helix domains." [a]

[a] https://www.ncbi.nlm.nih.gov/Structure/cdd/cddsrv.cgi?uid=cl21459

At the time of writing, the pfam database contained 19503 protein sequences belonging to the PadR family (PF03551) distributed over 4480 different species. This species distribution can be visualized on pfam in a so called Sunburst graph, which can be seen in Figure 1.3 (Pfam 2019).

Although PadR-like proteins have also been found in some *Archaea*, they are especially common in members of the bacterial domain of life. It is also apparent from the sunburst graph that the Gram-positive bacterial phyla *Firmicutes* and *Actinobacteria* represent the biggest portion of the total PadR diversity (nearly 75 % of all the sequences). Members of the *Actinobacteria* are an essential part of the global carbon cycle as they are major degraders of plant biomass. They mainly live as saprophytes making up around 10 % of soil microbioms or as symbionts associated with herbivorous animals (Lewin et al. 2016, Trivedi et al. 2016). The *Firmicutes* on the other hand only make up a small portion of soil microbiomes (around 2 %), while they can be found in abundance in manure or the gastrointestinal track of animals and constitute a major part of the human gut microbiome (Mao et al. 2015, Jandhyala et al. 2015, Trivedi et al. 2016, Rieke et al. 2018). It seems as if both the *Actinobacteria* and the *Firmicutes* do not necessarily grow in the same niches, but that they do co-exist in soil environments.

Figure 1.3: Sunburst representation of PadR sequences on Pfam (Pfam 2019). The sequences of PadR-like proteins in the Pfam database grouped according to their phylogeny. As of June 2019 the tree comprised 19503 sequences across 4480 species, of which 4177 were *Bacteria* and 303 *Archaea*. Sequences from the *Listeriaceae* are highlighted red in the upper left corner at around 11 o'clock. The red part on the right represents archaeal protein sequences.

1.3.2 PadR - the transcriptional regulator of phenolic acid decarboxylase

Initial research on PadR showed that it regulates the expression of the genes *padA* or *padC*, encoding phenolic acid decarboxylases. These enzymes increase the tolerance of bacteria to this class of compounds by degrading the toxic phenolic acids (Barthelmebs et al. 2000a, Barthelmebs et al. 2000b, Tran et al. 2008). Under normal conditions PadR binds to the *padA* promoter and prevents transcription of the gene (Gury et al. 2004). In the presence of phenolic acids, like p-coumaric acid, the binding of PadR to its operator does not occur (Gury et al. 2004). It thus seems that in response to phenolic acid stress, decarboxylases that degrade the toxic compounds are specifically induced. The role of the repressor PadR is to prevent the transcription of the decarboxylase genes when not needed, while it is activated in the presence of inducing compounds.

The binding of *B. subtilis* PadR to the DNA is principally mediated by a winged helix-turn-helix domain (Park et al. 2017). The beta-sheets of PadR also interact with the DNA, but the interaction is mostly unspecific bonding to the phosphate backbone of the DNA helix (Park et al. 2017). Binding of PadR to its operator prevents the transcription from the *padC* promoter it controls (Nguyen et al. 2011). The operator sequence recognized by PadR-like transcription factors is generally between 16 and 22 base pairs long and consists of an inverted repeat and a variable spacer region (Gury et al. 2004, Agustiandari et al. 2008, Nguyen et al. 2011, Fibriansah et al. 2012). The ATGT/ACAT inverted repeat has been suggested to be the canonical sequence for PadR-like repressors (Fibriansah et al. 2012). The operator of *B. subtilis* consists of two similar sites one containing the canonical ATGT-8N-ACAT repeat and overlapping the -10 promoter box, the other with an imperfect repeat overlapping the transcription start site (Nguyen et al. 2011). In *B. cereus* the protein bcPadR1 also recognizes a region overlapping the -10 box of the promoter (Fibriansah et al. 2012). PadR-like repressors therefore seem to interfere with transcription by blocking RNA polymerase from accessing the promoter region.

Transcription of PadR-controlled genes can be induced by addition of phenolic acids like *p*-coumaric acid (Tran et al. 2008). This acid was crystallized in complex with PadR, showing that a PadR monomer binds one molecule of the effector in a pocket between the N-terminal and the C-terminal domains (Park et al. 2017). This binding seemed to be predominantly enthalpy-driven by mainly hydrophilic interactions. Upon effector binding, conformational changes in the protein lead to a dissociation from the DNA. The mechanism of induction thus involves the thermodynamically favored binding of effector to the protein, followed by structural re-arrangements that lead to the dissociation from the DNA (Park et al. 2017). The promoter is then free to bind RNA polymerase and initiate transcription of the phenolic acid decarboxylase.

Despite the diversity of PadR-like sequences, only a few proteins of the PadR family have

been extensively studied. The biological functions assigned to proteins of this family range from virulence gene control in *Vibrio cholerae* by AphA (Kovacikova et al. 2003), over control of multi-drug-resistance pumps by LmrR in *Lactococcus lactis* (Agustiandari et al. 2008), all the way to the regulation of circadian rhythms by Pex in *Synechococcus elongates* (Takai et al. 2006). The next section will look at the PadR-like proteins that can be found in *L. monocytogenes*.

1.4 PadR-like transcription factors in *L. monocytogenes*

According to the Pfam database, the genome of *L. monocytogenes* harbors five genes belonging to the PadR family:

1. ***lmo0422*** - renamed *lstR* (Zhang et al. 2005)
2. ***lmo0599*** - renamed *lltR* (Hauf et al. 2019b)
3. ***lmo0719*** - renamed *lftR* (Kaval et al. 2015)
4. ***lmo1213***
5. ***lmo1408*** - renamed *ladR* (Huillet et al. 2006)

The PadR-like protein Q734F6 from *Bacillus cereus* has been crystallized and its structure deduced from X-ray diffraction data (Fibriansah et al. 2012). Recently, the crystal structure of LftR has also been determined (Lee et al. 2019). The overall structure of LftR is nearly identical to Q734F6, so it seems likely that other PadR-like proteins have a similar structural layout. Based on the crystallographic results, the secondary elements of the other PadR-like proteins can be inferred. The N-terminal HTH domain involved in DNA binding of transcription factors is followed by two beta-sheets and another helix important for dimerization and substrate recognition (Fibriansah et al. 2012, Lee et al. 2019).

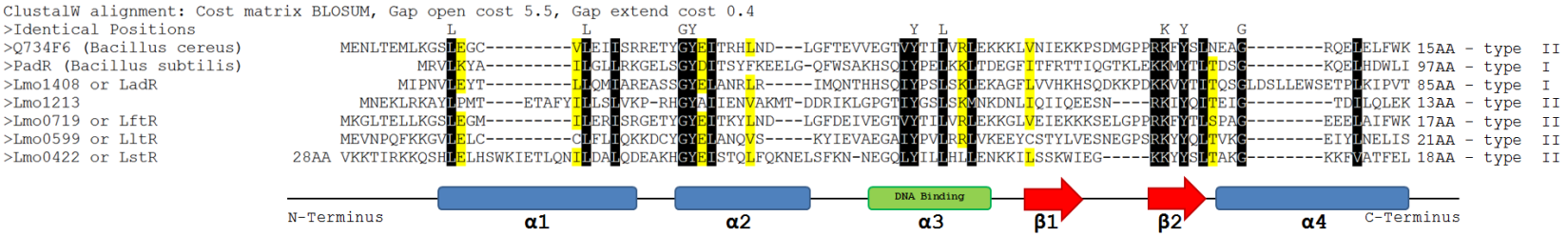

Figure 1.4: Alignment of listerial PadR-like protein sequences with the sequence of PadR from *B. subtilis* and the PadR-like protein Q734F6 from *B. cereus*. The N-terminal helix-turn-helix domain (comprised by helices $\alpha 1-3$) is important for interactions with the DNA and includes the putative DNA binding helix $\alpha 3$. The two beta sheets ($\beta 1-2$) and a dimerization helix ($\alpha 4$) at the C-terminus are also characteristic for PadR-like proteins. Proteins with a long C-terminal helix belong to the PadR-subfamily of type I, while proteins with a short C-terminal helix belong to type II.

Figure 1.4 shows a protein alignment of the five PadR-like proteins from *Listeria monocytogenes* compared to PadR from *B. subtilis* and the PadR-like protein Q734F6 from *B. cereus* with the secondary structural elements depicted at the bottom of the figure 1.4. Amino acids strongly conserved among all the proteins (highlighted in black) can be found in all of the helices and in the second beta-sheet. Such highly conserved amino acids are likely to be important for the function of the proteins (Poteete et al. 1992). For example the conserved Y–L–L (tyrosine–leucine–leucine) motive in the third helix (the putative DNA binding helix of the HTH domain) could to be important for the interaction with the DNA. Supporting this conjecture, it has been shown that the exchange of tyrosine in the Y–L–L motif for an alanine or the deletion of the beta-wing (the two beta-sheets shown in red in figure 1.4) abrogated DNA binding of LftR (Lee et al. 2019).

The C-terminal regions of the PadR-like proteins shown in figure 1.4 are either around 20 to 30 amino acids long or significantly longer (with over 100 amino acids). For example *B. subtilis* PadR and LadR from *L. monocytogenes* have significantly longer C-terminal domains than the other proteins placing them in the PadR subfamily I. All other PadR-like proteins, representing the shorter sequences (*lstR*, *lftR*, *lltR* and *lmo1213* in *L. monocytogenes*), belong to subfamily II. The next pages will briefly summarize the literature knowledge about the PadR-like proteins of *L. monocytogenes*.

1.4.1 LadR regulates *mdrL* expression

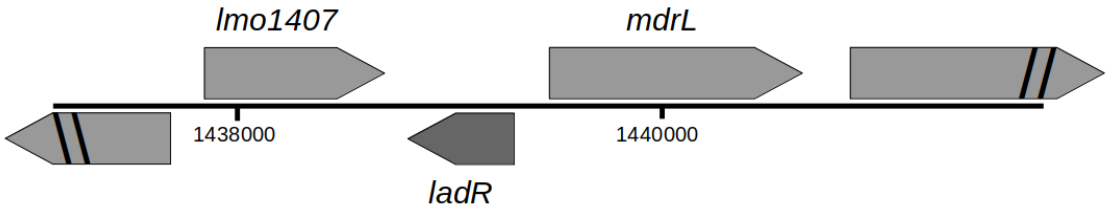

Figure 1.5: Genomic context of *L. monocytogenes ladR*.

While screening a transposon library in *L. monocytogenes* LO28 a mutant that showed altered hemolysis in the presence of cellobiose was identified (Huillet et al. 1999). Cellobiose normally inhibits hemolysis by suppressing PrfA-mediated haemolysin A activation (Milenbachs et al. 2003). In the mutant, the transposon had inserted between the genes *lmo1408*, called *orfA*, and *lmo1409* (see figure 1.5). The *lmo1409* gene shows significant similarity to **m**ulti**d**rug **r**esistance transporters and was therefore re-named *mdrL* (L for ***L****isteria*, Huillet et al. 1999). Lmo1408 (renamed LadR) was shown to repress the transcription of *mdrL* under standard conditions (Huillet et al. 2006). Transcripts of

the *mdrL* gene were detectable in the presence of the synthetic laser dye rhodamine 6G, whereas no *mdrL* transcripts were observed in the absence of the inducer (Huillet et al. 2006). However, evidence for rhodamine 6G transport by MdrL is still outstanding.

The genes *ladR* and *mdrL* have been associated with resistance to disinfectants (Romanova et al. 2006, Tamburro et al. 2015, Jiang et al. 2018). For example, *mdrL* is over-expressed in *L. monocytogenes* exposed to sub-lethal benzalkonium concentrations (Tamburro et al. 2015). MdrL was initially investigated as a potential exporter of benzalkonium (a disinfectant commonly used in the food industry), because it was one of two described efflux pumps in *L. monocytogenes* at that time (Romanova et al. 2006). A direct link between MdrL and benzalkonium resistance was also claimed (Jiang et al. 2018). These authors could show an increased lag phase when *mdrL* was deleted, but the MIC of benzalkonium was unaffected (Jiang et al. 2018). In another project, a transposon library was screened for mutants with an altered type I interferon response in macrophages (Crimmins et al. 2008). This study found one mutant with a disrupted *ladR* gene. In this *ladR* mutant the two genes *mdrL* and *mdrM* were induced 30-fold and 3-fold respectively (Crimmins et al. 2008). They found a contribution of MdrM but not of MdrL to the interferon response, so it seems likely that LadR exerts a weak repressive effect on *mdrM* that caused this phenotype (Crimmins et al. 2008) while *mdrL*, the main target gene of LadR repression, remains without a clearly defined function.

1.4.2 LstR - a lineage-specific thermal regulator

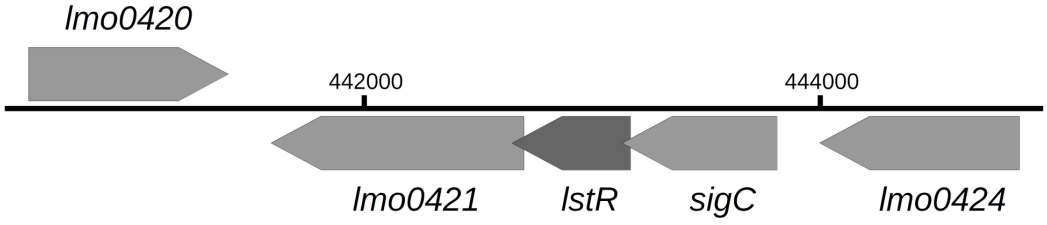

Figure 1.6: Genomic context of *L. monocytogenes lstR*.

A detailed examination of the genomes of the most common clinical serotypes of *L. monocytogenes* led to the observation that strains belonging to lineage I lack an operon containing genes for the extra-cytoplasmic function sigma factor *sigC* (*lmo0423*), an unknown gene coding for a protein of the PadR family (*lmo0422*, now called *lstR*), and a *rodA*/*ftsW* paralog (*lmo0421*) (Zhang et al. 2003). At that time the operon was identified to be absent in lineage I, the function of those genes (see figure 1.6) was completely unknown. Further characterization of the operon led to the description of *lstR* (for **l**ineage-**s**pecific **t**hermal

regulator) as being responsible for resistance to heat (Zhang et al. 2005). According to these results, the sigma factor SigC is important for the temperature-dependent expression of the one operon and the RodA/FtsW paralog mediates the heat adaptive response (Zhang et al. 2005). Other sigma factors of *L. monocytogenes* are the housekeeping sigma factor SigA, SigB involved in the general stress response and virulence (Kazmierczak et al. 2003), SigH involved in intracellular growth (Romeroa and Morikawa 2016) and SigL involved in the response to various stressful conditions (Mattila et al. 2012).

Transcriptomic and proteomic studies of alternative sigma factors mutants of *L. monocytogenes* confirmed the auto-regulatory nature of this operon by proving the transcriptional dependence of *lmo0422/lmo0421* on SigC. No other genes were identified as being regulated by SigC (Chaturongakul et al. 2011, Mujahid et al. 2013a). It has also been shown, that stable L-forms of *Listeria monocytogenes* acquired a mutation in *lmo0421* (Studer et al. 2016). As L-form bacteria lack the cell wall, they are assumed to be stabilized by mutations in cell wall synthesis genes. Therefore, the mutation of this RodA homolog could be a hint that it indeed has a function in the synthesis of the cell wall like other RodA proteins (Meeske et al. 2016, Emami et al. 2017).

1.4.3 LftR regulates the expression of the *lieAB* transporter genes

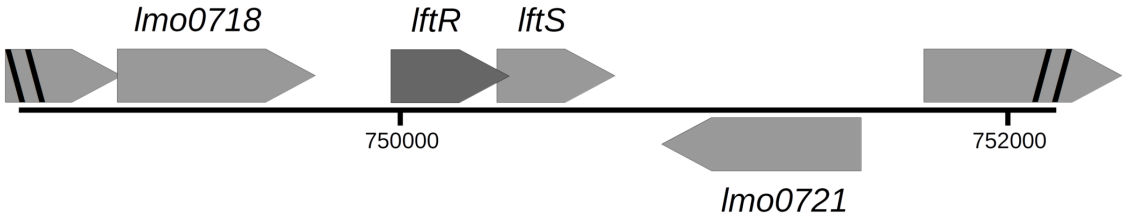

Figure 1.7: Genomic context of *L. monocytogenes lftR*.

LftR has been identified recently and named the **l**isterial protein **f**acilitating invasion and **t**ranscriptional **r**egulator (Kaval et al. 2015). It is encoded in a bicistronic operon together with *lftS*, a gene of unknown function (see figure 1.7). LftR negatively regulates the expression of the operon *lmo0979-lmo0980*, coding for a putative ABC-type transporter (Kaval et al. 2015). The tight regulation of the transporter is necessary for an efficient invasion into HeLa cells (Kaval et al. 2015), again linking a transporter regulated by a protein of the PadR family to virulence as was the case for LadR and the pump MdrL (Huillet et al. 2006). The exact role of the efflux pump did not become clear though. The transporter genes *lmo0979-0980* were renamed *lieAB* for **l**isterial **i**mporter of **e**thidium bromide as artificial substrate, because the pump imports ethidium bromide

in an ATP-consuming manner (Kaval et al. 2015). The active import of a toxic substance like ethidium bromide does not make any biological sense, though. Therefore, despite these discoveries the biological function of the LieAB transporter and LftR still remained hidden.

1.4.4 Lmo0599 and Lmo1213 - two uncharacterized PadR-like proteins

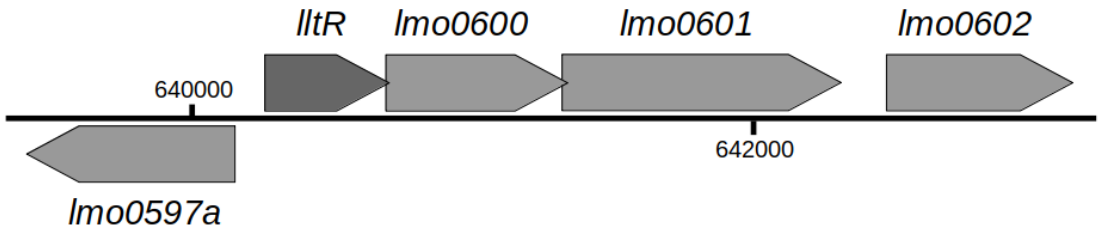

Figure 1.8: Genomic context of *L. monocytogenes lltR*.

Beside the proteins described above, two uncharacterised PadR-like proteines are also encoded in the genome of *L. monocytogenes*. At the time of writing, no knowledge existed about function of the two remaining PadR-like proteins Lmo0599 and Lmo1213. The gene *lmo0599* is located at the beginning of the three gene *lmo0599-lmo0600-lmo0601* operon (see figure 1.8). Lmo0600 is a DUF1700 domain-containing potential transmembrane protein and Lmo0601 contains a DUF4097 domain showing some homology to bacterial adhesins.

The gene *lmo1213* encoding a putative PadR-like repressor forms a bicistronic operon together with *lmo1214* (see figure 1.9). The latter gene codes for a DUF2812 containing protein without any known function.

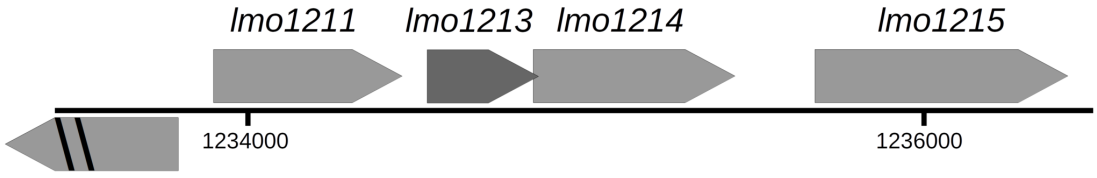

Figure 1.9: Genomic context of *L. monocytogenes lmo1213*.

1.5 Aims of this study

The genome of *L. monocytogenes* contains five genes that show significant homology to the PadR family of transcriptional regulators. Three of these have been studied previously (Zhang et al. 2005, Huillet et al. 2006, Kaval et al. 2015). Still, the biological role of these proteins has not yet been clearly defined and knowledge about effector molecules exists only for LadR (Huillet et al. 2006).

In general, PadR-like proteins seem to regulate gene expression in response to certain environmental stimuli. In the course of this work, deletion mutants were constructed to determine the regulon structure of the PadR-like proteins. Promoter-*lacZ* constructs are made to screen for conditions or substances that induce the expression of the normally repressed genes. Further, the interaction of LftR with promoters it controls was studied to identify and validate the possible LftR-binding motif.

Chapter 2

Materials and Methods

2.1 Primers

During the course of this work a range of genetic manipulations were done. All oligonucleotides used to generate the desired nucleic acid material are listed in the following table (table 2.1). They were synthesized by Eurofins Genomics GmbH or Integrated DNA Technologies, Inc. The lyophilized oligonucleotides were dissolved to 100 μM in molecular biology grade water from Carl Roth GmbH + Co. KG.

Table 2.1: Primers used in this study.

Name	Sequence	Use
SaH032	CAGATCTATCGATGCATGCCATGGAGGAAAG GAAGAGGAGAATTATG	*lmo1408* deletion US FW
SaH033	AATTCAGAGGTGCTATTGTGTCGACAAAAAC CGGCGAACTTAATATTCGC	*lmo1408* deletion US RV
SaH034	ATTAAGTTCGCCGGTTTTTGTCGACACAATA GCACCTCTGAATTTC	*lmo1408* deletion DS FW
SaH035	CCTCGCGTCGGGCGATATCGGATCCGGCCGA TATTTGAACAAATGG	*lmo1408* deletion DS RV
SaH036	CTCGCGTCGGGCGATATCGGATCCCAGGGAG ATAGCTACTAGGG	*lmo0422* deletion DS FW

continues on next page

SaH037	AGGAGGTTTAATCGTCGACATGAGTTCTTCT ACATTTGAAG	*lmo0422* deletion DS RV
SaH038	TGTAGAAGAACTCATGTCGACGATTAAACCT CCTTTTTCATCTTATTC	*lmo0422* deletion US FW
SaH039	CAGATCTATCGATGCATGCCATGGGTTAATC ATGGTGGGCGTCG	*lmo0422* deletion US RV
SaH052	GATCTATCGATGCATGCCATGGATGGAGGTT AACCCGCAGTTC	*lmo0599* in pMAD FW
SaH053	GCTTCTAGAATTCGAGCTCCCTTATTCATTT ACTGCTTCCCCCTC	*lmo0599* in pMAD RV
SaH058	CCGGTAGCAAGAGCAGCAGTAAAAGAAGA GTACTGTTC	*lmo0599*: C145G, T146C, T147A, A151G, G152C, T145G, T155C FW
SaH059	TTTTACTGCTGCTCTTGCTACCGGATAAATA GCACCTTC	*lmo0599*: C145G, T146C, T147A, A151G, G152C, T145G, T155C RV
SaH079	AGAACTAGTGGATCCCACGCTAATCTTGATG AGAAATGCC	P_{lftR} in pBP117 RV
SaH090	CGGGAAGCCCTGGGACG	check insertion of promoters in pBP117
SaH091	TGGCCTTCCTGTAGCCAGC	check insertion of promoters in pBP117
SaH099	GTTGTAAAACGACGGGGAATTCCATTTGAAT ACAACCTTCTTTCC	P_{lieAB}in pBP117 RV
SaH109	CTAGAACTAGTGGATCCCGCATGTTCTTAGC GACTGC	$P_{lmo0422}$ in pBP117 FW
SaH110	GTAAAACGACGGGGAATTCCATTTAAGTTTC ACCTTCTTCTGC	$P_{lmo0422}$ in pBP117RV
SaH113	CTAGAACTAGTGGATCCCTATCTTGGGAATG CTTATGAAC	$P_{lmo1409}$ in pBP117 FW
SaH114	GTAAAACGACGGGGAATTCCATAATACAACT ACACTTCCC	$P_{lmo1409}$ in pBP117RV
SaH115	CTAGAACTAGTGGATCCCTCACGCATAAACT TATCTCTCC	$P_{lmo0599}$ in pBP117 FW

continues on next page

SaH116	CGACGGGGAATTCCTGCAGCATGCTAACTCC TCCATTCTG	$P_{lmo0599}$ in pBP117RV
SaH170	CTAGAACTAGTGGATCCCTCAAACCGTCCGT TCAG	P_{lieAB}(193 bp) in pBP117 FW
SaH171	CTAGAACTAGTGGATCCCACAAAAGTCATTT CAGATGA	P_{lieAB}(152 bp) in pBP117 FW
SaH172	CTAGAACTAGTGGATCCCTGACTTTTTTATT GACACATCC	P_{lieAB}(122 bp) in pBP117 FW
SaH173	CTAGAACTAGTGGATCCCACTCGGTGTTACT ATGTAG	P_{lieAB}(97 bp) in pBP117 FW
SaH174	CTAGAACTAGTGGATCCCTGACTTTTTTATT GACACTACCGCAACTCGGTGTTACTAT-CAAGTAGTAATAAGTAATACAGAATACCG	P_{lieAB}(122 bp): A-104T, T-103A, G-82C, T-81A FW
SaH175	CTATCGATGCATGCCATGGTCCATCTTCCTC CTCCAG	*lmo0422* in pMAD DS FW
SaH176	GCACATGCAGCTGAAAACAAGAAAATCCTA TC	*lmo0422*: T268G, T269C, C274G, T275C, C277G, T278C DS RV
SaH177	AGCTGCATGTGCCAGAATATAAAGCTGACC	*lmo0422*: T268G, T269C, C274G, T275C, C277G, T278C US FW
SaH178	CTGCAGAAGCTTCTAGAATTCGACAGCGGA AGATTTAACG	*lmo0422* in pMAD US RV
SaH179	CTATCGATGCATGCCATGGTGGCAAGGATGA GGAGC	*lmo0421* deletion DS FW
SaH180	CTTTATGAGTTAATTTAGTGTATAACCGACA TG	*lmo0421* deletion DS RV
SaH181	CACTAAATTAACTCATAAAGAAGCCTCCTC	*lmo0421* deletion US FW
SaH182	CGTGCTAGGTTTGAGAAG	*lmo0421* deletion US RV
SaH185	CCCATGGAAAAGGATCCATGGAGGTTAACC CGCAGTTC	*lmo0599* into pIMK3 FW
SaH186	CGAATTCCTGCAGCCCGGGTTATTCATTTAC TGCTTCCCCCTC	*lmo0599* into pIMK3 RV
SaH187	CTAGAACTAGTGGATCCCTTTTTTATTGACA CATCCGCAACTCGGTGTTA CTATGTAGAT-CATTTAAGTAATACAGAATACCGGTG	P_{lieAB}(118 bp): T-78A, A-77T, G-76C, T-75A, A-74T, A-73T FW

continues on next page

SaH188	GTAACACCGGTATTGACATAATGTTATTACT ACTACATAGTAACACCG	P_{lieAB}(122 bp) US RV: bp-69...-61 GTAAT-ACAG → CATTATGTC
SaH189	CACTACTCAGTAAGTGGCCATAACTGTATTA CTTATTACTACTACATAG	P_{lieAB}(122 bp) US RV: bp-60...-51 AATACCG-GTG → TTATGGCCAC
SaH190	ATTAAAACCCCACATGAGTCATTCACCGGTA TTCTGTATTACTTATTAC	P_{lieAB}(122 bp) US RV: bp-50...-41 TTACT-GAGTA → AATGACT-CAT
SaH191	CTTCTTTCCATTTTTTATTTTTTGGGGTGTA CTCAGTAACACCGGTATTC	P_{lieAB}(122 bp) US RV: bp-40...-31 GTGGGGTTTT → CACCCCAAAA
SaH192	TACAACCTTCTTTCCTAAAAAATAAAAAACC CCACTACTCAGTAACACC	P_{lieAB}(122 bp) US RV: bp-30...-21 AATAAAAAAT → TTATTTTTTA
SaH208	CTTTAAGAAGGAGATATACATATGAAAGGAC TTACCGAGTTACTC	*lftR* into pSH304 FW
SaH209	CGAACTGCGGGTGGCTCCATGGCGCTTGCC CTCCTTTAAC	*lftR* into pSH304 RV
SaH210	CTTTAAGAAGGAGATATACATATGTTTAATT GGTACAAAAAATACCG	*lftS* into pSH304 FW
SaH211	CGAACTGCGGGTGGCTCCATGGTTTAATCGA ATCTCGCAATTTCTGACG	*lftS* into pSH304 RV
SaH212	CTATCGATGCATGCCATGGATGGAGGTTAAC CCGCAGTTC	*lmo0600* deletion US FW
SaH213	AGTGATGTTTATTCATTTACTGCTTCCCCCT	*lmo0600* deletion US RV
SaH214	TGAATAAACATCACTTAAGCAAAAAACT	*lmo0600* deletion DS FW
SaH215	CTGCAGAAGCTTCTAGAATTCTCATCTTCTT CAGGCACCGT	*lmo0600* deletion DS RV
SaH216	CTATCGATGCATGCCATGGTGACCTTGGTAA GCCAGAAG	*lmo0601* deletion US FW
SaH217	TTCGATTTTATGCATTTTTCCCGCCTCC	*lmo0601* deletion US RV
SaH218	TGCATAAAATCGAAAAATAAAAAATCAGTG CGCT	*lmo0601* deletion DS FW

continues on next page

SaH219	CTGCAGAAGCTTCTAGAATTCAGCTCCGTGC CAAGTCC	*lmo0601* deletion DS RV
SaH227	CTGTATTTGTTATTACTACTACATAGTAACA CC	P_{lieAB}(122 bp): G-69C, T-68A US RV
SaH228	GTAATAACAAATACAGAATACCGGTGT	P_{lieAB}(122 bp): G-69C, T-68A DS FW
SaH229	TCTGTAAAACTTATTACTACTACATAGTAAC ACC	P_{lieAB}(122 bp): A-67T, A-66T US RV
SaH230	TAATAAGTTTTACAGAATACCGGTGTTAC	P_{lieAB}(122 bp): A-67T, A-66T DS FW
SaH231	GTATTCTGATTTACTTATTACTACTACATAG	P_{lieAB}(122 bp): T-65A, A-64T US RV
SaH232	ATAAGTAAATCAGAATACCGGTGTTACTG	P_{lieAB}(122 bp): T-65A, A-64T DS FW
SaH233	CGGTATTCACTATTACTTATTACTACTACAT AG	P_{lieAB}(122 bp): C-63G, A-62T US RV
SaH234	AAGTAATAGTGAATACCGGTGTTACTGAG	P_{lieAB}(122 bp): C-63G, A-62T DS FW
SaH235	ACCGGTATAGTGTATTACTTATTACTACTAC A	P_{lieAB}(122 bp): G-61C, A-60T US RV
SaH236	GTAATACACTATACCGGTGTTACTGAGTAG	P_{lieAB}(122 bp): G-61C, A-60T DS FW
SaH237	ACACCGGTTATCTGTATTACTTATTACTACT AC	P_{lieAB}(122 bp): A-59T, T-58A US RV
SaH238	AATACAGATAACCGGTGTTACTGAGTAG	P_{lieAB}(122 bp): A-59T, T-58A DS FW
SaH239	TAACACCGCAATTCTGTATTACTTATTACTA C	P_{lieAB}(122 bp): A-57T, C-56G US RV
SaH240	TACAGAATTGCGGTGTTACTGAGTAGTGG	P_{lieAB}(122 bp): A-57T, C-56G DS FW
SaH241	AGTAACACGCGTATTCTGTATTACTTATTAC TAC	P_{lieAB}(122 bp): C-55G, G-54C US RV
SaH242	CAGAATACGCGTGTTACTGAGTAGTG	P_{lieAB}(122 bp): C-55G, G-54C DS FW
SaH243	TCAGTAACTGCGGTATTCTGTATTACTTATT ACTAC	P_{lieAB}(122 bp): G-53C, T-52A US RV

continues on next page

SaH244	GAATACCGCAGTTACTGAGTAGTGGGGT	P_{lieAB}(122 bp): G-53C, T-52A DS FW
SaH245	CAGTAAGACCGGTATTCTGTATTACTTATTA C	P_{lieAB}(122 bp): G-51C US RV
SaH246	ACCGGTCTTACTGAGTAGTGGGGTTT	P_{lieAB}(122 bp): G-51C DS FW
SaH253	CTATCGATGCATGCCATGGTCTCTGGCTTGT TTTAACC	*sigC* deletion US FW
SaH254	TTAGGTACCGAATCGAACGACAGCGGAAG	*sigC* deletion US RV
SaH255	TTCGGTACCTAAGAAAAAACTAGATGCAGT AC	*sigC* deletion DS FW
SaH256	CTGCAGAAGCTTCTAGAATTCTGCAGAAGA AGGTGAAAC	*sigC* deletion DS RV
SaH257	CTATCGATGCATGCCATGGTCGTGCTATGTT TATTTGGGC	internal fragment for disruption of *lmo1071* with pMAD FW
SaH258	CTGCAGAAGCTTCTAGAATTCTTATTAACCC ATACCAATCCCA	internal fragment for disruption of *lmo1071* with pMAD RV
SaH259	CTATCGATGCATGCCATGGTCTGCTTTCACC CATTC	*lmo2427-2428* deletion US FW
SaH260	ATGGCCTCTTAAAATGAAAATACAGAAGTC	*lmo2427-2428* deletion US RV
SaH261	CATTTTAAGAGGCCATTGTTTTCCGTC	*lmo2427-2428* deletion DS FW
SaH262	CTGCAGAAGCTTCTAGAATTCTGATTTAGTG GCGTATGG	*lmo2427-2428* deletion DS RV
SaH263	CTATCGATGCATGCCATGGTTATTACCCACC GCTCCCAATC	internal fragment for disruption of *lmo2688* with pMAD FW
SaH264	CTGCAGAAGCTTCTAGAATTCACGAGTTATG GTGTTGCTG	internal fragment for disruption of *lmo2688* with pMAD RV
SaH265	AAAGTAGGTTTGATGTCAACC	P_{lftRS} modification US RV

continues on next page

SaH266	CAAACCTACTTTCATATACTATATACTTGTA CCTAGTAACAACTAGTAG	P_{lftRS}: G-51C, T-50A, A-49T, T-48A DS FW
SaH267	CAAACCTACTTTGTATTACTATTATGTTGTA CCTAGTAACAACTAGTAG	P_{lftRS}: A-41T, T-40A, A-39T, C-38G DS FW
SaH268	CAAACCTACTTTGTATATGTATATACTTGTA CCTAGTAACAACTAGTAG	P_{lftRS}: T-47A, A-46T, C-45G DS FW
SaH269	CTGCAGAAGCTTCTAGAATTCCCGGATTATT TTATCGGTGTTC	internal fragment for disruption of *lmo2687* with pMAD FW
SaH270	CTATCGATGCATGCCATGGTTATTATCCCCG AACCAACAGC	internal fragment for disruption of *lmo2687* with pMAD RV
SaH273	CTGTATATGTTATATGTACTACATAGTAACA CCGAGTTGC	P_{lieAB}(122 bp): G-76C, T-75A, A-74T, G-69C, T-68A, A-67T US RV
SaH274	GTAGTACATATAACATATACAGAATACCGGT GTTACTG	P_{lieAB}(122 bp): G-76C, T-75A, A-74T, G-69C, T-68A, A-67T DS FW
SaH276	CCGGTATTCTGTATTTGTTATTTGTACTACA TAGTAACACC	P_{lieAB}(122 bp): G-76C, T-75A, G-69C, T-68A US RV
SaH277	CCGGTATTCTGTATTTGTTAAAACTACTACA TAGTAACACC	P_{lieAB}(122 bp): A-74T, A-73T, G-69C, T-68A US RV
SaH278	CCGGTATTCTGTATTTGTATTTACTACTACA TAGTAACACC	P_{lieAB}(122 bp): T-72A, A-71T, G-69C, T-68A US RV
SaH279	CCGGTATTCTGTATTTGATATTACTACTACA TAGTAACACC	P_{lieAB}(122 bp): A-70T, G-69C, T-68A US RV
SaH280	CAAATACAGAATACCGGTGT	P_{lieAB}(122 bp) modification DS FW
SaH283	CTATCGATGCATGCCATGGGGTGCGGTCATA TCTGGATG	*lmo0420* deletion US FW
SaH284	CAAAATCTCGCTCTAATCATCTGTTTAAACT CC	*lmo0420* deletion US RV
SaH285	GATTAGAGCGAGATTTTGATCCGATCTTTGG C	*lmo0420* deletion DS FW

continues on next page

SaH286	CTGCAGAAGCTTCTAGAATTCGGTTGGTTCG GCAAGGG	*lmo0420* deletion DS RV
SHW306	GAGTCAGTGAGCGAGGAAG	binds p15A origin region

2.2 Plasmids

All plasmids used in this work can be found in the table below (table 2.2).

Table 2.2: Plasmids used in this study.

Name	Genotype	Construction
pBP117	*lacZ neo*	(Hauf et al. 2019a)
pET11a	*bla* P_{T7} *lacI*	Novagen
pIMK2	P_{help} *neo*	(Monk *et al.*, 2008)
pIMK3	P_{help}-*lacO lacI neo*	(Monk *et al.*, 2008)
pMAD	*bla erm bgaB*	(Arnaud et al., 2004)
pSAM1	*bla erm* Δ*lmo1408*	*lmo1408* upstream (SaH032, SaH033) and downstream (SaH034, SaH035) BamHI/NcoI in pMAD
pSaH001	*bla erm bgaB* Δ*lmo1408*	BamHI/NcoI cut fragment from pSAM1 into pMAD
pSaH002	*bla erm bgaB* Δ*lmo0422*	*lmo0422* upstream (SaH036, SaH037) and downstream (SaH038, SaH039) BamHI/NcoI in pMAD
pSaH003	*bla erm bgaB* Δ*lmo0422*	pSaH002 cut BamHI, PCR purified and religated

continues on next page

pSaH004	*bla erm bgaB-lmo0599*	*lmo0599* (SaH052, SaH053) EcoRI/NcoI into pMAD
pSaH005	*bla erm bgaB-lmo0599*: C145G, T146C, T147A, A151G, G152C, T145G, T155C	PCR around pSaH004 (SaH058, SaH059) and DpnI digest
pSaH010	P_{lieAB}(266 bp)-*lacZ neo*	(Hauf et al. 2019a)
pSaH011	P_{lftRS}(315 bp)-*lacZ neo*	(Hauf et al. 2019a)
pSaH012	$P_{lmo0423}$(370 bp)-*lacZ neo*	370 bp upstream of *lmo0423* (SaH109, SaH110) BamHI/EcoRI into pBP117
pSaH013	*bla erm bgaB ΔsigB (lmo0895)*	(Hauf et al. 2019a)
pSaH014	$P_{lmo1409}$(347 bp)-*lacZ neo*	347 bp upstream of *lmo1409* (SaH113, SaH114) BamHI/EcoRI into pBP117
pSaH015	$P_{lmo0599}$(201 bp)-*lacZ neo*	201 bp upstream of *lmo0599* (SaH115, SaH116) BamHI/EcoRI into pBP117
pSaH018	P_{gpsB}(237 bp)-*lacZ neo*	(Hauf et al. 2019a)
pSaH019	P_{divIVA}(214 bp)-*lacZ neo*	(Hauf et al. 2019a)
pSaH026	P_{lieAB}(193 bp)-*lacZ neo*	193 bp upstream of *lieAB* (SaH170, SaH099) BamHI/EcoRI into pBP117
pSaH027	P_{lieAB}(152 bp)-*lacZ neo*	152 bp upstream of *lieAB* (SaH171, SaH099) BamHI/EcoRI into pBP117
pSaH028	P_{lieAB}(122 bp)-*lacZ neo*	122 bp upstream of *lieAB* (SaH172, SaH099) BamHI/EcoRI into pBP117

continues on next page

pSaH029	P_{lieAB}(97 bp)-*lacZ neo*	97 bp upstream of *lieAB* (SaH173, SaH099) BamHI/EcoRI into pBP117
pSaH030	P_{lieAB}(122 bp): A-104T, T-103A, G-82C, T-81A-*lacZ neo*	122 bp upstream of *lieAB* (SaH174, SaH099) BamHI/EcoRI into pBP117
pSaH031	P_{lieAB}(118 bp): T-78A, A-77T, G-76C, T-75A, A-74T, A-73T-*lacZ neo*	118 bp upstream of *lieAB* (SaH187, SaH099) BamHI/EcoRI into pBP117
pSaH032	*bla erm bgaB* Δ*lmo0421*	*lmo0421* upstream (SaH179, SaH180) and downstream (SaH181, SaH182) EcoRI/NcoI in pMAD
pSaH033	*bla erm bgaB-lmo0422*: T268G, T269C, C274G, T275C, C277G, T278C	upstream (SaH175, SaH176) and downstream (SaH177, SaH178) of *lmo0422* DNA binding helix into pMAD by OE-PCR
pSaH034	*bla erm bgaB* Δ*lmo0421-lmo0422*:T268G, T269C, C274G, T275C, C277G, T278C	PCR around pSaH032 (SaH176, SaH177) and DpnI digest
pSaH035	P_{help}-lacO-lmo0599 lacI neo * BackBone SEQUENCE UNCERTAIN	*lmo0599* (SaH185, SaH186) into pIMK3 by OE-PCR
pSaH036	*bla erm bgaB-lftRS* repair allel	(Hauf et al. 2019a)
pSaH037	P_{help}-lacO-lmo0599 lacI neo	*lmo0599* cut NcoI/SalI from pSaH035 and ligated into pSW25 cut NcoI/SalI

continues on next page

pSaH038	P_{lieAB}(122 bp): bp-69...-61 GTAATACAG → CATTATGTC -*lacZ neo*	P_{lieAB}upstream (SHW306, SaH188) and downstream (SaH091, SaH195) fused by PCR (SaH099, SaH172), then BamHI/EcoRI into pBP117
pSaH039	P_{lieAB}(122 bp): bp-60...-51 AATACCGGTG → TTATGGCCAC-*lacZ neo*	P_{lieAB}upstream (SHW306, SaH189) and downstream (SaH091, SaH196) fused by PCR (SaH099, SaH172), then BamHI/EcoRI into pBP117
pSaH040	P_{lieAB}(122 bp): bp-50...-41 TTACTGAGTA → AATGACTCAT -*lacZ neo*	P_{lieAB}upstream (SHW306, SaH190) and downstream (SaH091, SaH197) fused by PCR (SaH099, SaH172), then BamHI/EcoRI into pBP117
pSaH041	P_{lieAB}(122 bp): bp-40...-31 GTGGGGTTTT → CACCCCAAAA -*lacZ neo*	P_{lieAB}upstream (SHW306, SaH191) and downstream (SaH091, SaH198) fused by PCR (SaH099, SaH172), then BamHI/EcoRI into pBP117
pSaH042	P_{lieAB}(122 bp): bp-30...-21 AATAAAAAAT → TTATTTTTTA-*lacZ neo*	P_{lieAB}upstream (SHW306, SaH192) and downstream (SaH091, SaH199) fused by PCR (SaH099, SaH172), then BamHI/EcoRI into pBP117
pSaH043	*bla* P_{T7} *lacI lftR*-strep	*lftR* (SaH208, SaH209) NdeI/SalI into pSH304
pSaH044	*bla* P_{T7} *lacI lftS*-strep	*lftS* (SaH210, SaH211) NdeI/SalI into pSH304

continues on next page

pSaH045	*bla erm bgaB-lmo0599*: C145G, T146C, T147A, A151G, G152C, T145G, T155C Δ*lmo0600*	*lmo0600* US (SaH212, SaH213) and DS (SaH214, SaH215) from LMSH3 into pMAD by OE-PCR
pSaH046	*bla erm bgaB-lmo0599*: C145G, T146C, T147A, A151G, G152C, T145G, T155C Δ*lmo0601*	*lmo0601* US (SaH216, SaH217) and DS (SaH218, SaH219) from LMSH3 into pMAD by OE-PCR
pSaH047	P_{lieAB}(122 bp): G-69C, T-68A-*lacZ neo*	P_{lieAB}US (SHW306, SaH227) and DS (SaH091, SaH228) from pSaH028 fused by PCR (SHW306, SaH091), then BamHI/EcoRI into pBP117
pSaH048	P_{lieAB}(122 bp): A-67T, A-66T-*lacZ neo*	P_{lieAB}US (SHW306, SaH229) and DS (SaH091, SaH230) from pSaH028 fused by PCR (SHW306, SaH091), then BamHI/EcoRI into pBP117
pSaH049	P_{lieAB}(122 bp): T-65A, A-64T-*lacZ neo*	P_{lieAB}US (SHW306, SaH231) and DS (SaH091, SaH232) from pSaH028 fused by PCR (SHW306, SaH091), then BamHI/EcoRI into pBP117
pSaH050	P_{lieAB}(122 bp): C-63G, A-62T-*lacZ neo*	P_{lieAB}US (SHW306, SaH233) and DS (SaH091, SaH234) from pSaH028 fused by PCR (SHW306, SaH091), then BamHI/EcoRI into pBP117

continues on next page

pSaH051	P_{lieAB}(122 bp): G-61C, A-60T-*lacZ neo*	P_{lieAB}US (SHW306, SaH235) and DS (SaH091, SaH236) from pSaH028 fused by PCR (SHW306, SaH091), then BamHI/EcoRI into pBP117
pSaH052	P_{lieAB}(122 bp): A-59T, T-58A-*lacZ neo*	P_{lieAB}US (SHW306, SaH237) and DS (SaH091, SaH238) from pSaH028 fused by PCR (SHW306, SaH091), then BamHI/EcoRI into pBP117
pSaH053	P_{lieAB}(122 bp): A-57T, C-56G-*lacZ neo*	P_{lieAB}US (SHW306, SaH239) and DS (SaH091, SaH240) from pSaH028 fused by PCR (SHW306, SaH091), then BamHI/EcoRI into pBP117
pSaH054	P_{lieAB}(122 bp): C-55G, G-54C-*lacZ neo*	P_{lieAB}US (SHW306, SaH241) and DS (SaH091, SaH242) from pSaH028 fused by PCR (SHW306, SaH091), then BamHI/EcoRI into pBP117
pSaH055	P_{lieAB}(122 bp): G-53C, T-52A-*lacZ neo*	P_{lieAB}US (SHW306, SaH243) and DS (SaH091, SaH244) from pSaH028 fused by PCR (SHW306, SaH091), then BamHI/EcoRI into pBP117

continues on next page

pSaH056	P_{lieAB}(122 bp): G-51C-*lacZ neo*	P_{lieAB}US (SHW306, SaH245) and DS (SaH091, SaH246) from pSaH028 fused by PCR (SHW306, SaH091), then BamHI/EcoRI into pBP117
pSaH062	*bla erm bgaB* Δ*lmo2427-2428*	*lmo2427-2428* US (SaH259, SaH260) and DS (SaH261, SaH262) into pMAD by OE-PCR
pSaH063	P_{lftRS}(315 bp): G-51C, T-50A, A-49T, T-48A -*lacZ neo*	P_{lftRS} US (SaH079, SaH265) and DS (SaH108, SaH266) fused by PCR (SaH079, SaH108), then into pBP117 by OE-PCR
pSaH064	P_{lftRS}(315 bp): A-41T, T-40A, A-39T, C-38G-*lacZ neo*	P_{lftRS} (SaH079, SaH265) and DS (SaH108, SaH267) fused by PCR (SaH079, SaH108), then into pBP117 by OE-PCR
pSaH065	P_{lftRS}(315 bp): T-47A, A-46T, C-45G-*lacZ neo*	P_{lftRS} (SaH079, SaH265) and DS (SaH108, SaH268) fused by PCR (SaH079, SaH108), then into pBP117 by OE-PCR
pSaH066	*bla erm bgaB-lmo1071* bp:53-594-TAATAA	*lmo1071* fragment (SaH257, SaH258) into pMAD by OE-PCR
pSaH067	*bla erm bgaB -lmo2687* bp:24-730-TAATAA	*lmo2687* fragment (SaH269, SaH270) into pMAD by OE-PCR
pSaH068	*bla erm bgaB -lmo2688* bp:73-724-TAATAA	*lmo2688* fragment (SaH263, SaH264) into pMAD by OE-PCR

continues on next page

pSaH069	*bla erm bgaB-lmo0423*: T117G, A121C, A122C	*sigC* US (SaH253, SaH254) and DS (SaH255, SaH256) into pMAD by OE-PCR
pSaH070	P_{lieAB}(122 bp): G-76C, T-75A, A-74T, G-69C, T-68A, A-67T-*lacZ neo*	P_{lieAB}US (SaH172, SaH273) and DS (SaH099, SaH274) fused by PCR (SaH172, SaH099), then BamHI/EcoRI into pBP117
pSaH071	P_{lieAB}(122 bp): G-76C, T-75A, G-69C, T-68A-*lacZ neo*	P_{lieAB}US (SaH172, SaH276) and DS (SaH099, SaH280) fused by PCR (SaH172, SaH099), then BamHI/EcoRI into pBP117
pSaH072	P_{lieAB}(122 bp): A-74T, A-73T, G-69C, T-68A-*lacZ neo*	P_{lieAB}US (SaH172, SaH277) and DS (SaH099, SaH280) fused by PCR (SaH172, SaH099), then BamHI/EcoRI into pBP117
pSaH073	P_{lieAB}(122 bp): T-72A, A-71T, G-69C, T-68A-*lacZ neo*	P_{lieAB}US (SaH172, SaH278) and DS (SaH099, SaH280) fused by PCR (SaH172, SaH099), then BamHI/EcoRI into pBP117
pSaH074	P_{lieAB}(122 bp): A-70T, G-69C, T-68A-*lacZ neo*	P_{lieAB}US (SaH172, SaH279 and DS (SaH099, SaH280) fused by PCR (SaH172, SaH099), then BamHI/EcoRI into pBP117

continues on next page

pSaH077	*bla erm bgaB* Δ*lmo0420*	*lmo0420* upstream (SaH283, SaH284) and downstream (SaH285, SaH286) into pMAD by OE-PCR
pSaH078	P_{lieAB}(120 bp): G-69C, T-68A, A-57T, C-56G-*lacZ neo*	P_{lieAB}downstream from pSaH47 (SaH091, SaH240) used as primer with SHW306 to amplify modified operator from pSaH047, then BamHI/EcoRI into pBP117
pSW25	P_{help}-*lacO-mreB lacI neo*	Sabrina Wamp (*mreB* (SW53/SW54) cut NcoI/SalI into pSH207 cut NotI/PstI)
pSH207	P_{help}-*lacO-spoIIIJ lacI neo*	BamHI/SalI *spoIIIJ* fragment from pSH198 into pIMK3
pSH198	P_{help}-*spoIIIJ* neo	Dr. Sven Halbedel
pSH304	*bla* P_{T7} *lacI-divIVA*-strep	Dr. Sven Halbedel

2.3 Bacterial strains

The standard host for cloning procedures like plasmid propagation and amplification was *Escherichia coli* Top 10. All work with *L. monocytogenes* was done in the background of strain EGD-e. Table 2.3 contains all other strains used.

Table 2.3: Bacterial strains used in this study.

Name	**Genotype**	**Construction**
LMKK26	Δ*lftS*	(Kaval et al. 2015)

continues on next page

LMKK31	Δ*lftRS*	(Kaval et al. 2015)
LMKK42	Δ*lftR rsbT*^{C10T}	(Kaval et al. 2015)
LMS160	Δ*lieAB*	(Kaval et al. 2015)
LMS168	Δ*lftRS* Δ*lieAB*	(Kaval et al. 2015)
LMS169	Δ*lftR* Δ*lieAB*	(Kaval et al. 2015)
LMSH001	Δ*lmo1408 (ladR)*	pSaH001 → EGD-e
LMSH002	Δ*lmo0422 (lstR)*	pSaH003 → EGD-e
LMSH003	*lmo0599*:L49A, R51A, L52A	pSaH005 → EGD-e
LMSH005	*attB::*P$_{lieAB}$(266 bp)-*lacZ neo*	(Hauf et al. 2019a)
LMSH006	Δ*lftR rsbT*^{C10T} *attB::*P$_{lieAB}$(266 bp)-*lacZ neo*	(Hauf et al. 2019a)
LMSH007	*attB::*P$_{lftRS}$(315 bp)-*lacZ neo*	(Hauf et al. 2019a)
LMSH008	Δ*lftR rsbT*^{C10T} *attB::*P$_{lftRS}$(315 bp)-*lacZ neo*	(Hauf et al. 2019a)
LMSH009	Δ*lmo0895 (sigB)*	(Hauf et al. 2019a)
LMSH010	*attB::*P$_{lmo1409}$(347 bp)-*lacZ neo*	pSaH014 → EGD-e
LMSH011	Δ*lmo1408 (ladR) attB::*P$_{lmo1409}$(347 bp)-*lacZ neo*	pSaH014 → LMSH001
LMSH012	*attB::*P$_{lmo0423}$(315 bp)-*lacZ neo*	pSaH012 → EGD-e
LMSH013	Δ*lmo0422 (lstR) attB::*P$_{lmo0423}$(315 bp)-*lacZ neo*	pSaH012 → LMSH002
LMSH014	*attB::*P$_{lmo0599}$(201 bp)-*lacZ neo*	pSaH015 → EGD-e
LMSH015	*lmo0599*:L49A, R51A, L52A *attB::*P$_{lmo0599}$(201 bp)-*lacZ neo*	pSaH015 → LMSH003
LMSH016	*attB::aphA3 int*	(Hauf et al. 2019a)
LMSH017	*attB::*P$_{gpsB}$(237 bp)-*lacZ neo*	(Hauf et al. 2019a)
LMSH018	*attB::*P$_{divIVA}$(214 bp)-*lacZ neo*	(Hauf et al. 2019a)
LMSH024	Δ*lmo0895 (sigB) attB::*P$_{lieAB}$(266 bp)-*lacZ neo*	(Hauf et al. 2019a)
LMSH025	Δ*lmo0895 (sigB) attB::*P$_{lftRS}$(315 bp)-*lacZ neo*	(Hauf et al. 2019a)
LMSH026	Δ*lftR*	(Hauf et al. 2019a)
LMSH027	Δ*lftS attB::*P$_{lieAB}$(266 bp)-*lacZ neo*	(Hauf et al. 2019a)
LMSH028	Δ*lftS attB::*P$_{lftRS}$(315 bp)-*lacZ neo*	pSaH011 → LMKK26
LMSH030	*attB::*P$_{lieAB}$(193 bp)-*lacZ neo*	pSaH026 → EGD-e
LMSH031	*attB::*P$_{lieAB}$(152 bp)-*lacZ neo*	pSaH027 → EGD-e
LMSH032	*attB::*P$_{lieAB}$(122 bp)-*lacZ neo*	pSaH028 → EGD-e

continues on next page

LMSH033	*attB::*P_{lieAB}(97 bp)-*lacZ neo*	pSaH029 → EGD-e
LMSH034	Δ*lftR attB::*P_{lieAB}(266 bp)-*lacZ neo*	(Hauf et al. 2019a)
LMSH035	Δ*lftR* Δ*lmo0979-0980*	(Hauf et al. 2019a)
LMSH036	*attB::*P_{lieAB}(122 bp):A-104T, T-103A, G-82C, T-81A -*lacZ neo*	pSaH030 → EGD-e
LMSH037	Δ*lftS attB::*P_{lieAB}(122 bp):A-104T,T-103A,G-82C,T-81A -*lacZ neo*	pSaH030 → LMKK26
LMSH038	*attB::*P_{lieAB}(118 bp):T-78A,A-77T,G-76C,T-75A,A-74T,A-73T-*lacZ neo*	pSaH031 → EGD-e
LMSH039	*lmo0422*:T268G, T269C, C274G, T275C, C277G, T278C	pSaH033 → EGD-e
LMSH040	Δ*lmo0421, lmo0422*:T268G, T269C, C274G, T275C, C277G, T278C	pSaH034 → LMSH39
LMSH042	*lmo0599*:L49A, R51A, L52A *attB::*P_{help}-*lacO-lmo0599 lacI neo*	pSaH0037 → LMSH3
LMSH043	*lftS* revertant	(Hauf et al. 2019a)
LMSH044	*attB::*P_{lieAB}(122 bp):bp-69...-61 GTAATACAG → CATTATGTC-*lacZ neo*	pSaH038 → EGD-e
LMSH045	*attB::*P_{lieAB}(122 bp):bp-60...-51 AATACCGGTG → TTATGGCCAC-*lacZ neo*	pSaH039 → EGD-e
LMSH046	*attB::*P_{lieAB}(122 bp):bp-50...-41 TTACTGAGTA → AATGACTCAT-*lacZ neo*	pSaH040 → EGD-e
LMSH047	*attB::*P_{lieAB}(122 bp):bp-40...-31 GTGGGGTTTT → CACCCCAAAA-*lacZ neo*	pSaH041 → EGD-e
LMSH048	*attB::*P_{lieAB}(122 bp):bp-30...-21 AATAAAAAAT → TTATTTTTTA-*lacZ neo*	pSaH042 → EGD-e
LMSH049	*lftS* revertant *attB::*P_{lieAB}(266 bp)-*lacZ neo*	(Hauf et al. 2019a)
LMSH050	*lmo0599*:L49A, R51A, L52A, Δ*lmo0600*	pSaH045 → LMSH3
LMSH051	*lmo0599*:L49A, R51A, L52A, Δ*lmo0601*	pSaH046 → LMSH3
LMSH052	*attB::*P_{lieAB}(122 bp):G-69C, T-68A-*lacZ neo*	pSaH047 → EGD-e
LMSH053	*attB::*P_{lieAB}(122 bp):A-67T, A-66T-*lacZ neo*	pSaH048 → EGD-e
LMSH054	*attB::*P_{lieAB}(122 bp):T-65A, A-64T-*lacZ neo*	pSaH049 → EGD-e
LMSH055	*attB::*P_{lieAB}(122 bp):C-63G, A-62T-*lacZ neo*	pSaH050 → EGD-e
LMSH056	*attB::*P_{lieAB}(122 bp):G-61C, A-60T-*lacZ neo*	pSaH051 → EGD-e

continues on next page

LMSH057	*attB::*P_{lieAB}(122 bp):A-59T, T-58A-*lacZ neo*	pSaH052 → EGD-e
LMSH058	*attB::*P_{lieAB}(122 bp):A-57T, C-56G-*lacZ neo*	pSaH053 → EGD-e
LMSH059	*attB::*P_{lieAB}(122 bp):C-55G, G-54C-*lacZ neo*	pSaH054 → EGD-e
LMSH060	*attB::*P_{lieAB}(122 bp):G-53C, T-52A-*lacZ neo*	pSaH055 → EGD-e
LMSH061	*attB::*P_{lieAB}(122 bp):G-51C-*lacZ neo*	pSaH056 → EGD-e
LMSH063	*lmo0422*:T268G, T269C, C274G, T275C, C277G, T278C *attB::*$P_{lmo0423}$(315 bp)-*lacZ neo*	pSaH012 → LMSH39
LMSH064	Δ*lftRS attB::*P_{lieAB}(266 bp)-*lacZ neo*	(Hauf et al. 2019a)
LMSH065	Δ*lieAB attB::*P_{lieAB}(266 bp)-*lacZ neo*	(Hauf et al. 2019a)
LMSH066	Δ*lftS* Δ*lieAB*	(Hauf et al. 2019a)
LMSH067	Δ*lmo2427-2428*	pSaH062 → EGD-e
LMSH068	Δ*lmo2427-2428 lmo0422*:T268G, T269C, C274G, T275C, C277G, T278C	pSaH062 → LMSH39
LMSH069	*attB::*P_{lftRS}(315 bp):G-51C, T-50A, A-49T, T-48A -*lacZ neo*	pSaH063 → EGD-e
LMSH070	*attB::*P_{lftRS}(315 bp):A-41T, T-40A, A-39T, C-38G-*lacZ neo*	pSaH064 → EGD-e
LMSH071	*attB::*P_{lftRS}(315 bp):T-47A, A-46T, C-45G-*lacZ neo*	pSaH065 → EGD-e
LMSH072	*lmo1071::pSaH066*	pSaH066 → EGD-e
LMSH073	*lmo2687::pSaH067*	pSaH067 → EGD-e
LMSH074	*lmo2688::pSaH068*	pSaH068 → EGD-e
LMSH075	*lmo0422*:T268G, T269C, C274G, T275C, C277G, T278C *lmo1071::pSaH66*	pSaH066 → LMSH39
LMSH076	*lmo0422*:T268G, T269C, C274G, T275C, C277G, T278C *lmo2687::pSaH067*	pSaH067 → LMSH39
LMSH077	*lmo0422*:T268G, T269C, C274G, T275C, C277G, T278C *lmo2688::pSaH068*	pSaH068 → LMSH39
LMSH078	Δ*lmo2427-2428 lmo1071::pSaH066*	pSaH066 → LMSH67
LMSH079	Δ*lmo2427-2428 lmo2687::pSaH067*	pSaH067 → LMSH67
LMSH080	Δ*lmo2427-2428 lmo2688::pSaH068*	pSaH068 → LMSH67
LMSH081	Δ*lmo2427-2428 lmo0422*:T268G, T269C, C274G, T275C, C277G, T278C *lmo1071::pSaH066*	pSaH066 → LMSH68

continues on next page

LMSH082	Δ*lmo2427-2428 lmo0422*:T268G, T269C, C274G, T275C, C277G, T278C *lmo2687::pSaH067*	pSaH067 → LMSH68
LMSH083	Δ*lmo2427-2428 lmo0422*:T268G, T269C, C274G, T275C, C277G, T278C *lmo2688::pSaH068*	pSaH068 → LMSH68
LMSH088	Δ*lmo0421*	pSaH032 → EGD-e
LMSH089	*lmo0423*:T117G, A121C, A122C	pSaH069 → EGD-e
LMSH090	*lmo0423*:T117G, A121C, A122C *lmo0422*:T268G, T269C, C274G, T275C, C277G, T278C	pSaH069 → LMSH39
LMSH091	*attB::*P_{lieAB}*(120 bp)*:G-76C, T-75A, A-74T, G-69C, T-68A, A-67T-*lacZ neo*	pSaH070 → EGD-e
LMSH092	*attB::*P_{lieAB}*(120 bp)*:G-76C, T-75A, G-69C, T-68A-*lacZ neo*	pSaH071 → EGD-e
LMSH093	*attB::*P_{lieAB}*(120 bp)*:A-74T, A-73T, G-69C, T-68A-*lacZ neo*	pSaH072 → EGD-e
LMSH094	*attB::*P_{lieAB}*(120 bp)*:T-72A, A-71T, G-69C, T-68A-*lacZ neo*	pSaH073 → EGD-e
LMSH095	*attB::*P_{lieAB}*(120 bp)*:A-70T, G-69C, T-68A-*lacZ neo*	pSaH074 → EGD-e
LMSH096	*lmo0423*:T117G, A121C, A122C *attB::*P_{l}*mo*0423(315 bp)-*lacZ neo*	pSaH012 → LMSH089
LMSH097	*lmo0423*:T117G, A121C, A122C *lmo0422*:T268G, T269C, C274G, T275C, C277G, T278C *attB::*P_{l}*mo*0423(315 bp)-*lacZ neo*	pSaH012 → LMSH090
LMSH098	Δ*lftR attB::*P_{lieAB}(122 bp)-*lacZ neo*	pSaH028 → LMSH26
LMSH100	Δ*lftR attB::*P_{lftRS}(315 bp)-*lacZ neo*	pSaH011 → LMSH26
LMSH101	Δ*lftR attB::*P_{lieAB}(122 bp) G-69C, T-68A-*lacZ neo*	pSaH047 → LMSH26
LMSH102	Δ*lftR attB::*P_{lftRS}(315 bp):A-41T, T-40A, A-39T, C-38G-*lacZ neo*	pSaH064 → LMSH26
LMSH104	*lmo0599*:L49A, R51A, L52A A640221G, P_{lltR} -35 box mutation	LMSH3 cold growth suppressor
LMSH105	*lmo0599*:L49A, R51A, L52A A640869 deletion, Lmo0600 frame shift	LMSH3 cold growth suppressor
LMSH106	*lmo0599*:L49A, R51A, L52A A640758C, Lmo0600 Q45P	LMSH3 cold growth suppressor

continues on next page

LMSH107	*lmo0599*:L49A, R51A, L52A A640221G, P_{lltR} -35 box mutation	LMSH3 cold growth suppressor
LMSH108	*lmo0599*:L49A, R51A, L52A A640869 deletion, Lmo0600 frame shift	LMSH3 cold growth suppressor
LMSH109	*lmo0599*:L49A, R51A, L52A G640611T, Lmo0600 RBS mutation, LltR E104D	LMSH3 cold growth suppressor
LMSH110	*lmo0599*:L49A, R51A, L52A, Δ*lmo0601* C640782A, Lmo0600 P53Q	LMSH51 cold growth suppressor
LMSH111	*lmo0599*:L49A, R51A, L52A, Δ*lmo0601* C640871T, Lmo0600 Q83*	LMSH51 cold growth suppressor
LMSH112	*lmo0599*:L49A, R51A, L52A, Δ*lmo0601* C640757T, Lmo0600 Q45*	LMSH51 cold growth suppressor
LMSH113	*lmo0599*:L49A, R51A, L52A, Δ*lmo0601* G640346T, LltR C16F	LMSH51 cold growth suppressor
LMSH114	*lmo0599*:L49A, R51A, L52A, Δ*lmo0601* 133 bp insertion in *lmo0600*, Lmo0600 frame shift	LMSH51 cold growth suppressor
LMSH115	*lmo0599*:L49A, R51A, L52A, Δ*lmo0601* C640757T, Lmo0600 Q45*	LMSH51 cold growth suppressor
LMSH116	*lmo0599*:L49A, R51A, L52A, Δ*lmo0601* 8 bp insertion in *lmo0600*, Lmo0600 frame shift	LMSH51 cold growth suppressor
LMSH117	*lmo0599*:L49A, R51A, L52A, Δ*lmo0601* G640731A, Lmo0600 G36E	LMSH51 cold growth suppressor
LMSH118	Δ*lmo0420*	pSaH077 → EGD-e
LMSH119	Δ*lmo0420* Δ*lmo2427-2428*	pSaH062 → LMSH88
LMSH120	*attB::*P_{lieAB}*(120 bp)*:G-69C, T-68A, A-57T, C-56G-*lacZ neo*	pSaH078 → EGD-e
LMSH121	G750063A, LftR G27S	aurantimycin-resistant suppressor
LMSH122	A750155 deletion, LftR frame shift	aurantimycin-resistant suppressor
LMSH123	G749972T, P_{lftR} RBS mutation	aurantimycin-resistant suppressor
LMSH124	G750063A, LftR G27S	aurantimycin-resistant suppressor

continues on next page

LMSH125	A750080 deletion, LftR frame shift	aurantimycin-resistant suppressor
LMSH126	A750155 deletion, LftR frame shift	aurantimycin-resistant suppressor
LMSH127	A750080 deletion, LftR frame shift	aurantimycin-resistant suppressor
LMSH128	G749973T, P_{lftR} RBS mutation	aurantimycin-resistant suppressor
LMSH129	C750039T, LftR premature stop	aurantimycin-resistant suppressor
LMSH130	A750182 deletion, LftR frame shift	aurantimycin-resistant suppressor
LMSH131	A750155 deletion, LftR frame shift	aurantimycin-resistant suppressor
LMSH132	C750121T, LftR T46M	aurantimycin-resistant suppressor
LMSH133	C750062A, LftR premature stop	aurantimycin-resistant suppressor
LMSH134	A insertion after A750155, LftR frame shift	aurantimycin-resistant suppressor
LMSH135	A750080 deletion, LftR frame shift	aurantimycin-resistant suppressor
LMSH136	A749939G, P_{lftR} -10 box mutation	aurantimycin-resistant suppressor
LMSH137	T750252 deletion, LftR frame shift	aurantimycin-resistant suppressor
LMSH138	A750155 deletion, LftR frame shift	aurantimycin-resistant suppressor
LMSH139	A750155 deletion, LftR frame shift	aurantimycin-resistant suppressor
LMSH140	A750155 deletion, LftR frame shift	aurantimycin-resistant suppressor
LMSH141	Δ*lftS* G750193A, LftR G70D	LMKK26 aurantimycin suppressor
LMSH142	Δ*lftS* C750141T, LftR R53C	LMKK26 aurantimycin suppressor

continues on next page

LMSH143	Δ*lftS* C750141T, LftR R53C	LMKK26 aurantimycin suppressor
LMSH144	Δ*lftS* C750141T, LftR R53C	LMKK26 aurantimycin suppressor
LMSH145	Δ*lftS* C749998T, LftR T5I	LMKK26 aurantimycin suppressor
LMSH146	Δ*lftS* G750237T, LftR premature stop	LMKK26 aurantimycin suppressor
LMSH147	Δ*lftS* C750141T, LftR R53C	LMKK26 aurantimycin suppressor
LMSH148	Δ*lftS* C750141T, LftR R53C	LMKK26 aurantimycin suppressor
LMSH149	Δ*lftS* T750252 deletion, LftR frame shift	LMKK26 aurantimycin suppressor
LMSH150	Δ*lftS* G750253A, LftR premature stop	LMKK26 aurantimycin suppressor
LMSH151	Δ*lftS* G750165T, LftR premature stop	LMKK26 aurantimycin suppressor
LMSH152	Δ*lftS* T750252 deletion, LftR frame shift	LMKK26 aurantimycin suppressor
LMSH153	Δ*lftS* T750252 deletion, LftR frame shift	LMKK26 aurantimycin suppressor
LMSH154	Δ*lftS* G750237T, LftR premature stop	LMKK26 aurantimycin suppressor
LMSH155	Δ*lftS* C750141T, LftR R53C	LMKK26 aurantimycin suppressor
LMSH156	Δ*lftS* C750141T, LftR R53C	LMKK26 aurantimycin suppressor
LMSH157	Δ*lftS* T750252 deletion, LftR frame shift	LMKK26 aurantimycin suppressor
LMSH158	Δ*lftS* T750252 deletion, LftR frame shift	LMKK26 aurantimycin suppressor
LMSH159	Δ*lftS* C750141T, LftR R53C	LMKK26 aurantimycin suppressor
LMSH160	Δ*lftS* C750141T, LftR R53C	LMKK26 aurantimycin suppressor

continues on next page

LMSH162	Δ*lftR attB::*P_{lieAB}(120 bp):G-69C, T-68A, A-57T, C-56G-*lacZ neo*	pSaH078 → LMSH26
LMSH163	*attB::*P_{lieAB}(122 bp):A-57T, C-56G-*lacZ neo*	pSaH053 → LMSH26

2.4 DNA based work

Molecular cloning was done *in silico* with Geneious and Clone Manager software and oligonucleotides were designed using these software products. Oligonucleotides were ordered from Eurofin Genomics GmbH or Integrated DNA Technologies Inc. in lyophilized form and dissolved to 100 μM in molecular biology grade water from Carl Roth GmbH + Co. KG.

2.4.1 Preparation of genomic DNA

Genomic DNA to was extracted from overnight cultures. For use as a PCR template, 1 ml of the culture was harvested by centrifugation in a 2 ml microcentrifuge tube and the cells were resuspended in water. Around 300 mg glass beads (1 mm diameter) were then added to the suspension and the samples lysed at 30 Hz for 5 minutes using the TissueLyser II from QIAGEN. After lysis, the suspension was centrifuged at 13,000 x g for 2 minutes and the supernatant used immediately as a PCR template.

When high quality DNA was needed, a chloroform-phenol extraction was performed. For this purpose, 1 ml of an overnight culture was harvested, the cell pellet re-suspended in 400 μl of TES buffer before addition of lysozyme (10 mg/ml). The mixture was incubated at 37C for 60 minutes to lyse the cells. Afterwards, 40 μl 20 % SDS and 400 μl phenol:chloroform:isoamyl alcohol mix (25:24:1) were added and mixed vigorously. Centrifugation at 13,000 x g for 4 minutes separated phases and the upper phase was transferred into a new 1.5 ml microcentrifuge tube. Another extraction with 500 μl chloroform was performed before the DNA was precipitated from the aqueous phase by the addition of 1 ml of 100 % ethanol. The DNA was pelleted by centrifugation, washed with 70 % ethanol, air-dried and re-suspended in 100 μl molecular biology grade water.

2.4.2 PCR

Standard PCR

Standard PCR reactions for molecular cloning were done using Phusion®-High Fidelity DNA Polymerase in HF Buffer. Colony and check PCR reactions used *Taq* Polymerase in ThermoPol Buffer. Both enzymes were produced by New England Biolabs, Inc. Deoxynucleotides were ordered as a premix of 10 mM dATP, dCTP, dGTP and dTTP from Thermo Fisher Scientific. The annealing temperature was varied depending on primer melting temperature, but was 58°C for most reactions. The make-up of the PCR reactions and the standard PCR protocols for both polymerases can be found in table 2.4 and 2.5.

Table 2.4: Composition and PCR protocol for Taq PCR reactions.

***Taq* Polymerase PCR**	ThermoPol buffer	1 x
	dNTPs	0.4 mM
	Primer	0.4 μM
	Taq polymerase	0.02 U/μl
	Template less than	1 μg
***Taq* PCR Protocol**		
Initial denaturation	95°C	5 min
30 cycles of:		
Denaturation	95°C	5 sec
Annealing	58°C	5 sec
Extension	68°C	30 sec/kb
Pause	16°C	∞

Table 2.5: Composition and PCR protocol for Phusion PCR reactions.

Phusion polymerase PCR	HF buffer	1 x
	dNTPs	0.4 mM
	Primer	0.4 μM
	Phusion polymerase	0.02 U/μl
	Template less than	1 μg
Phusion PCR protocol		
Initial denaturation	95°C	5 min
30 cycles of:		
Denaturation	95°C	5 sec
Annealing	58°C	5 sec
Extension	72°C	30 sec/kb
Final extension	72°C	1 min
Pause	16°C	∞

Overlap extension PCR - OE-PCR

To join two DNA fragments using PCR or to insert a fragment into a plasmid the primers were designed in a way that an overlapping region between the two fragments or between the fragment and the plasmid backbone had a melting temperature of around 45°C. Single fragments to be joined were produced in a first round of PCR. The two fragments were used as template in a second PCR using only the outer primers to join them together.
To insert a DNA fragment into a plasmid, the plasmid was cut near the intended site of insertion using a restriction endonuclease. The plasmid and insert were then added as template to a PCR reaction without primers. The standard protocol used to insert DNA fragments into pMAD or pIMK derivatives can be found in table 2.6. 1 μl of DpnI was added to a 30 μl PCR reaction after cycling and the mix was incubated at 37°C for at least one hour. Afterwards the PCR mix (5 μl) was transformed into *E. coli* Top 10.

Table 2.6: PCR protocol for insertion of fragments into a plasmid.

PCR protocol		
Initial denaturation	95°C	15 min
30 cycles of:		
Denaturation	95°C	30 sec
Annealing	45°C	30 sec
Extension	72°C	14 min
Final extension	72°C	14 min
Pause	16°C	∞

Colony PCR

Using a sterile toothpick, material from a single colony was transferred into a well of an 8-well strip as well as onto a new agar plate. For *L. monocytogenes*, the 8-well strip was closed and placed in a microwave for 2 minutes at 900 W. For *E. coli* the microwave treatment was omitted. 20 μl PCR mix was then added and the PCR performed according to the standard protocol after an incubation for 15 minutes at 95°C.
To confirm genome modifications in *L. monocytogenes*, an 0.5 ml aliquot from an over night culture was pelleted in a 2 ml microcentrifuge tube and the supernatant was discarded. Around 500 mg 0.1 mm diameter glass beads and 750 ml sterile water were added. The samples were then placed in the Qiagen TissueLyser II and shaken for 5 minutes at 30 Hz. Afterwards samples were centrifuged for 2 minutes at 13,000 x g and 5 μl of the supernatant was used as template for a standard PCR reaction of 25 μl total volume.

2.4.3 Agarose gel electrophoresis

To check the product purity and size of PCR reactions or of plasmid digests, samples were loaded onto agarose gels containing 1 % agarose in 1x TAE buffer. Small gels (6 cm) were run at a constant voltage of 100 V and big gels (15 cm) at 150 V until a sufficient separation of the DNA fragments was achieved. For size comparison the GeneRuler 1 kb DNA Ladder from Thermo Fisher Scientific was used. After electrophoresis the DNA was stained by incubating the gels in 400 ml TAE containing 4 drops of a 5 mg/ml ethidium bromide solution for around 15 minutes. The stained DNA was visualized using a Gel Doc™XR+ Gel Documentation System from Bio-Rad Laboratories Inc.

50x TAE buffer	Tris	2 M
sterilized by filtration	acetic acid	1 M
	EDTA	50 mM
pH was adjusted to 8.3 with acetic acid. For use, the buffer was diluted to 1x.		

2.4.4 DNA purification

To purify the DNA produced after PCR or endonuclease digest, the NucleoSpin®Gel and PCR Clean-up Kit from MACHEREY-NAGEL GmbH Co. KG was used. In most cases Buffer NTI was diluted 1:1 with ddH_2O in order to prevent purification of small fragments like primers. Otherwise the manufactures protocol was followed. Elution was done with about half the original samples volume of molecular biology grade water.

2.4.5 Plasmid purification

Plasmid harboring *E. coli* were grown over night in 4 ml LB containing the appropriate antibiotic. Cells were harvested by centrifugation and the plasmid extracted with the QIAprep Spin Miniprep Kit from QIAGEN GmbH following the manufacturer's protocol. Molecular biology grade water (100 μl) was used to elute the plasmid from the column.

2.4.6 Endonuclease digestion

To check plasmids for the presence of inserts of a defined size, to create compatible ends for cloning, to linearize plasmids or to simply check for the presence of a restriction site, DNA was cut with endonucleases. One volume of DNA was mixed with the appropriate amount of enzyme and restriction buffer, as recommended by the enzyme manufacturer. The digest was incubated at the temperature recommended by the manufacturer for one hour. After the digest, the fragments produced were visualized by agarose gel electrophoresis or purified and used for cloning or PCR. All enzymes and buffers were ordered from New England Biolabs, Inc.

2.4.7 Ligation

Ligation of DNA fragments was done over night in 20 μl volume with T4 DNA Ligase from New England Biolabs. The Ligation mix was prepared following the manufactures protocol and placed in a lukewarm water bath. The water bath was covered with a lid and placed at 6°C over night. The ligation mix (5 μl) was transformed into competent *E. coli* the next day.

2.4.8 Sanger sequencing

Sanger sequencing was employed in order to confirm the DNA sequences of PCR products or plasmids. The composition of a sequencing reaction and the cycling conditions used are listed in table 2.8 and table 2.9 respectively. The BigDye™reagents were ordered from Thermo Fisher Scientific.

Table 2.8: Composition of a Sanger sequencing reaction. * The DNA amount used was varied with size of the product to be sequenced.

Composition	DNA* 1000 bp PCR product	20 ng
	or plasmid	200 ng
	Primer (10μM)	0.5 μl
	BigDye 3.1	0.5 μl
	5x ABI buffer	2 μl
	water	ad 10 μl

Table 2.9: PCR protocol for Sanger sequencing. * The annealing temperature was varied according to primer melting temperature.

PCR protocol		
Initial denaturation	96°C	2 min
25 cycles of:		
Denaturation	96°C	10 sec
Annealing*	45-60°C	5 sec
Extension	60°C	4 min
Hold	4°C	∞

2.5 RNA based work

2.5.1 Cultivation

For RNA extraction, over-night cultures were diluted to an OD_{600} of 0.05 and grown to mid-exponential phase (3 hours) at 37°C using a shaking frequency of 250 rpm. This pre-culture with all cells in the same growth stage was used to inoculate pre-warmed medium (37°C) at an OD_{600} of 0.05. Once the culture reached an OD_{600} of 0.5 $\pm$ 0.05 a volume of 25 ml was mixed with 25 ml of ice-cold killing buffer and incubated on ice for 5 min. Cells were harvested by centrifugation at 10,000 x g and 4°C for 5 min. After re-suspension of the cell pellet in 1 ml killing buffer, the cells were transferred to a microcentrifuge tube, spun down at 13,000 x g for 30 sec and stored at -80°C until RNA extraction.

Killing Buffer	Tris/HCl pH 7.5	20 mM
sterilized by filtration	$MgCl_2$	5 mM
	NaN_3	20 mM

2.5.2 RNA extraction

RNA isolation was performed using the phenol/chloroform protocol adapted from Völker et al. 1994. Here, the cell pellet was re-suspended in 1 ml lysis buffer I and incubated on ice for 5 min with 100 μg/ml lysozyme. Meanwhile, 300 μl lysis buffer III were prepared and pre-heated to 95°C in a 2 ml microcentrifuge tube. The cell suspension was centrifuged at 5000 x g and 4°C for 5 minutes. The pellet was re-suspended in lysis buffer II. The suspension in buffer II was added to pre-heated buffer III and incubated at 95°C for exactly 5 min. After this incubation 600 μl phenol:chloroform:isoamylalcohol mixture (25:24:1) was added and shaken at room temperature at 700 rpm for 5 min. The mixture was centrifuged at 13,000 x g for 5 min to separate the phases and the upper aqueous phase was transferred to a new 1.5 ml microcentrifuge tube containing 600 μl phenol:chloroform:isoamylalcohol mixture. After repeating the phenol/chloroform extraction once, the aqueous phase was transferred to a tube containing 600 μl chloroform:isoamylalcohol (25:1). After shaking vigorously, the mixture was centrifuged as before and a second chloroform purification step was performed. The remaining upper aqueous phase was then transferred to an RNase-free plastic tube. Nucleic acids were precipitated over night at -20°C using 1.5 volumes of 100 % ethanol and 0.1 volumes of

3 M sodium acetate (pH 5.2). After precipitation nucleic acids were pelleted by centrifugation at 13,000 x g and 4°C for 15 minutes. The pellet was washed once with 500 μl 70 % ethanol. After washing and another round of centrifugation at 13,000 x g and 4°C for 15 minutes the supernatant was removed completely and the pellet was left to dry at room temperature under a laminar flow hood. Dry pellets were dissolved in 100 μl RNAse-free water and kept on ice or stored at -80°C.

Lysis Buffer I	Sucrose	25 %
sterilized by filtration	Tris/HCl pH 8.0	20 mM
	NaN_3	0.25 mM
Lysis Buffer II	NaCl	200 mM
sterilized by filtration	EDTA	3 mM
Lysis Buffer III	NaCl	200 mM
sterilized by filtration	EDTA	3 mM
	SDS	1 %

2.5.3 RNA quantification

RNA concentration was measured using the Qubit RNA BR Assay Kit and the Qubit Fluorometer from Thermo Fisher Scientific following the manufacturer's instructions. Shortly, the Qubit RNA BR Reagent was diluted 1:200 in Qubit RNA BR Buffer and 198 μl mixed with 2 μl RNA sample. For the standards 190 μl working solution and 10 μl standard were used. After mixing the samples were incubated at room temperature for 2 minutes and then measured.

2.5.4 RNA gel electrophoresis

For RNA electrophoresis gels, 1.5 % agarose was dissolved in 1x MOPS buffer and 6 % formaldehyde was added once the mix cooled to 60°C. RNA was thawed on ice and 4 μg of RNA were diluted in 10μl RNase-free water plus 10 μl RNA loading dye. The mix was then incubated at 65°C for 10 minutes, before being cooled on ice for 5 minutes, loaded onto the gel and run in 1x MOPS buffer at 120 V for 1.5 hours.

10x MOPS Buffer	MOPS	200 mM
	sodium acetate	50 mM
	EDTA	10 mM
RNA Loading Dye	Formamide	65 %
	Formaldehyde	12 %
	10x MOPS	20 %
	Sucrose	2 %
	Bromophenol	0.2 %
	Xylene cyanol	0.2 %

2.5.5 Northern blotting

RNA separated in a formaldehyde agarose gel was fragmented for 2 minutes using UV illumination. The gel was then placed onto a positively charged nylon membrane and RNA blotted onto the membrane using a vacuum blotter at 55 mbar. For the first 10 minutes of blotting the gel was covered with RNA hydrolysis solution. The hydrolysis solution was then replaced with 0.1 M Tris-HCl solution at pH 7.4 for 5 minutes to neutralize the hydrolysis solution. The Tris solution was then removed and 20x SSPE was added for blotting. Blotting was done for 2.5 hours while 20x SSPE buffer was replenished when the amount on top of the gel markedly decreased. After blotting the membrane was air dried and RNA cross-linked via UV illumination for 2 minutes. To visualize rRNA the membrane was then stained with methylene blue solution for 5 minutes and de-stained three times with sterile water for 3 minutes. The methylene blue stained rRNA served as a loading control. Membranes were air-dried after de-staining and stored until mRNA detection.

RNA Hydrolysis Solution	NaOH	50 mM
	NaCl	10 mM
20x SSPE	NaCl	3 M
	NaH_2PO_4	200 mM
	EDTA	20 mM
Methylene Blue Solution	methylene blue	100 mg
	3M sodium acetate pH 5.2	13.2 ml
	glacial acetic acid	2 ml

2.5.6 Detection of specific mRNA transcripts

RNA probes

Specific RNA transcripts were detected using DIG-labelled, single stranded RNA probes around 800 bp in length (or less for smaller target genes). For this purpose, an 800 bp fragment of the gene to be detected was amplified with PCR. The primer annealing at the 3' end of the gene also contained the T7 polymerase promoter. The PCR product was purified and the RNA probe complementary to the mRNA transcript that should be detected was synthesized using the DIG Northern Starter Kit and T7 Polymerase form Roche Diagnostics GmbH. A 10-fold dilution series of the RNA probes (until 10^{-5}) was spotted (1 μl) onto nylon membrane and immobilized by UV cross linking. The efficiency of probe synthesis was evaluated following the detection procedure described in the DIG Northern Starter Kit manual. Good quality probes gave a detectable signal even if diluted 100,000-fold.

mRNA detection

Nylon membranes with cross-linked RNA were placed in a tight sealing tube and 1 ml hybridization buffer was added per 5 cm^2 of membrane. The membrane was rotating continuously during pre-hybridized at 68°C for one hour. 15 μl of the DIG labelled RNA probes were added to 5 ml hybridization buffer and the mix was incubated at 95°C for 10 minutes, cooled on ice for 2 minutes and then stored at room temperature until use. The pre-hybridization solution was discarded and the RNA probes were added to the membrane while taking care that the membrane did not fall dry. Hybridization with RNA probe was performed at 68°C over night with continuous rotation. On the next day, RNA probes were collected and frozen at -20°C for re-use. The membrane was washed twice at room temperature (5 minutes) with 1 ml 2x SSC + 0.1 % SDS per 2 cm^2 of membrane. Two more washes were performed at 68°C with 0.2x SSC + 0.1 % SDS. Afterwards, the detection of the RNA probe bound to the blot followed the detection procedure outlines in the DIG Northern Starter Kit manual.

20x SSC	NaCl	3	M
pH 7	NaCitrate	0.3	M
Hybridization Buffer	SSC	5	x
	N-Lauroylsarcosin-Na	0.1	%
	SDS	7	%
	Blocking Solution	1	%
	Formamide	50	%

2.5.7 RNA sequencing

RNA quality control

The RNA extracted was confirmed to be of high quality and not degraded before preparing sequencing libraries. To this end, a quality check on the Agilent 2100 Bioanalyzer System using the RNA 6000 Nano Kit following the manufacturer's instructions was performed. Shortly, fresh RNA 6000 Nano gel matrix was prepared (stable for about one month) and 9 μl thereof were dispensed into the matrix well. The matrix was pushed into the chip by applying pressure using the syringe with the plunger placed at 1 cm. The 9 μl matrix was also added to the two wells at the top right. Afterwards, 5 μl marker were added to all remaining wells, followed by 1 μl of the ladder or RNA sample. After mixing on the IKA vortexer for 1 minute, samples were immediately run on the Bioanalyzer. Only RNA with intact rRNA peaks was used for DNA digestion and rRNA removal.

DNA digest

Contaminating DNA was removed from RNA samples using the RNAse-Free DNase Set from Qiagen starting with 10 μg of total RNA calculated according to Qubit measurement results. The necessary amount of RNA sample was brought to a final volume of 87.5 μl using RNase-free water. Then, 10 μl Buffer RDD and 2.5 μl DNase I were added. After mixing the samples were incubated at room temperature for 10 minutes. After the DNA digest, the absence of residual DNA was tested by the amplification of a fragment of *L. monocytogenes* genomic DNA in 30 PCR cycles. The PCR reaction was separated on an agarose gel and PCR products visualized using ethidium bromide staining. Samples yielding a detectable PCR product indicating residual DNA were discarded.

Purification and removal of small RNAs

RNA was then purified using RNA Clean & Concentrator-5 from Zymo Research. Here, only large RNAs >200 nt were purified as specified in the manufacturer's protocol. Shortly, RNA Binding Buffer was diluted with pure ethanol to a final concentration of 50 %. 200 μl of the resulting buffer was added to the DNase digest and transferred to a spin column. After centrifugation at 10,000 x g for 30 seconds, 400 μl of RNA Prep Buffer were added, centrifuged as before and the flow through was discarded. The column was washed twice with RNA Wash Buffer (first 700 μl, then 400 μl). Once the final wash buffer had been discarded, the columns were dried by centrifugation at 10,000 x g for 2 minutes. RNA was eluted with 15 μl RNase-free water. After DNA digest and

purification, quality and quantity of the RNA were again determined, before proceeding to the removal of the rRNA.

rRNA removal

rRNA was removed using the Ribo-Zero®rRNA Removal Kit from Illumina using approximately 3 μg of purified RNA as the input. First, the magnetic beads were washed by adding 225 μl bead solution to a plastic tube, placing it on the magnetic stand for 2 minutes, discarding the supernatant, re-suspending the beads in 225 μl RNase-free water and then repeating the washing procedure once more. After the second wash, the beads were re-suspended in 65 μl Magnetic Bead Resuspension Solution, adding 1 μl RiboGuard RNase Inhibitor. RNA sample was then mixed with 4 μl Ribo-Zero Reaction Buffer and as much RNase-free water as necessary to get a final volume of 30 μl. To the 30 μl, 10 μl Ribo-Zero Removal Solution was added and the samples incubated for 10 minutes at 68°C followed by 5 minutes at room temperature. The 40 μl RNA sample were then added to the 65 μl magnetic beads prepared before and mixed immediately. After all samples were incubated for at least 5 minutes at room temperature, they were placed at 50°C for 10 minutes. Then, they were put on the magnetic stand for 1 minute and 85 μl of the supernatant transferred to an RNase-free plastic tube. The remaining RNA was precipitated by adding 95 μl RNase-free water, 18 μl 3 M sodium acetate, 2 μl 10 mg/ml glycogen stock, 600 μl pure ethanol and incubating over night at -20°C. On the next day, samples were centrifuged at 10,000 x g and 4°C for at least 30 minutes and washed twice with freshly prepared 70 % ethanol. Each wash was followed by a 5 minute centrifugation at 10,000 x g and 4°C. After the ethanol had been removed, the samples were completely dried under a laminar flow hood.

Library preparation

For Illumina library preparation the TruSeq®Stranded mRNA Kit was used. The protocol (TruSeq®) started with the addition of 19.5 μl Fragment Prime Finish Mix to the RNA pellet obtained after rRNA removal and precipitation (see above). The samples were then transferred to PCR tubes and incubated at 98°C for 8 minutes, before being cooled to 4°C. A 17 μl aliquot of the sample was transferred to a new PCR tube. First Strand Synthesis Act D mix was prepared by adding 1 μl Superscript II to 9 μl First Strand Synthesis Act D stock. An 8 μl aliquot of the First Strand Synthesis Act D mix was added to the 17 μl RNA sample. The first strand was synthesized by incubation at 25°C for 10 minutes followed by 42°C for 15 minutes, 70°C for 15 minutes and 4°C hold. The second strand was synthesized by first adding 5 μl Resuspension Buffer to each sample and then adding 20 μl Second Strand Marking Mix. The mixture was incubated at 16°C for 1 hour. A 50 μl aliquot of the transcribed DNA was added to a new plastic tube and purified by adding 90 μl AMPure XP beads. The mix was incubated for 15 minutes at room temperature and

then placed on a magnetic stand for 5 minutes. Of the supernatant 135 µl was removed and 200 µl 80 % ethanol added. Following a 30 second incubation, all supernatant was removed and 80 % ethanol added again. Once the last ethanol had been removed, the samples were left to dry (until cracks in the pellet appeared). To dissolve the DNA, 17.5 µl Resuspension Buffer was added. The beads were re-suspended and then pelleted again on the magnetic stand. Of the supernatant 15 µl were transferred to a new PCR tube. Then, 2.5 µl Resuspension Buffer and 12.5 µl A-Tailing Mix were added. The samples were then incubated at 37°C for 30 minutes, followed by 70°C for 5 minutes and 4°C on hold. Afterwards, 2.5 µl Resuspension Buffer, 2.5 µl Ligation Mix and 2.5 µl of the desired adapter were added. The mix was incubated for 10 minutes at 30°C, before 5 µl Stop Ligation Buffer were added. Now, the samples were purified two times using AMPure XP beads again. To the 42.5 µl sample 42 µl AMPure XP beads were added. The mix was incubated for 15 minutes at room temperature and then placed on a magnetic stand for 5 minutes. Of the supernatant 79.5 µl was removed and 200 µl 80 % ethanol added. Following a 30 second incubation, all supernatant was removed and 80 % ethanol added again. Once the last ethanol had been removed, the samples were left to dry (until cracks in the pellet appeared). To dissolve the library fragments, the beads were re-suspended in 52.5 µl Resuspension Buffer and then pelleted again on the magnetic stand. Of the supernatant, 50 µl was transferred to a new plastic tube and 50 µl AMPure XP beads added again. The mix was incubated for 15 minutes at room temperature and then placed on a magnetic stand for 5 minutes. Of the supernatant 95 µl was removed and 200 µl 80 % ethanol added. Following a 30 second incubation, all supernatant was removed and 80 % ethanol added again. Once the last ethanol had been removed, the samples were left to dry (until cracks in the pellet appeared). To dissolve the library fragments, the beads were re-suspended in 22.5 µl Resuspension Buffer and then pelleted again on the magnetic stand. Of the supernatant, 20 µl was amplified by PCR. For this purpose, 5 µl Primer Cocktail and 25 µl PCR Master Mix were added to the 20 µl samples. A PCR for 12 to 15 cycles, depending on initial RNA input, was sufficient to have a good concentration of the final library.

Table 2.15: PCR protocol for the library amplification PCR.

PCR Protocol			
Initial denaturation	98°C	30	sec
12-15 cycles of:			
Denaturation	98°C	10	sec
Annealing	60°C	30	sec
extension	72°C	30	sec
Final extension	72°C	5	min
Pause	4°C	∞	

After the PCR, the library was purified using 50 μl AMPure XP beads. After incubation for 15 minutes at room temperature, the mix was placed on a magnetic stand for 5 minutes. Of the supernatant 95 μl was removed and 200 μl 80 % ethanol added. Following a 30 second incubation, all supernatant was removed and 80 % ethanol added again. Once the last ethanol had been removed, the samples were left to dry (until cracks in the pellet appeared). To dissolve the library fragments, the beads were re-suspended in 32.5 μl Resuspension Buffer and then pelleted again on the magnetic stand. Of the supernatant, 30 μl was transferred to a new plastic tube and stored at -20°C until further analysis.

Library quality control

The quality of the produced DNA libraries was assessed using the Agilent 2100 Bioanalyzer System with the DNA 120000 Kit. After preparation of the chip according to the manufacturer's instruction 1 μl of the library was loaded and analysed. The presence of the typical library peak with a size of approximately 300 base pairs indicated a good quality library. The library concentration was determined using the Qubit dsDNA HS Assay. Here, the Qubit dsDNA HS Reagent was diluted 1:200 in Qubit dsDNA HS Buffer. Of the working solution 190 μl were transferred to plastic tubes and 10 μl standard or sample added. After mixing, the samples were incubated at room temperature for 2 minutes and then measured. Common library yields were around 200 nM.

Sequencing

Sequencing of the libraries was performed on the Illumina Miseq in paired-end mode (2 times 76 bp) with v3 chemistry. The pooling of 4-5 samples per run gave a sufficient coverage to estimate differential expression. Pooling was performed according to Illuminas "TruSeq Library Prep Pooling Guide".

Transcriptomic analysis

The quality of the sequencing data was assessed using fastqc and quantification of mRNA transcripts against the *L. monocytogenes* EGD-e cDNA (EMBL-EBI 2018) downloaded via the ensemblgenomes ftp server (Kersey et al. 2018) and was done using the Salmon0.8.2 software (Patro et al. 2017). The differential expression ratio was determined as the ration of average expression from three biological replicates in the mutant compared to the wild type. Transcript counts from three biological replicates were Log2-transformed (to normalize for strongly deviating expression across the replicates) and used to calculate *P* values using Students t-test. The following criteria were used to select genes with significant differential expression:

- an expression level of at least 10 TPM
- a *P* value less than 0.01
- an absolute differential expression factor of more than 2

2.6 Protein based work

2.6.1 Protein over-expression and purification

Proteins were overproduced in *E. coli* BL21 cells carrying a plasmid with an IPTG inducible version of the protein of interest linked to a Strep-Tag®. The required antibiotic was always added to the cultures to prevent loss of the plasmid. An over night culture was used to inoculate 500 ml medium at an OD_{600} of 0.05. After reaching an OD_{600} of 0.5 at 37°C, protein expression was induced by addition of 1 mM IPTG. 2 hours after induction, the culture was harvested by centrifugation and the cells were re-suspended in ZAP buffer (12 ml) containing 1 mM PMSF. Cells were sonified at 40 % power output on ice (three times 30 seconds). Afterwards the cell suspension was passed three times through the EmulsiFlex C3 from Avestin Europe GmbH. Cell debris was removed by centrifugation for 30 minutes at 10,000 g.
The strep-tag®containing protein was then purified from the lysate using 1 ml strep-tactin®superflow from IBA GmbH in chromatography columns from Bio-Rad Laboratories GmbH. Strep-tactin®was added to the columns and equilibrated with 2 ml Buffer W. Afterwards, the cell lysate was added to bind the tagged protein. Unbound proteins were removed by washing 5 times with Buffer W. The specifically bound protein was eluted in 6 fractions with 0.5 ml Buffer E and stored at -20°C.

ZAP Buffer	Tris-HCl pH7.5	50 mM
	NaCl	200 mM
	EDTA	20 mM
Buffer W	Tris-HCl pH8.0	100 mM
	NaCl	150 mM
	EDTA	1 mM
Buffer E	Tris-HCl pH8.0	100 mM
	NaCl	150 mM
	Desthiobiotin	2.5 mM

2.6.2 Isolation of cellular proteins

20 ml medium were inoculated at an OD_{600} of 0.05 with cells from an over night culture. They were grown until the desired growth phase was reached. Cells were usually harvested (centrifugation at 6,000 g, 4°C, 10 minutes) in late exponential phase around an OD_{600} of 1. The cell pellet was washed once in ZAP buffer and re-suspended in 1 ml ZAP supplemented with 1 mM PMSF to inhibit protein degradation by proteases. The cell suspension was then transferred to a 15 ml tube and sonicated on ice for 10 minutes at 40 % power output. The lysate was transferred into a microcentrifuge tube and cell debris was removed by centrifugation at 13,000 x g for one minute at 4°C. The supernatant was transferred into a new microcentrifuge tube and the centrifugation repeated. The solution obtained after this second centrifugation was considered to be the total cellular protein extract.

2.6.3 Quantification of protein concentrations

To determine the protein concentration of solutions, Roti®-Nanoquant solution by Carl Roth GmbH + Co. KG was used following the manufacturer's instructions.

2.6.4 ONPG β-galactosidase assay

To quantify β-galactosidase activity in *L. monocytogenes*, the respective strains were grown over night and then re-inoculated at on OD_{600} of 0.05 into 5 ml fresh BHI broth containing inducer substances where applicable. The culture was incubated at 37°C (250rpm) for around 3 hours or until reaching an OD_{600} of 0.5 ± 0.1. Cells were harvested by centrifugation at 6500 x g for 5 minutes, re-suspended in 600 μl ddH_2O and transferred to a 2 ml micro centrifuge tube. Cells were pelleted at 13000 x g speed for 30 seconds and re-suspended in 1200 μl Z-Buffer. Afterwards, the samples were lysed by sonification at 40 % power output for 10 minutes. Debris was removed from the lysates by centrifugation at 13000 x g for 2 min. The protein concentration was then determined using 50 μl sample aliquots and 950 μl Roti®-Nanoquant working solution. Otherwise the manufacturer's instructions were followed. 1000 μl of Z-Buffer and of the samples (diluted where necessary due to high β-galactosidase activity) were transferred to a new 2 ml micro centrifuge tube and incubated at 30°C for 10 min. 200 μl of a 4 mg/ml ONPG

solution (dissolved in Z-Buffer without 2-mercaptoethanol) were then added to all samples and a timer started. Once the first sample turned distinctly yellow, the reaction was stopped by addition of 500 μl 1M $NaCO_3$, the time noted and the sample OD_{600} at 420 nm measured against the Z-Buffer blank. β-galactosidase activity in Miller Units (MU) was calculated according to equation 2.1.

5x Z-Buffer	Na_2HPO_4	60 mM
	NaH_2PO_4	40 mM
	KCl	10 mM
	$MgSO_4$	1 mM

The pH was adjusted to 7 with NaOH (10 M) and the buffer sterilized by autoclaving. Before use, it was diluted to 1x and 0.15 % (v/v) 2-mercaptoethanol were added.

$$1MU = 1000 * \frac{OD_{420}}{t * c_{protein}} \tag{2.1}$$

t = time in [minutes]
$c_{protein}$ = Protein concentration [μg/μl]

2.7 Microbiology

2.7.1 Cultivation

Bacteria were grown on agar plates and stored at 6°C for up to one month. For longer periods, bacteria were stored at -80°C in 25% glycerol. Standard cultivation of all bacterial strains was done at 37°C and 250 rpm for liquid cultures. As a standard measure of growth, the optical density (OD) of liquid cultures at 600 nm was measured using a Beckman Coulter DU 720 Spectrophotometer.

Media and antibiotics

E. coli was cultivated on LB medium or agar (1.5 % agar) using ampicillin (100 μg/ml) or kanamycin (50 μg/ml) to select clones carrying resistance genes.
L. monocytogenes was cultivated in BHI medium or agar (1.5 % agar) using erythromycin (5 μg/ml) or kanamycin (50 μg/ml) to select clones carrying resistance genes.

X-Gal was added to the medium at 100 μg/ml to monitor for β-galactosidase activity. IPTG was used at a final concentration of 1 mM to induce expression from the *lac* operator.

2.7.2 Genetic engineering

Manipulation of *E. coli*

To prepare chemically competent *E. coli* cells, an over night culture was diluted 1:100 in 40 ml fresh medium and grown for 3 hours at 37°C with shaking at 250 rpm. Cells were then collected by centrifugation (5,000 x g for 10 minutes at 4°C), re-suspended in 12.5 ml ice-cold 0.1 M $CaCl_2$ and incubated on ice for at least 30 minutes. The cells were then pelleted at 5,000 x g for 5 minutes at 4°C and re-suspended in 1 ml 0.1 M $CaCl_2$. Glycerol was added to a final concentration of 8 % and aliquots were stored at - 80°C until use.

Chemically competent cells were thawed on ice and 100 μl of this cell suspension were added to a microcentrifuge tube containing DNA to be transformed (e.g. one μl plasmid DNA or 5 μl PCR reaction or ligation). Cells and DNA were mixed by flicking the tube and then incubated on ice for at least 30 minutes. The cells were then heat shocked for one minute at 42°C in a water bath and immediately afterwards placed on ice again for at least 3 minutes. Room temperature LB was added to the cells after the incubation on ice and the tubes were placed at 37°C with shaking at 250 rpm. After one hour at 37°C, the cells were pelleted at 13,000 x g for 1 minute and plated on LB containing the necessary antibiotic(s) and X-Gal when needed.

Manipulation of *L. monocytogenes*

In order to prepare *L. monocytogenes* for electroporation, an over night culture was diluted 1:50 in 40 ml BHI and grown for 3 hours at 37°C with shaking at 250 rpm. Then, ampicillin was added at a final concentration of 100 μg/ml and the cells were incubated for another 2 hours at 37°C with shaking at 250 rpm. Cells were harvested by centrifugation at 6,500 x g for 5 minutes and washed twice in 15 ml SGWB. After the last wash step, the cells were re-suspended in 10 ml SGWB and lysozyme was added (final concentration of 10 μg/ml). The cells were incubated for 20 to 30 minutes at 37°C with shaking at 250 rpm and then pelleted a last time (at 5,000 x g for 10 minutes) before being re-suspended in 1 ml SGWB and stored at -80°C until use.

SGWB	Glycerol	50 %
sterilized by filtration	Sucrose	500 mM
pH was adjusted to 7 with 100 m	M NaOH.	

80 μl electrocompetent *L. monocytogenes* suspension was added to a microcentrifuge tube containing approximately 1 μg precipitated plasmid DNA and mixed shortly by pipetting. 75 μl of the cells were then transferred to a 2 mm electroporation cuvette and pulsed at 25 μF, 200 Ω and 2,400 V. Afterwards, 1 ml of room temperature BHI was added and the cells incubated for 1 hour at 37°C for pIMK derivatives or for 1.5 hours at 30°C for pMAD derivatives before being plated on BHI agar containing the necessary antibiotics and X-Gal or IPTG when necessary.

To modify genome sections in *L. monocytogenes* the vector pMAD was used (Arnaud et al. 2004). After transformation with a vector carrying a 300 to 800 bp sized region of homology to the genome of *L. monocytogenes*, transformants were grown at 30°C for 3 days on plates containing erythromycin and X-Gal. Single colonies were then streaked onto new erythromycin, X-Gal plates and incubated at 42°C for two days to integrate the plasmid into the genome. 3 to 5 single, blue colonies were then used to inoculate 3 ml BHI and incubated at 30°C for 2 hours and 42°C for 4 hours afterwards before a dilution series to 10^{-5} was plated on BHI + X-Gal plates. After 2 days at 42°C, white colonies were picked, checked for the desired modification by PCR and transferred to a new BHI + X-Gal and a BHI + X-Gal + erythromycin plate at 37°C. Once loss of plasmid was proven by inability to grow on erythromycin and white color of the colonies, clones with the desired modification -according to PCR results- were streaked to single colonies, one colony used to inoculate an over night culture for permanent storage and material from this final culture was also used to proof the desired modifications and loss of plasmid by PCR.

2.7.3 Disc diffusion assay

The growth inhibition of different substances was tested by measuring the zone of inhibition around a filter disc soaked with a solution of the inhibitor. To do so, fresh BHI agar plates were inoculated with material from an over night culture by dipping a sterile collection swap into the culture and streaking the material onto the surface of the agar plate in three directions. Plates were shortly dried after being inoculated. During the drying period, Whatman™ paper disc 6 mm in diameter were prepared with the rough side facing down. Then 10 μl of a solution of the substance to be tested were spotted onto the discs, which were then placed (rough side down) onto the prepared agar plates in

triplicate. The diameter of the inhibition zone was measured after over night incubation at 37°C.

2.7.4 Growth curves

Manual Growth Curves
For manual measurement of bacterial growth, 20 ml medium were inoculated at an OD_{600} of 0.05 and incubated at the specified temperature. For cultivations at 30, 37 and 42°C samples were shaken at 250 rpm in New Brunswick™Innova®42 or 43 incubators and OD_{600} measured every hour in a Beckman Coulter DU 720 Spectrophotometer. Cultivation at 6°C was performed statically and the OD measured every 24 hours after vortexing of the samples.

Automatic Growth Curves
Automatic OD measurement during the course of batch growth was performed using the Multiskan Sky or Multiskan Go Microplate Spectrophotometer from Thermo Fisher Scientific. A 96 well plate containing 100 μl medium (including inhibitory substances of twice the concentration to be tested where applicable) was prepared and cells from an over night culture were diluted in fresh medium to an OD_{600} of 0.1. 100 μl of this dilution was added to the 100 μl medium prepared in the 96 well plate. The plate was incubated at 37°C with shaking at high frequency for 10 seconds followed by a pause of 20 to 50 seconds. OD_{600} was read every 5 or 15 minutes for 24 hours.

2.7.5 Lysozyme mediated lysis

In order to determine the susceptibility to lysozyme, an over night culture was used to inoculate a 20 ml culture. The cells were grown from OD_{600} 0.05 to mid-exponential phase and then harvested at 6,000 x g for 5 minutes. The pellet was re-suspended in the volume of 50 mM Tris-HCl, pH 8.0 necessary to get an OD_{600} of 0.8. From the re-suspension 6 ml was transferred to a new tube and 2.5 μg/ml lysozyme were added. The mix was incubated at 37°C with shaking at 250 rpm while measuring the OD_{600} every 15 minutes.

2.7.6 Agar plate based screen for *lacZ* induction

To screen substances for the induction of promoter-*lacZ* fusions 1 volume of BHI broth was mixed with $1/1000$ volume of an over night culture of the bacteria and $1/500$ volume of X-Gal stock solution (50 mg/ml). To this mix 1 volume hot molten 1.5 % BHI Agar was added, shortly but vigorously mixed and the plates poured immediately afterwards. After solidification of the plates, 1 μl of a solution of the substance to be tested (usually 1 mM concentration) was spotted onto the surface and left to dry. After drying, the plates were incubated over night at 37°C and inspected for blue coloration indicating induction of the promoter-*lacZ* fusion. A total of 681 substances tested (at 1 mM in DMSO) were part of the DZIF (German Centre for Infection Research) Natural Compound Library. It contained secondary metabolites from streptomycetes (340 substances), myxobacteria (253 substances) and fungi (88 substances), collected during screens at the University of Tübingen, the HIPS (Helmholtz Institute for Pharmaceutical Research Saarland) and the HZI (Helmholtz Centre for Infection Research). The compounds were stored at 10 mM in DMSO and dispensed as 1 mM solutions into 96 well plates using the STARlet liquid handling system (Hamilton Robotics). The substances were randomized and encrypted by a barcode system for non-biased screening.

2.7.7 MIC determination - broth dilution

To determine the MIC, BHI medium containing twice the concentration of antibiotic to be tested was prepared and 100 μl aliquots thereof added to a 96 well flat bottom plate. All antibiotics were tested in geometric dilution series spanning the expected MIC range. Strains were grown over night and then diluted to OD_{600} 0.1 before 100 μl of this inoculum was added to the antibiotic containing medium prepared in the 96 well plate. Plates were either incubated at 37°C in the Multiskan Sky or Multiskan Go Microplate Spectrophotometer from Thermo Fisher Scientific with automatic OD_{600} measurement (see Automatic Growth Curves) or incubated statically at 37°C for 18 to 24 hours, followed by OD_{600} measurement in a Tecan Sunrise Plate reader. MIC was determined to be the highest concentration of the antibiotic where the OD did not increase more than two-fold after 24 hours.

2.7.8 Lysis by aurantimycin

20 ml BHI broth were inoculated at an OD_{600} of 0.05 and incubated at 37°C with shaking at 250 rpm until an OD_{600} of 0.5 $\pm$ 0.1 was reached. After harvest by centrifugation, the cells were re-suspended in enough 50 mM Tris pH 8.0 for the OD_{600} to be around 2. 100 μl of this cell suspension were added to a 96 well plate containing 100 μl 50 mM Tris pH 8.0 with aurantimycin A (at a final concentration of 2 mg/ml), where applicable. To energize the cells, 2.5 g/l glucose was added when indicated. The lysis of cells was monitored at 37°C by measuring OD_{600} in 5 minute intervals using the Multiskan Go Microplate Spectrophotometer from Thermo Fisher Scientific.

2.7.9 Selection of aurantimycin-resistant suppressors

To select for aurantimycin-resistant suppressor mutants, the wild type and the Δ*lftS* mutant were each inoculated into 40 wells of a 96 well plate and grown in the Multiskan Go Microplate Spectrophotometer at 37°C for 24 hours. The medium contained a final aurantimycin concentration of 750 ng/ml. For each strain, cells from 20 different wells were then streaked to single colonies on BHI agar. Single colonies were picked, grown over night in liquid culture. An aliquot of the liquid culture was stored at -80°C. Aurantimycin-resistance of the suppressors was confirmed by monitoring the OD_{600} in a MIC assay (see section on MIC determination - broth dilution) using the Multiskan Go Microplate Spectrophotometer from Thermo Fisher Scientific.

2.7.10 Selection of lltR* cold growth suppressors

Δ*lltR* and and *lltR** Δ*lmo0601* strains grown on BHI agar at 6°C for at least 3 months formed big colonies on a background of weak growth. These big colonies were picked and streaked to single colonies, before being grown in liquid BHI at 37°C. An aliquot of the liquid culture was preserved at -80°C. The growth phenotype at 6°C was confirmed on BHI agar using the parental strains as controls.

2.7.11 Scanning or transmission electron microscopy

Electron microscopy was performed by Lars Möller and Gudrun Holland at the RKI in Berlin. Strains were grown to mid-exponential phase under standard conditions. A 10 ml culture was harvested at 4629 x g for 2 minutes and re-suspended in 1 ml fixative (2.5 % glutaraldehyde and 1 % formaldehyde in 0.05 M HEPES buffer). After a two hour incubation at room temperature, the samples were stored at 4°C until analysis.

Chapter 3

Results

3.1 The regulons of the PadR-like repressors as determined by RNA sequencing

The first step in determining the function of the PadR-like repressors in *L. monocytogenes* was to determine the genes they regulate. In order to characterize the regulons of the PadR-like transcription factors, mutants in each individual PadR-like repressor were constructed using the pMAD plasmid system (Arnaud et al. 2004). The clean deletion mutant for *lftR* was constructed perviously (Kaval et al. 2015). Clean deletion mutants for *ladR* (Δ*lmo1408*, strain LMSH1) and *lstR* (Δ*lmo0422*, strain LMSH2) were obtained, but all attempts to delete *lltR* (*lmo0599*) failed, because the plasmids were unstable in *E. coli* (data not shown). As a result, instead of generating a deletion mutant, the *lltR* gene was cloned into pMAD and three conserved amino acids in the DNA binding helix mutated. The mutations introduced were L49A, R51A, L52A and the resulting strain was named LMSH3. It will be referred to as the *lltR** mutant. The conserved lysine in position 49 (see figure 1.4) has previously been shown to be very important for DNA binding, so the mutation of this amino acid alone should be sufficient to abrogate DNA binding by LltR (Park et al. 2017).

The transcriptomes of the mutants and the wild type were determined using RNA sequencing. This technique allows the quantification of mRNA transcripts so that the transcript abundances in the mutants can be compared to the wild type. All strains were grown under standard conditions until the mid-exponential phase, quenched in ice-cold buffer and then harvested by centrifugation. The RNA was extracted using a chloroform-phenol based method, because this protocol was easily scalable to obtain large amounts of high quality RNA. The large RNA amounts obtained (around 50 μg per 25 ml bac-

terial culture) might not be needed for RNA sequencing, but are essential for Northern blotting procedures. Other column-based extraction procedures gave significantly lower yields. Residual DNA and RNAs smaller than 200 nucleotides were removed to enrich the mRNA transcripts. Further, the bacterial rRNA was removed by hybridization to homologous sequences immobilized on magnetic beads. The RNA library was prepared from the enriched mRNA following the Illumina protocol (see methods section).

To identify the ideal sequencing depth for listerial samples, the number of samples per Illumina MiSeq run was gradually increased in the RNA sequencing experiments. Table 3.1 lists the sequencing runs, samples analysed and the amount of data obtained in each experiment.

Table 3.1: RNA sequencing runs. Information on the RNA sequencing runs, the samples analysed and the number of raw reads obtained.

Sequencing Run	**Samples Analysed**	**Million Reads per sample**	**Total Reads per run**
Run 1	EGD-e replicate 1	22.2	39.0 M
	LMKK42 (Δ*lftR rsbT*^{C10T}) replicate 1	16.8	
Run 2	EGD-e replicate 2	11.2	38.4 M
	LMKK42 (Δ*lftR rsbT*^{C10T}) replicate 2	10.4	
	EGD-e replicate 3	10.7	
	LMKK42 (Δ*lftR rsbT*^{C10T}) replicate 3	6.08	
Run 3	EGD-e replicate 4	8.01	29.3 M
	LMSH1 (Δ*ladR*) replicate 1	9.27	
	LMSH2 (Δ*lstR*) replicate 1	6.08	
	LMSH3 (*lltR**) replicate 1	5.91	
Run 4	EGD-e replicate 5	2.48	23.2 M
	LMSH1 (Δ*ladR*) replicate 2	3.18	
	LMSH2 (Δ*lstR*) replicate 2	2.85	
	LMSH3 (*lltR**) replicate 2	3.21	
	EGD-e replicate 6	3.02	
	LMSH1 (Δ*ladR*) replicate 3	3.04	
	LMSH2 (Δ*lstR*) replicate 3	2.67	
	LMSH3 (*lltR**) replicate 3	2.73	

Eight parallel samples were analysed in run number 4, still yielding sufficient sequencing reads to reliably detect differential gene expression. Therefore, up to 8 samples could be analysed in one run.

3.1.1 RNA sequencing data exploration and cut-off definition for weakly expressed genes

The genes significantly regulated should be identified by comparing mutant transcript counts to those of the wild type. After initial quality checks for Illumina sequencing data (not shown), the number of transcripts (TPM - transcripts per million sequenced bases) for all annotated *L. monocytogenes* genes was quantified using the quasi-mapping approach implemented in the software Salmon (Patro et al. 2017). Other quantification methods like mapping of the reads (using Geneious, Star or bowtie), followed by quantifications and differential expression analysis (using again Geneious or edgeR) or analysis using Rockhopper were not chosen after an initial assessment (data not shown), because they required more computing power while yielding the same results or results that were more difficult to interpret due to the implemented statistics.

Genes that are regulated by the PadR-like repressors should be expressed at a higher level in the mutants lacking these transcription factors. To gain a first impression of the transcriptomic changes, the number of transcripts detected in the mutant (TPM values) can be plotted against the TPM values of the wild type (see top row in figure 3.1). The three replicates are represented by black, red and blue points, respectively. These plots revealed that the data are highly skewed. Some strongly expressed genes dominate the plot, while most genes have a relatively low expression level and cluster in the lower left part of the plots (see figure 3.1 upper row). For the Δ*lftR* and Δ*lstR* mutants, some genes seem to be differentially expressed, because much higher TPM values are detected in the mutant than in the wild type as indicated by the cluster of points located above the diagonal.

Logarithmic transformation is one way to reduce the skewness of the data (Zwiener et al. 2014). Log transformation of the x axis spreads the genes more evenly across the plot (see figure 3.1 middle row). In these plots, genes with higher expression in the mutant separate more clearly from the the other genes that are expressed at identical levels in the mutant and the wild type. Still, genes that are strongly expressed in the wild type (right margin of the plots) show a high variation in expression between different replicates.

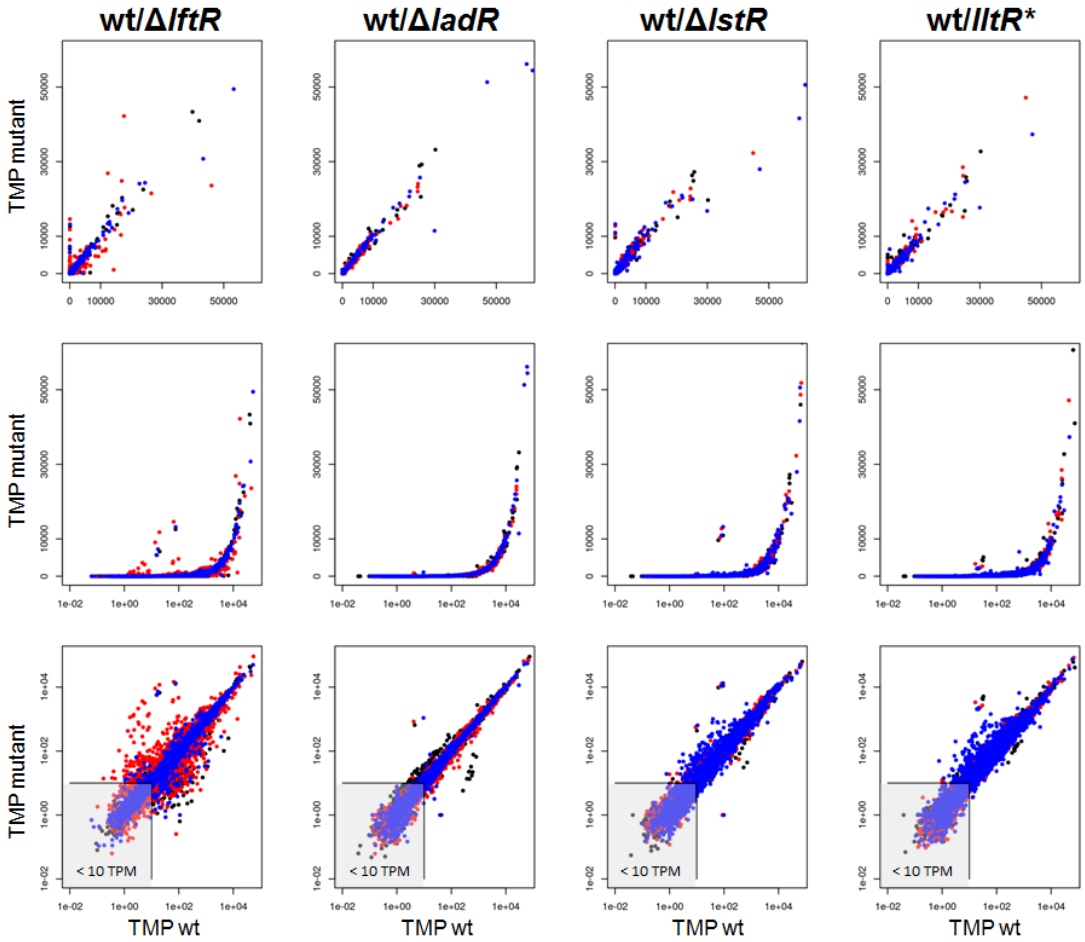

Figure 3.1: TPM/TMP plots comparing *padR* mutants and the wild-type. Plotting of the transcript number (TPM) detected for each gene in the Δ*lftR* (LMKK42), Δ*ladR* (LMSH1), Δ*lstR* (LMSH2) and *lltR** (LMSH3) mutants (y axis) versus the transcript number in the wild type (x axis). The three replicates are shown in black, red and blue color. The gray shaded area indicates points excluded from analysis, because they lie below the minimum 10 TPM cut-off. Note that the axis scales vary from all linear (top), over x axis logarithmic (middle), to both axes logarithmic (bottom).

The remaining skewness can be removed by also scaling the y axis logarithmically. The resulting double logarithmic graphs for the RNA-sequencing data show clusters of genes that are up-regulated in all three replicates (black, red and blue points are present in the cluster) for all four repressors (see figure 3.1 bottom row). The log transformation was therefore also used in further analysis. From the Δ*ladR* plot it can also be seen, that the differences between replicates increase significantly for genes with low expression levels (increasing spread of the points on the bottom left). This random variation is the reason, why weakly expressed genes are usually excluded from RNA sequencing analysis (Łabaj

and Kreil 2016). In this work a cut-off value of 10 TPM was chosen for further analysis. This cut-off is shown by the lines in the plots on the bottom. Points falling into this bottom left region, highlighted in gray, fail to meet the cut-off criterion and are excluded from the analysis.

A standard measure for differentially expressed genes is the differential expression ratio. This ratio is shown in figure 3.2 for all mutant/wild type combinations. The graphs show the differential expression ratios for all genes in each of the three replicates. The area shaded gray indicates the zone in which genes failed to meet the minimum 2-fold difference between mutant and wild type and/or the minimum detection level of 10 TPM (see previous section). For all PadR-type repressors, a small cluster of genes that are highly up-regulated (around 100-fold) in all three replicates (presence of black, red and blue points) can be seen around the middle of the x axis. This data suggests that these genes are specifically negatively regulated by the respective repressor. Genes up- or down-regulated in only one replicate can for example be found in the case of the wt/Δ*lftR* (red dots) or the wt/Δ*ladR* comparison (black dots, figure 3.2). Such effects cannot be based on the proteins investigated and represent outliers, because they were found in only one replicate.

When comparing the wt/Δ*lftR* plot to the others, a striking difference is a cloud of down-regulated genes that was not found for the other regulators (see figure 3.2). The next sections will take a closer look at the up and down-regulated genes for each repressor by also looking at statistically significant differences. The statistical significance was determined using a t-test on the log transformed count data from the three replicates (see Materials and Methods).

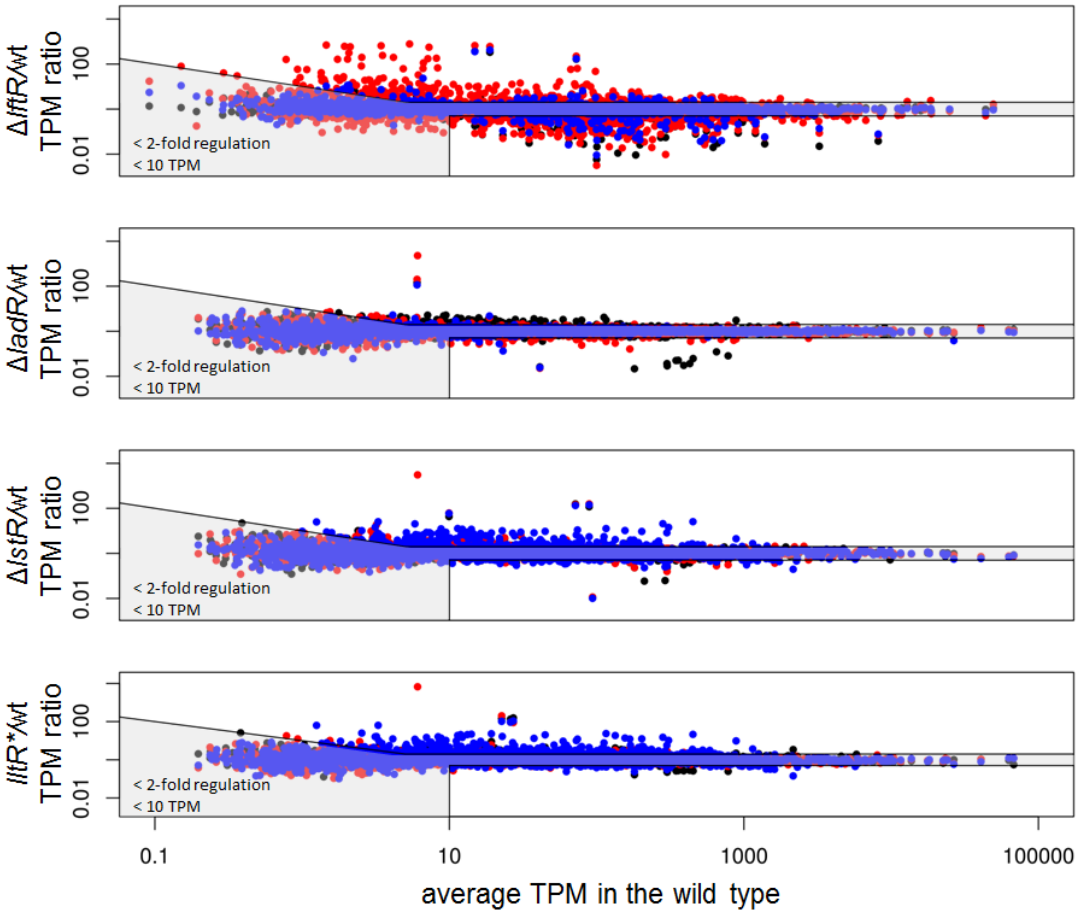

Figure 3.2: Differential expression ratios comparing *padR* mutants and the wild type. for all genes in the Δ*liftR* (LMKK42), Δ*ladR* (LMSH1), Δ*lstR* (LMSH2) and *lltR** (LMSH3) mutants. The genes were ordered according to the average expression in the wild type. The three replicates are indicated by black, red and blue points. The black lines indicate the threshold to be crossed for genes to be considered up- or down-regulated based on a minimum 2-fold ratio between mutant and wild type, as well as a minimum count of 10 TPM.

3.1.2 Genes differentially expressed in the Δ*lftR* mutant

Instead of only looking at genes that were strongly regulated, all genes that can be said to be statistically significantly regulated were determined next. As a measure of statistical significance, *P*-values comparing wild type and mutant expression levels were calculated using Student's t-test. The statistical significance level was chosen to be 1 %. The Δ*lftR* mutant (LMKK42) did show the most complex regulatory pattern of all the transcriptomes examined. In total, there were 8 up-regulated (see table 3.2) and 16 down-regulated genes (see table 3.3). Among the up-regulated genes, the strongest difference was found for the *lmo0979-0980* (*lieAB*) operon. It can be seen from table 3.2 that this operon was nearly 500-fold higher expressed in the mutant than in the wild type. The gene *lftS*, part of the *lftRS* operon, was also strongly up-regulated (150-fold). The *lftRS* operon thus seems to be autoregulatory. Compared to the strong regulation of *lieAB* and *lftRS* the other up-regulated genes were only weakly influenced by the deletion of *lftR*. Noticeably, *lmo0981* and *lmo0982*, two genes immediately downstream of *lieAB* were also up-regulated 7- and 4-fold, respectively.

Table 3.2: Genes up-regulated in the Δ*lftR* mutant (LMKK42).

Locus	Induction Ratio	Standard Deviation	*P*-value	Function
lmo0979	466	173	2.8E-04	ABC-type transporter ATPase subunit LieA
lmo0980	454	139	4.7E-04	ABC-type transporter membrane subunit LieB
lmo0719	187	32.1	2.9E-07	hypothetical protein LftS
lmo0981	7.15	2.04	6.5E-03	transporter
lmo0982	4.46	1.15	7.1E-03	peptidase
lmo2678	2.75	0.55	1.4E-03	XRE family transcription regulator
lmo2679	2.69	0.45	1.7E-03	histidine kinase
lmo2834	2.15	0.20	9.8E-05	oxidoreductase

Down-regulated genes were also observed in the Δ*lftR* mutant. All of the down-regulated genes (see table 3.3) are under the transcriptional control of the alternative sigma factor SigB (Hain et al. 2008, Oliver et al. 2009 or Mujahid et al. 2013b). The shared control of all these genes by SigB suggests an interaction of LftR-controlled genes with SigB or the SigB activation pathway.

Table 3.3: Genes down-regulated in the Δ*lftR* mutant (LMKK42).

Locus	Induction Ratio	Standard Deviation	*P*-value	Function
lmo0434	0.42	0.037	7.1E-03	InlB
lmo0670	0.12	0.098	6.2E-03	hypothetical protein
lmo1427	0.11	0.030	6.5E-03	OpuCB
lmo1425	0.10	0.018	2.1E-03	OpuCD
lmo1426	0.10	0.006	1.6E-03	OpuCC
lmo1428	0.08	0.021	4.1E-03	OpuCA
lmo0669	0.08	0.030	5.8E-03	oxidoreductase
lmo0602	0.07	0.018	2.1E-03	transcription regulator
lmo2748	0.07	0.013	4.1E-03	hypothetical protein
lmo0937	0.06	0.021	9.3E-03	hypothetical protein
lmo2230	0.05	0.017	9.5E-03	arsenate reductase
lmo2213	0.04	0.020	9.5E-03	hypothetical protein
lmo0994	0.04	0.025	8.3E-03	hypothetical protein
lmo0263	0.04	0.027	8.9E-03	InlH
lmo0596	0.04	0.015	4.3E-03	hypothetical protein
lmo0913	0.03	0.023	8.9E-03	aldehyde dehydrogenase

The Δ*lftR* mutant was investigated for SigB-controlled phenotypes, because all of the down-regulated genes were controlled by SigB. SigB-dependent phenotypes include chitinase activity and day light dependent coordination of swarming (Larsen et al. 2010, Tiensuu et al. 2013). Different strain backgrounds (Δ*lftR*, Δ*lftS*, Δ*lftRS*, Δ*lieAB*, Δ*lftR* Δ*lieAB*) revealed that only the Δ*lftR* (LMKK42) and Δ*lftR*Δ*lieAB* (LMS169) strains showed SigB-dependent phenotypes (data not shown). Both of these strains over-express *lftS*, therefore the SigB phenotype might be caused by LftS. Ectopic production of LftS on the other hand did not produce any of the SigB-associated phenotypes (data not shown). These phenotypes could also not be complemented by re-introduction of *lftR* in those mutants (data not shown). Lokking for other possible causes of the phenotypes it became obvious, that both mutants showing SigB-controlled phenotypes (Δ*lftR* and Δ*lftR* Δ*lieAB*) shared the same genetic background. The Δ*lftR* Δ*lieAB* strain LMS169 was constructed by deleting *lieAB* in the Δ*lftR* mutant LMKK42 (Kaval et al. 2015).

For these reasons, a another explanation for the observed behaviour was that a second mutation had occurred in *sigB* or any gene necessary for SigB activation. Close examination of the RNA sequencing data revealed a mutation in *rsbT*, a gene necessary for activation of SigB. This mutation introduced a premature stop codon in the *rsbT* transcript, which likely prematurely halted the translation process. For the Δ*lftR* strain LMKK42, the presence of a C to T transition at base pair 10 of the *rsbT* gene was confirmed by genome re-sequencing. The mutation found converts the fourth codon of *rsbT* from CAA, coding for the amino acid glutamine, to TAA, a stop codon (see figure 3.3). The resulting RsbT

protein thus is shortened from 136 amino acids to 3 amino acids and will in all likelihood have lost its functionality.

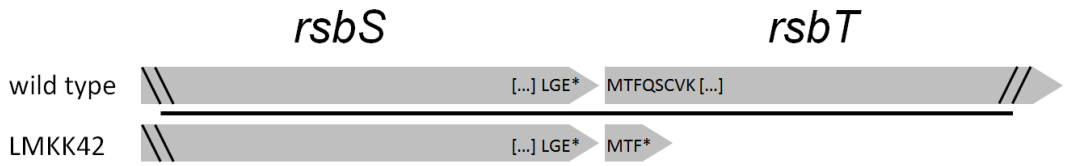

Figure 3.3: Genomic context of the *rsbT* mutation observed in the strain LMKK42 (Δ*lftR*). The C to T transition converts a CAA codon coding for glutamine to TAA, a stop codon ending translation. The resulting protein is thus shortened from 136 to three amino acids and most likely inactive.

RsbT inactivation causes a SigB null phenotype (Chaturongakul and Boor 2004), thus explaining the down-regulation of SigB-dependent genes observed in the Δ*lftR* and Δ*lftR* Δ*lieAB* mutants. A new Δ*lftR* mutant was subsequently constructed and readily obtained without second site mutations as confirmed by genome sequencing (data not shown). It must therefore be concluded that SigB had been inadvertently disrupted during the construction of the original Δ*lftR* mutant, a phenomenon that is not uncommon in *L. monocytogenes* (Quereda et al. 2013). Since this phenotype depends on SigB activity (Tiensuu et al. 2013), the abberant daylight-dependent coordination of swarming in strain LMKK42 (Kaval et al. 2015) must also be caused by the mutation in *rsbT*.

3.1.3 Genes differentially expressed in the Δ*ladR* mutant

Three genes were found to be significantly up-regulated in the Δ*ladR* mutant (LMSH1) (see table 3.4). The *mdrL* gene encoding a multi-drug efflux pump was the main regulatory target of LadR, with an induction ratio of over 150-fold, supporting the results of a previous study on this repressor (Huillet et al. 2006). Two more genes were also significantly up-regulated in the Δ*ladR* mutant. These were *lmo1618*, encoding the transcriptional regulator MarR, and *lmo1617*, encoding the efflux pump MdrM. The *mdrM* gene is known to be approximately 3-fold induced in a Δ*ladR* mutant (Crimmins et al. 2008) and forms an operon with *marR* (Toledo-Arana et al. 2009). Both genes can therefore be assumed to be transcribed together. The RNA sequencing data on the Δ*ladR* mutant thus confirmed previous knowledge.

Table 3.4: Genes up-regulated in the Δ*ladR* mutant (LMSH1).

Locus	Induction Ratio	Standard Deviation	*P*-value	Function
lmo1409	154	44	3.6E-4	MdrL multi-drug-transporter
lmo1618	4.3	0.4	3.3E-4	MarR family transcription regulator
lmo1617	2.6	0.8	9.4E-3	MdrM multi-drug-transporter

3.1.4 Genes differentially expressed in the Δ*lstR* mutant

In the Δ*lstR* mutant (LMSH2), several genes were differentially regulated. A summary of the up-regulated genes in the Δ*lstR* mutant is given in table 3.5. The genes with the highest induction rations around 140-fold were *lmo0421* (encoding a protein homologous to RodA and FtsW) and *lmo0423* (*sigC*). These highly up-regulated genes were already observed in the plots of the raw TPM values (see figure 3.1). The genes *sigC-lstR-lmo0421* form one operon (Toledo-Arana et al. 2009) that is negatively regulated by LstR (autoregulatory). Two other strongly up-regulated genes in the Δ*lstR* mutant are located directly downstream of the *sigC-lstR-lmo0421* operon. Improper termination of transcription after *lmo0421* could be a reason for this observation. Weak induction was observed for the genes *lmo2773* and *lmo2050*, but the 2-fold induction levels are of minor interest when compared to the 140-fold induction of the *sigC-lstR-lmo0421* operon.

Table 3.5: Genes up-regulated in the Δ*lstR* mutant (LMSH2).

Locus	Induction Ratio	Standard Deviation	*P*-value	Function
lmo0421	145	11.3	2.6E-5	RodA homologue
lmo0423	139	19.3	8.6E-7	RNA polymerase factor sigma C
lmo0420	55	10.2	1.1E-4	hypothetical protein
lmo0419	7	1.47	3.5E-3	hypothetical protein
lmo2773	2.4	0.53	3.5E-3	hypothetical protein
lmo2050	2.3	0.35	3.7E-3	excinuclease ABC subunit A

Looking at the transcripts with the strand-specific analysis software Rockhopper showed that in the Δ*lstR* mutant anti-sense RNA transcripts mapped to *lmo0420*, a gene oriented

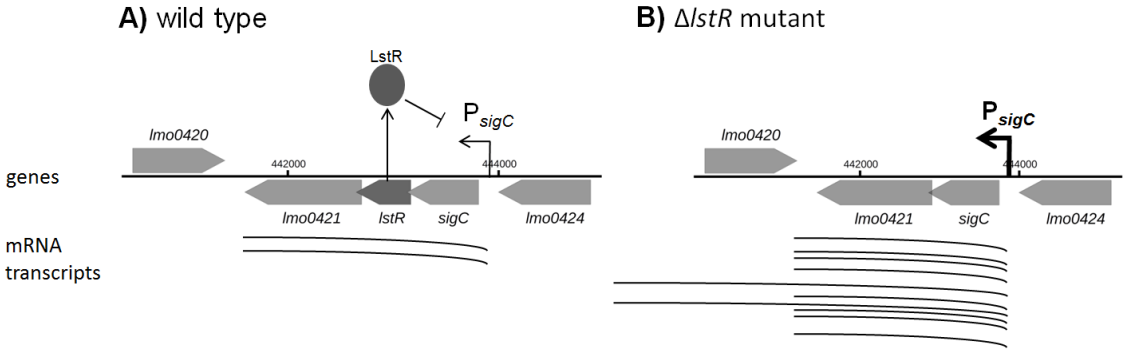

Figure 3.4: LstR-based control of the *sigC-lstR-lmo0421* operon in the wild type and in the absence LstR. Panel A: In the wild type, few mRNA transcripts are made from P_{sigC}. The amount of LstR produced is sufficient to repress activity of P_{sigC} to a basal level. Panel B: The repressor LstR is no longer present in the Δ*lstR* mutant and P_{sigC} becomes hyperactive producing many mRNA transcripts. Some of these transcripts are not properly terminated after *lmo0421*, the last gene of the operon, leading to transcription of the neighbouring region including *lmo0420* and *lmo0419*.

in opposite direction to the *sigC-lstR-lmo0421* operon. The complete de-repression of this autoregulatory operon is probably leading to incomplete termination of transcription after *lmo0421*. For this reason, long transcripts spanning the entire region from *sigC* until *lmo0419* are produced (see figure 3.4).

It is possible that the anti-sense RNA binds to the *lmo0420* mRNA and prevent its translation. From a proteomic perspective, the quantity of the Lmo0420 protein should be reduced in the mutant, possibly affecting the ability of this protein to accurately fulfil its function. The gene *lmo0419* is oriented in the same direction as the *sigC-lstR-lmo0421* operon. It should therefore be up-regulated in the Δ*lstR* mutant and the Lmo0419 protein amount should be increased. The exact influence on the proteome of the Δ*lstR* mutant needs to be investigated in further experiments. Two other genes (*lmo2773* and *lmo2050*) are up-regulated by a factor of slightly above two. This is barely above the 2-fold cut-off used for significant differences (see chapter Materials and Methods).

There were also four genes down-regulated in the Δ*lstR* mutant (see table 3.6). The putative role of LstR as a transcriptional repressor suggested that the deletion mutant should over-express the genes regulated by the repressor. Finding down-regulated genes was therefore somewhat surprising and could be a hint for secondary effects. These might be caused by the altered transcription profiles of up-regulated genes (see table 3.5). For example, the up-regulated genes could themselves be transcription factors that interfere with the expression of other genes, leading to their down-regulation. Interestingly, *lmo0416* and *lmo0417* are located in close vicinity of the *sigC-lstR-lmo0421* operon, so a direct influence may also be possible.

In summary, it seems that the PadR-like repressor LstR is responsible for the repression of its own operon *sigC-lstR-lmo0421*. Other genes were detected as being deferentially expressed, but this might be due to secondary effects caused by the complete disruption of regulation of the *sigC-lstR-lmo0421* operon. One effect of the complete de-repression seems to be an incomplete termination of transcription after the operon (see figure 3.4).

Table 3.6: Genes down-regulated in the Δ*lstR* mutant (LMSH2).

Locus	Induction Ratio	Standard Deviation	*P*-value	Function
lmo1597	0.47	0.042	8.3E-3	hypothetical protein
lmo0416	0.46	0.011	1.7E-3	transcriptional regulator
lmo0417	0.43	0.164	8.4E-3	hypothetical protein
lmo1839	0.22	0.057	7.4E-3	PyrP

3.1.5 Genes differentially expressed in the *lltR** mutant

In the strain LMSH3 the DNA binding site of LltR (Lmo0599) has been modified by the introduction of three amino acid exchanges (L49A, R51A, L52A) replacing the larger original amino acids with the small alanine residue. This should result in a phenotype similar to a *lmo0599* deletion mutant, because mutation of the conserved lysine in position 49 abrogated DNA binding in another PadR protein (Park et al. 2017). As expected, a set of up-regulated genes was observed when comparing the transcriptome of this mutant to the wild type. The RNA sequencing results are presented in table 3.7.

Table 3.7: Genes up-regulated in the *lltR mutant (LMSH3).**

Locus	Induction Ratio	Standard Deviation	*P*-value	Function
lmo0599	151	50	4.4E-5	PadR-like repressor LltR
lmo0600	118	34	1.2E-4	hypothetical protein
lmo0601	107	24	4.8E-5	hypothetical protein
lmo0602	12.7	9.2	1.1E-3	transcription regulator
lmo0954	3.78	1.06	2.5E-3	hypothetical protein
lmo2487	3.13	0.66	7.3E-3	hypothetical protein
lmo0955	2.64	0.62	2.7E-3	hypothetical protein
lmo1637	2.51	0.25	3.4E-4	hypothetical protein
lmo0047	2.44	0.43	2.9E-3	hypothetical protein
lmo1636	2.39	0.37	4.3E-3	ABC-Transporter

Most of the genes listed in table 3.7 are close to the threshold for significant differential expression (2-fold). Only the four genes at the top of the table, including the *lltR-lmo0600-lmo0601* operon and *lmo0602*, are highly over-expressed in the *lltR** mutant. The *lltR** operon is over 100-fold up-regulated and the next most strongly regulated gene, *lmo0602*, is located immediately downstream of this operon. These results clearly show that LltR, like LstR in the previous section, is mainly regulating the expression of its own operon. As was the case with the *lstR* operon, incomplete termination might cause over-expression of downstream genes.

3.1.6 Confirmation of the RNA sequencing results by measuring promoter activity in a β-galactosidase assay

To validate the results obtained with RNA sequencing, the activities of the promoters most strongly repressed by LftR, LadR, LstR and LltR were quantified using β-galactosidase measurements. For this purpose, the promoters of *lieA*, *mdrL*, *sigC* and *lltR* were fused to a promoter-less *lacZ* gene present on a plasmid. Initially, a 300 bp region upstream of the respective start codon should be cloned for all promoters, in order to include any regulatory elements that might be present in the upstream region. This was not possible for the *lltR* promoter, because the resulting plasmids were unstable in *E. coli*. The sequence had to be shortened to 201 bp to get a stable construct.

The plasmids carrying the promoter-*lacZ* fusions were then transformed into the wild type and the mutants lacking the cognate PadR-like repressor. A single copy of the pIMK based plasmids was integrated into the genome (Monk et al. 2008). The cells were then grown to mid-exponential phase and the LacZ activity (the amount of LacZ produced) was measured in an ONPG-based assay. The *lltR*, *lstR* and *lieA* promoters showed a measurable, but low activity in the wild type under the growth conditions used (see figure 3.5). In the mutant strains lacking the cognate PadR-like repressor the β-galactosidase activity was significantly higher (see figure 3.5). This confirmed the RNA sequencing data by showing on a protein activity level the up-regulation of:

- P_{mdrL} in the absence of *ladR* by 17-fold,
- P_{lltR} in the *lltR** mutant by 53-fold,
- P_{sigC} in the absence of *lstR* by 77-fold, and of
- P_{lieA} in the absence of *lftR* by 422-fold.

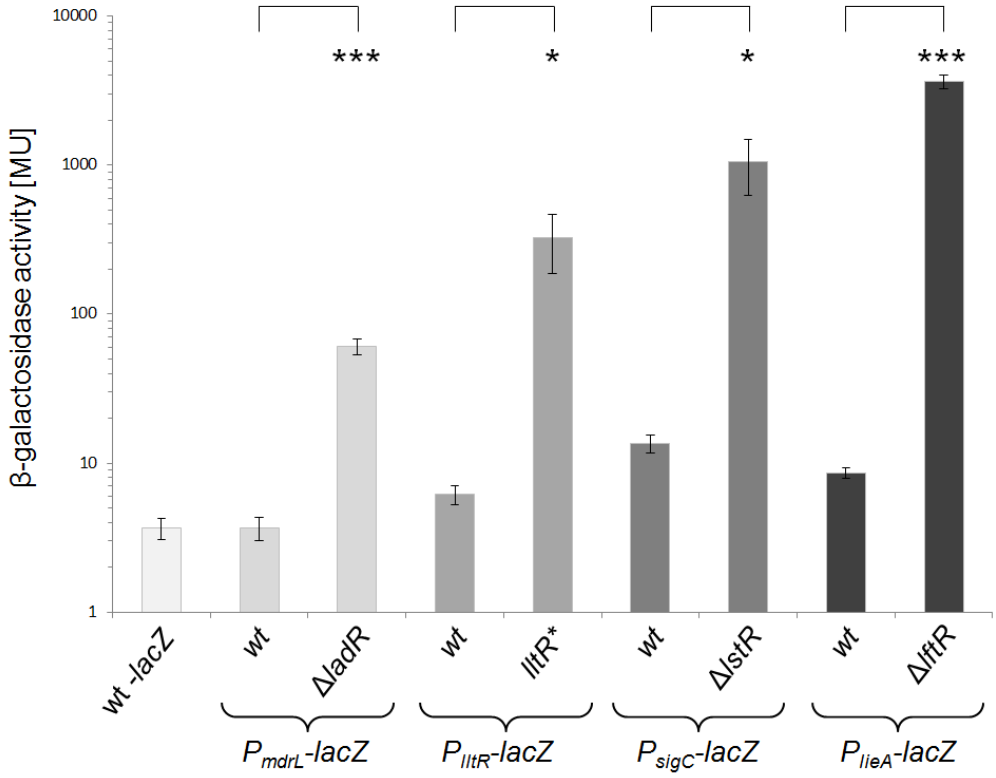

Figure 3.5: Confirmation of the RNA-sequencing results using a promoter-*lacZ*-based β-galactosidase assay. β-galactosidase activity of the *mdrL*, *lltR*, *lstR* and *lieA* promoters in the wild type (strains LMSH10, LMSH14, LMSH12 and LMSH5) and the mutants lacking the cognate PadR-type repressor (strains LMSH11, LMSH15, LMSH13, LMSH6). Cells were grown in BHI at 37°C until mid-exponential phase, harvested and then lysed by sonification. The activity of promoter-less *lacZ* is shown as a negative control. Three replicates were measured and the average is shown with standard deviation. Asterisks indicate the statistical significance (t-test) with $P<0.05$ *, $P<0.01$ **, $P<0.001$ ***

The RNA sequencing data also suggested that LftR represses transcription of its own operon *lftRS*. We wondered, if the transcripts of *lftS* could also be shown directly by Northern blotting. For this purpose, RNA extracts from the wild type and the Δ*lftR* mutant strain LMKK42 (carrying the *rsbT*^{C10T} mutation inactivating SigB) were prepared. Using an RNA probe complementary to the *lftS* transcript, it could be shown that *lftRS* (0.7 kb) is weakly transcribed in the wild type. In contrast, a strong signal for a 0.4 kb transcript (*lftS* only) was detected in the Δ*lftR*rsbT^{C10T} background (see figure 3.6). Importantly, no signal was detected in the *lftS* (LMKK26) and *lftRS* (LMKK31) mutants showing the specificity of the method. Finally, the deletion of *sigB* (LMSH9) did not affect the signal intensity of the *lftRS* transcript. This precludes an influence of the *rsbT*^{C10T} mutation on the expression of *lftRS*. The Northern blot thus confirmed the RNA sequencing data.

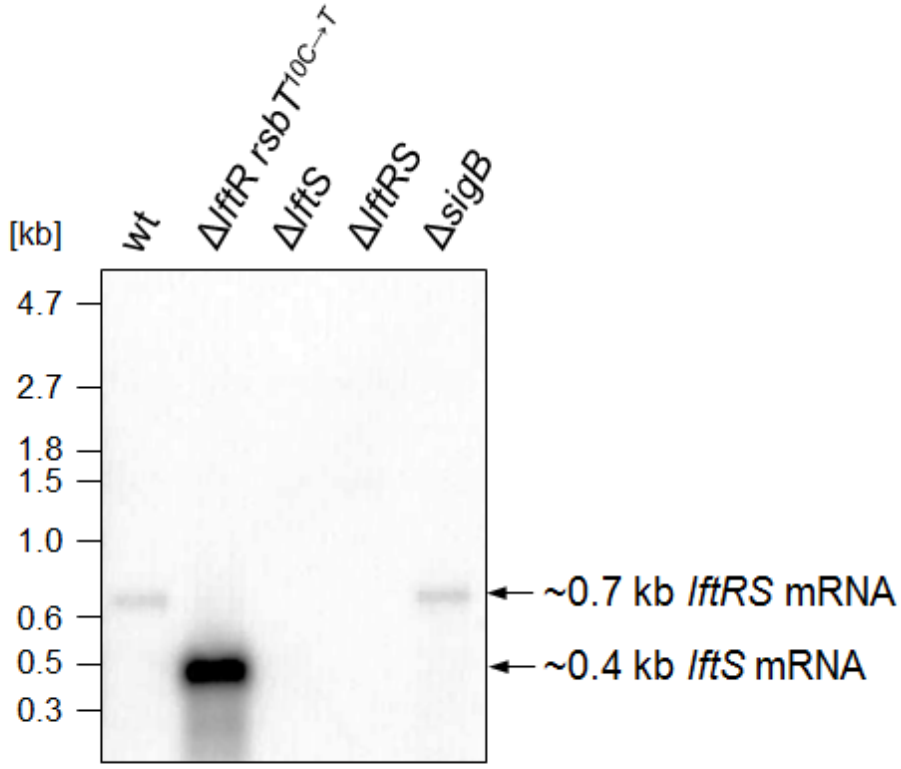

Figure 3.6: Direct detection of *liftS* transcripts. Northern blot showing the de-repression of *liftS* in the Δ*liftR rsbT*^{C10T} background, confirming *liftR* autoregulation. An *liftS* specific RNA probe detected a abundant *liftS* transcripts in the absence of the *liftR* (Δ*liftR rsbT*^{C10T} lane). RNA from strains LMKK26 (Δ*liftS*), LMKK31 (Δ*liftRS*) and LMSH9 (Δ*sigB*) were included as controls, proving the specificity of RNA-probe interaction by the absence of a signal in the Δ*liftS* strain and low transcription of the longer *liftRS* operon in the presence of *liftR*.

The RNA sequencing data showed that all four repressors strongly inhibit the transcription of a small set of genes (one to four genes or one to two operons) and seem to be auto-regulatory. The latter could not be shown for LadR, because we used a Δ*ladR* mutant and this gene is not part of an operon. Some weak but significant regulation of other genes was observed. In the case of LadR, this observation fits perfectly to previously published data (Crimmins et al. 2008).

3.2 Determination of conditions leading to the induction of genes controlled by PadR-like transcription factors

PadR-like transcription factors often activate genes in response to environmental signals, like the presence of toxic compounds (antibiotics or phenolic acids) or other stresses, for example heat (Zhang et al. 2005, Agustiandari et al. 2008, Nguyen et al. 2011, Heravi et al. 2015). One aim of this study was to identify conditions leading to the expression of genes controlled by the PadR-like repressors. In order to be able to screen different conditions and substances for induction, promoter-*lacZ* fusions were constructed as described in the previous section. It has been shown that these constructs are nearly inactive in the wildtype, but are strongly up-regulated in the respective repressor mutants (see figure 3.5).

Wild type cells carrying the reporter constructs P_{mdrL}-*lacZ*, P_{lltR}-*lacZ*, P_{sigC}-*lacZ* and P_{lieA}-*lacZ* (LMSH10, LMSH14, LMSH12 and LMSH05) were mixed with liquid BHI agar containing X-Gal as a chromogenic substrate for LacZ to pour plates. Concentrated solutions of different substances were spotted on top of the plates and the plate were incubated at 37°C over night. Under standard conditions no LacZ is produced, because the promoters are inactive (see figure 3.5). The plate therefore stays color-less. Under inducing conditions however, LacZ should be produced and catalyse X-Gal conversion to a deeply blue reactant. Using this method, around 750 different chemical substances and conditions such as cold, heat and pH were screened. 681 substances were compounds from the DZIF natural substance collection (Herrmann et al. 2017) consisting of secondary metabolites from streptomycetes (340 substances), myxobacteria (253 substances) and fungi (88 substances). A total of 67 commercially available substances or physical conditions were also tested for induction of some promoter-*lacZ* constructs. These are listed in table 3.8. Most compounds were dissolved in water or DMSO and saturated solutions spotted on agar.

Table 3.8: Substances and conditions screened beside the DZIF Natural Compound Collection. A ”plus” sign signifies ”induction”, a ”minus” sign signifies ”no induction”, a ”u” signifies ”unspecific induction” for all reporter strains and ”n.d.” signifies ”not determined”

Substance	**P**$_{lmo0979}$ **induction**	**P**$_{lmo0423}$ **induction**	**P**$_{lmo0599}$ **induction**	**P**$_{lmo1409}$ **induction**
Rhodamine 6G	+	-	-	-
Rhodamine B	+	n.d.	n.d.	n.d.
Ethidium bromide	-	-	-	-
Heat 42°C	-	-	-	-
Heat 48°C	-	-	-	-
Cold 6°C	-	-	-	-
Penicillin G	-	-	-	-
Phosphomycin	-	-	-	-
Bacitracin	-	-	-	-
Vancomycin	u	u	u	u
Benzalkonium	-	-	-	-
Vanillin	-	-	-	-
tert-Butylhydroquinone	-	-	-	-
Nalidixic acid	-	-	-	-
Erythromycin	-	+	-	-
Cycloserin	-	-	-	-
Cravacrol	-	-	-	-
Chloramphenicol	-	-	-	-
Acriflavine	-	-	-	-
Tetracycline	-	-	-	-
Gigasept	-	-	-	-
Grotanat	u	u	u	u
Lysozyme	-	-	-	-
Ethanol	-	-	-	-

continues on next page

DMSO	-	-	-	-
NaOH 10 M	-	-	-	-
HCl 37 %	u	u	u	u
EDTA 0.5 M	-	-	-	-
KCl	-	-	-	-
Spectinomycin	-	-	-	-
Ampicillin	-	-	-	-
Triton X-100	-	-	-	-
SDS	-	-	-	-
Deoxycholate	-	-	-	-
H_2O_2	-	-	-	-
Kanamycin	-	-	-	-
Daunomycin	-	-	-	-
Chromomycin	-	-	-	-
Josamycin	-	+	-	-
Rifampicin	-	-	-	-
Tylosin	-	+	-	-
Moenomycin	n.d.	-	-	-
Bile salts	n.d.	-	-	-
Streptomycin	n.d.	-	n.d.	n.d.
Cellobiose	n.d.	-	n.d.	n.d.
Sucrose	n.d.	-	n.d.	n.d.
Trehalose	n.d.	-	n.d.	n.d.
Rhamnose	n.d.	-	n.d.	n.d.
Maltose	n.d.	-	n.d.	n.d.
Spiramycin	n.d.	-	n.d.	n.d.
Acridine orange	-	n.d.	n.d.	n.d.
Riboflavin	-	n.d.	n.d.	n.d.
Tryptophane	-	n.d.	n.d.	n.d.
Folic acid	-	n.d.	n.d.	n.d.
Imidazol	-	n.d.	n.d.	n.d.

continues on next page

4-Hydroxybenzoate	-	n.d.	n.d.	n.d.
Salycilate	-	n.d.	n.d.	n.d.
Pyrogallol	-	n.d.	n.d.	n.d.
Indol	-	n.d.	n.d.	n.d.
Humic acid	-	n.d.	n.d.	n.d.
Emodin	-	n.d.	n.d.	n.d.
Methylene blue	-	n.d.	n.d.	n.d.
Congo red	-	n.d.	n.d.	n.d.
Nile red	-	n.d.	n.d.	n.d.
Fluorescein	-	n.d.	n.d.	n.d.
$FeCl_2$	-	n.d.	n.d.	n.d.
$ZnCl_2$	-	n.d.	n.d.	n.d.
NaN_3	-	n.d.	n.d.	n.d.
Menadione	-	n.d.	n.d.	n.d.

3.2.1 Conditions leading to the activation of LftR-controlled genes

It was known that LftR controls the transcription of the ABC-type transporter genes *lieAB* and that this transporter imports ethidium bromide into the cells (Kaval et al. 2015), but ethidium bromide did not . Conditions leading to the transcription of *lieAB* were unknown. Using the P_{lieA}-*lacZ* (LMSH05) reporter strain we screened for conditions leading to the activation of *lieAB* transcription. For the screening LMSH5 was grown in BHI agar containing X-Gal as a chromogenic substrate. Different chemicals were spotted on top of such agar plates. An induction of P_{lieA} would lead to the production of LacZ which in turn would convert X-Gal producing a deep blue end product that can easily seen by eye.

During these screens, it could be shown that LftR-controlled genes are activated by dyes of the rhodamine family (rhodamine B and rhodamine 6G were tested). A blue ring corresponding to the zone of induction is visible around the region where the dye was applied (see figure 3.7). On the other hand, a strain carrying a promoter-less *lacZ* reporter did not produce a color change indicating that the activity observed depends on P_{lieA}. Ethidium bromide, which had been shown to be an artificial substrate of the LieAB transporter (Kaval et al. 2015), did also not induce expression from P_{lieA}. This proved that ethidium bromide is indeed an artificial substrate that is accidentally being imported

by LieAB. Identical results were obtained when using strain LMSH7 carrying the P_{lftR}-*lacZ* reporter, confirming the regulation of both the P_{lieA} and P_{lftR} promoters by LftR (see figure 3.7).

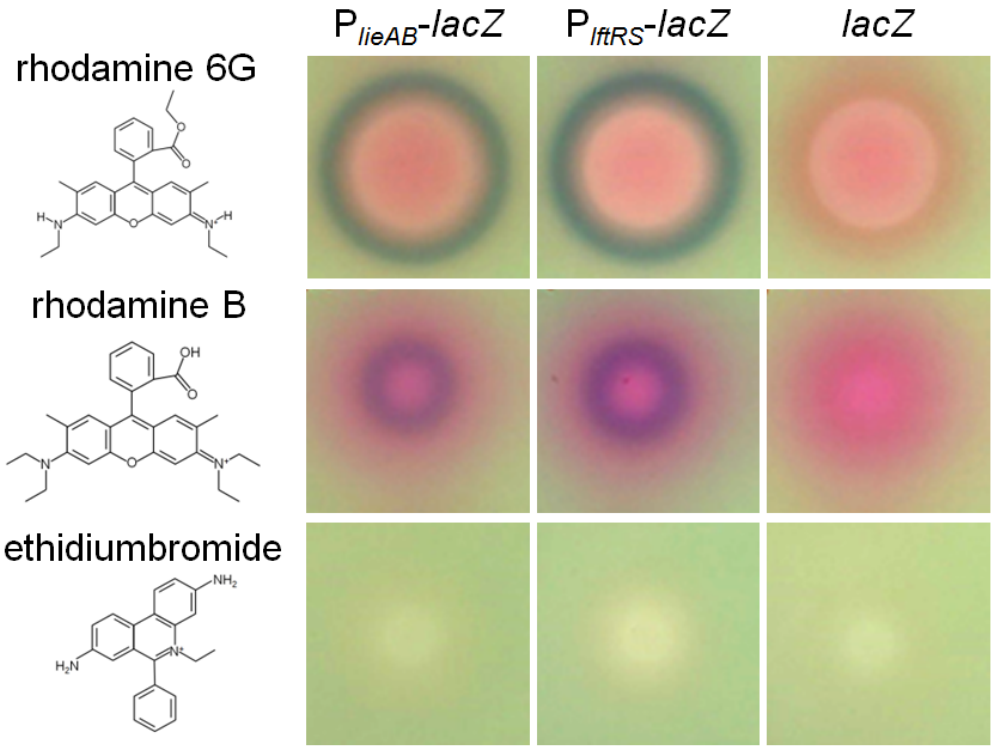

Figure 3.7: Rhodamine dyes induce LftR-regulated transcription. A volume of 2 μl of the dyes rhodamine 6G, rhodamine B and ethidium bromide (all at 5 mg/ml) was spotted on agar plates containing strain LMSH5 (P_{lieA}-*lacZ* reporter) or strain LMSH7 (P_{lftR}-*lacZ* reporter). After over night incubation at 37°C both strains showed a color change on the plates containing X-Gal as a chromogenic substrate in the presence of the rhodamine dyes. Strain LMSH16 carrying promoter-less *lacZ* did not show a color change indicating specificity of the induction to the *lieA* and *lftR* promoters. The artificial LieAB substrate ethidium bromide also does not induce reporter activity.

Rhodamine dyes induce the transcription from both of the LftR-controlled promoters, but it was not known how strong this induction was or in what concentration range the induction occurred. In order to quantify the induction observed with rhodamine 6G the strains LMSH5 (P_{lieA}-*lacZ*) and LMSH7 (P_{lftR}-*lacZ*) were inoculated at an OD_{600} of 0.05 into BHI medium containing increasing concentrations of rhodamine 6G and grown until mid-exponential phase at 37°C. After lysis by sonification, the LacZ activity was mea-

sured in using ONPG as a substrate. The maximal de-repression of the the *lieA* promoter was achieved at a rhodamine 6G concentration of 0.5 μg/ml (see figure 3.8). At this concentration the *lieA* promoter was induced 13.5-fold while the *lftR* promoter was induced 6.6-fold (see figure 3.8).

As a control for maximal de-repression, the activity of the P_{lieA}-*lacZ* (LMSH6) and P_{lftR}-*lacZ* reporter (LMSH8) was also measured in the Δ*lftR rsbT*^{C10T} mutant background lacking LftR. Compared to the strains LMSH6 and LMSH7 the induction by rhodamine 6G was only at 3.4 % (P_{lieA}) or 6.2 % (P_{lftR}) of the maximal capacity. It is important to note the different expression levels from the *lftR* and *lieA* promoters in the absence of an inducer. The expression level of *lftRS* is more than twice as high as that of *lieAB*. The higher expression might be needed to guarantee the proper regulation of *lieAB*. Panel B of figure 3.8 shows the structure of the dye and the induction of the P_{lieA}-*lacZ* reporter on agar containing X-Gal, when 2 μl rhodamine 6G (2.5 mg/ml) were spotted.

Rhodamine dyes are inducing expression of LftR-controlled genes, but they are of artificial origin (Cooksey 2016) and therefore unlikely to play any role in natural settings. It must be assumed that they are not the natural effectors of LftR. In order to identify potential naturally occurring effectors, a screening of the DZIF natural substance collection was initiated. Again, strain LMSH5 carrying the P_{lieA}-*lacZ* reporter was poured into BHI agar containing X-Gal. A volume of 1 μl of the substances from the natural compound collection were spotted onto the agar surface and left to dry before incubation over night at 37°. This screen revealed aurantimycin A as a potent, naturally occurring inducer of LftR-controlled gene expression (see figure 3.9, panel B). No other substances inducing transcription were found in the DZIF collection.

To quantify the strength of induction at given aurantimycin concentrations, strain LMSH5 (P_{lieA}-*lacZ*) was again inoculated at an OD_{600} of 0.05 into BHI medium containing increasing concentrations of the antibiotic and grown to mid-exponential phase at 37°C. Quantification of the resulting β-galactosidase activity revealed that aurantimycin induces gene expression from the *lieA* promoter in a dose dependent manner, but at much lower concentrations than rhodamine 6G (see figure 3.9, panel A). The structure of aurantimycin A and the induction it causes in the agar based assay are also shown for reference (see figure 3.9, panel B).

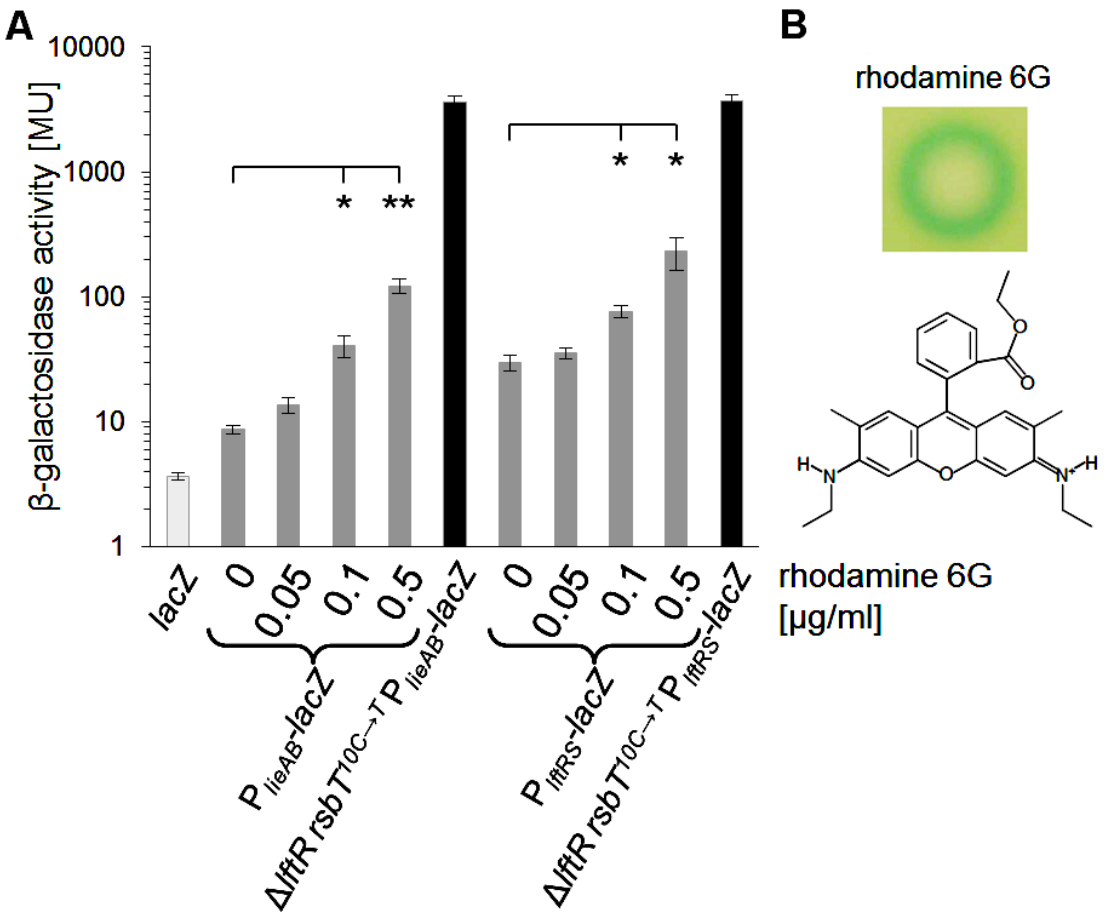

Figure 3.8: Quantification of the dose-dependent induction of P_{lieA} by rhodamine 6G. Panel A: In liquid culture, the β-galactosidase induced in strains LMSH5 (P_{lieA}-*lacZ* reporter) and LMSH7 (P_{lftR}-*lacZ* reporter) depends on the rhodamine 6G concentration. The strains were grown at 37°C in BHI containing the indicated concentrations of rhodamine 6G. The strains LMSH6 (Δ*lftR rsbT*^{C10T} P_{lieA}-*lacZ*) and LMSH8 (Δ*lftR rsbT*^{C10T} P_{lftR}-*lacZ*) were used as controls for maximal de-repression. Three replicates were measured and the average is shown with standard deviation. Asterisks indicate the statistical significance (t-test): $P<0.01$ *, $P<0.001$ **. Panel B: Induction of the P_{lieA}-*lacZ* reporter by 2 μl rhodamine 6G (2.5 mg/ml) on agar plates containing X-Gal after over night incubation and structure of rhodamine 6G.

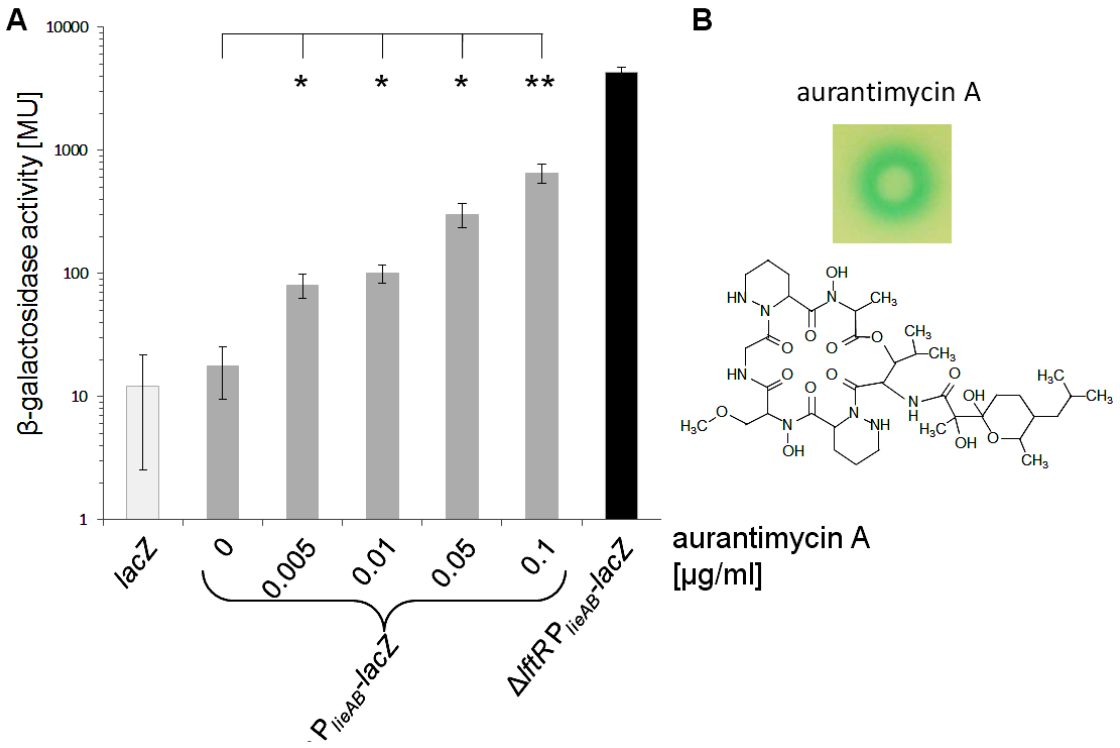

Figure 3.9: Quantification of the dose-dependent induction of P_{lieA} by aurantimycin A. Panel A: In liquid culture, aurantimycin induced β-galactosidase in strain LMSH5 (P_{lieA}-*lacZ* reporter) in a concentration-dependent manner. The cells were grown at 37°C in BHI containing the indicated concentrations of aurantimycin. Strain LMSH16 (promoter-less *lacZ*) and LMSH34 (Δ*lftR* P_{lieA}-*lacZ*) served as controls. Three replicates were measured and the average is shown with standard deviation. Asterisks indicate the statistical significance (t-test): $P<0.01$ *, $P<0.001$ **. Panel B: Induction of the P_{lieA}-*lacZ* reporter by 2 μl aurantimycin A (2.5 mg/ml) on agar plates containing X-Gal after over night incubation and structure of aurantimycin A.

3.2.2 Induction of LftR-controlled genes depends on LftS

The PadR-like transcriptional regulator LftR is encoded in an operon together with a second protein of unidentified function named LftS. The *lftRS* operon is induced in the presence of rhodamine dyes or aurantimycin A (see figure 3.7, figure 3.8 and figure 3.9). To test whether *lftS* plays a role in the regulation of P_{lieA} or P_{lftR}, the induction by rhodamine 6G and aurantimycin A was tested in a Δ*lftS* mutant background. To this end, the P_{lieA}-*lacZ* reporter was introduced into the Δ*lftS* mutant strain LMKK26 and into strain LMSH43 constructed by re-introducing *lftS* into LMKK26, yielding the strains LMSH27

and LMSH49 (labelled *lftS*$^+$). Spotting of 2 μl of rhodamine 6G and aurantimycin A (both at 2.5 mg/ml) onto plates containing the reporter strains and X-Gal showed that P$_{lieA}$-*lacZ* reporter construct gave the expected color signal in the wild type after over night incubation at 37°C (see figure 3.10). In the absence of *lftS*, there was no induction of the promoters. To show that this effect depends only on *lftS*, the *lftS* gene was re-introduced and the resulting *lftS*$^+$ strain did again show the expected color change, indicating that *lftS* is essential for the induction (see figure 3.10).

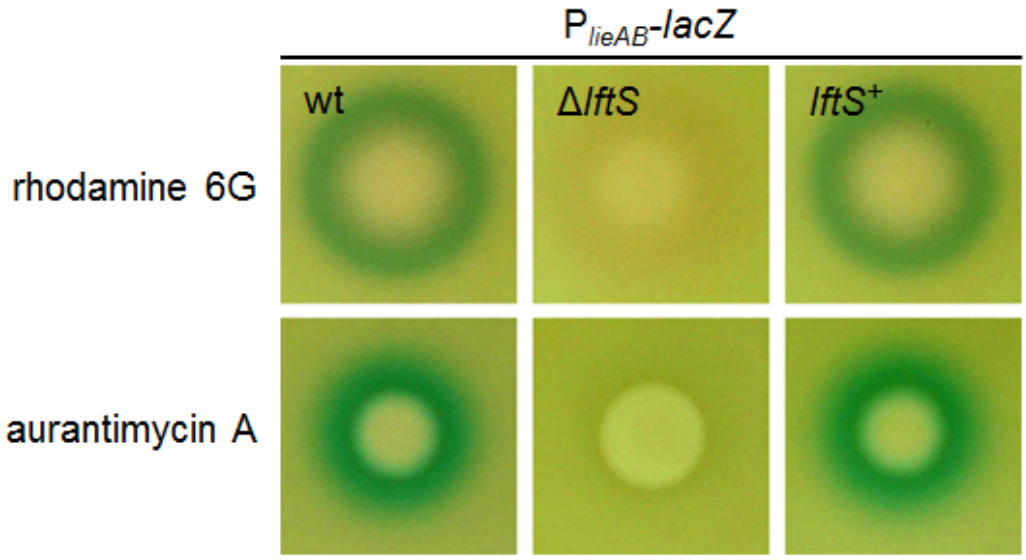

Figure 3.10: Effect of *lftS* on P$_{lieA}$ induction. Induction of the P$_{lieA}$-*lacZ* reporter in the agar based assay depends on the presence of *lftS*. A volume of 2 μl of 2.5 mg/ml rhodamine 6G or aurantimycin A was spotted on BHI agar plates with X-gal. The plates also contained strains LMSH5 (P$_{lieA}$-*lacZ* [labelled wt]), LMSH27 (Δ*lftS* P$_{lieA}$-*lacZ* [labelled Δ*lftS*]) or LMSH49 (*lftS* reverted P$_{lieA}$-*lacZ* [labelled *lftS*$^+$]) and were incubated over night at 37°C.

To determine whether the induction in the Δ*lftS* background was low or completely prevented, the β-galactosidase activity of the P$_{lieA}$-*lacZ* reporter construct in strain LMSH27 (Δ*lftS*) was quantified. The cells were grown at 37°C in BHI medium containing increasing aurantimycin A concentrations until reaching mid-exponential phase. Strain LMSH16 (promoter-less *lacZ*) and strain LMSH34 (Δ*lftR* P$_{lieA}$-*lacZ*) were used as controls. In the absence of *lftS*, the activity of the *lieA* promoter is essentially abolished, no matter at which aurantimycin A concentration the strain was grown (see figure 3.11). The results proved that *lftS* is absolutely essential for the induction observed in the wild type (see

figure 3.9).

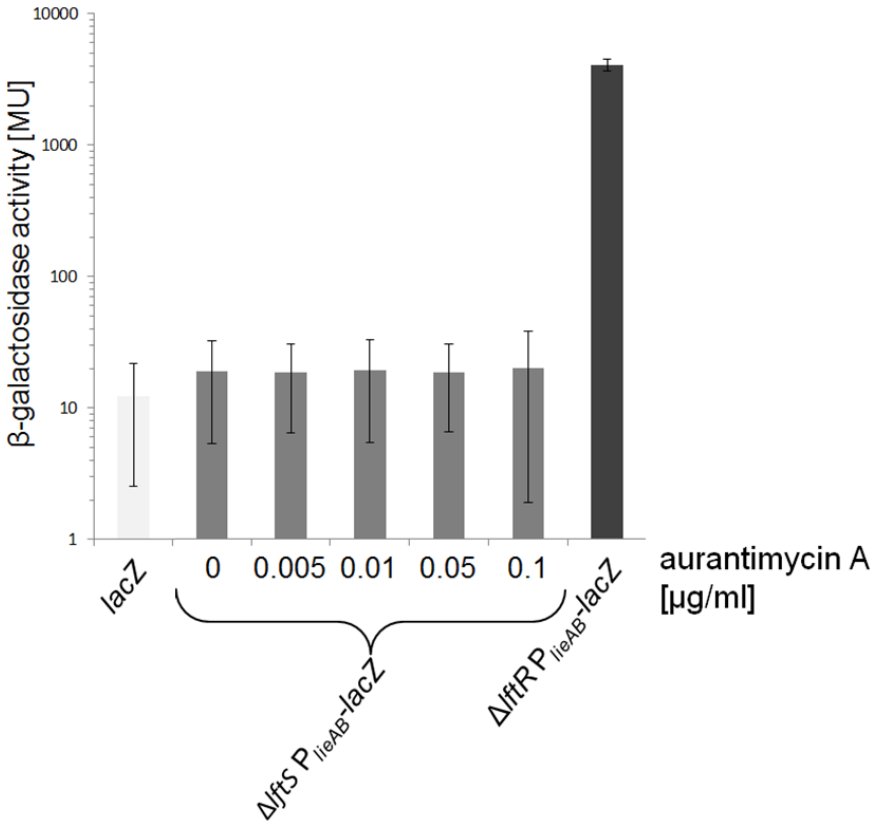

Figure 3.11: Quantification of the effect of *lftS* on P_{lieA} induction. The β-galactosidase activity of strain LMSH27 (Δ*lftS*) was quantified using the ONPG assay. The cells were grown at 37°C in BHI medium containing increasing aurantimycin concentrations until reaching mid-exponential phase. The strains LMSH16 (promoter-less *lacZ*) and LMSH34 (Δ*lftR* P_{lieA}-*lacZ*) are shown as controls for inactive and active *lacZ* transcription.

The observation that *lftS* is essential for the induction of LftR-controlled genes could mean that either LftS acts as an independent activator of transcription for those promoters or that LftS acts through LftR by relieving the LftR-dependent repression in the presence of effector molecules. To determine which is the case, the β-galactosidase activity of the P_{lieA}-*lacZ* reporter was measured for the wild type, the Δ*lftS*, Δ*lftR* and Δ*lftRS* mutants in the presence or absence of 50 ng/ml aurantimycin. Previously published results indicated, that the ABC transporter BceAB is required for the control of expression of the *bceAB* genes in *B. subtilis* (Bernard et al. 2007). To test if the *lieAB* genes also play a role in the induction process, the Δ*lieAB* mutant was included in the experiment.

The results clearly showed, that there is no activity in the Δ*lftS* mutant (see figure 3.12).

The identical promoter activity of the Δ*lftR* and Δ*lftRS* mutants implied that LftS does not have an effect on the promoter activity in absence of *lftR* (see figure 3.12). This indicates that LftS is not an independent activator, but acts through LftR. The Δ*lieAB* mutant behaved like the wild type ruling out the possibility that the transporter LieAB is involved in gene regulation. Therefore, LftR is the dominant factor for repression of the *lieAB* genes and LftS acts on LftR to activate transcription in the presence of effector.

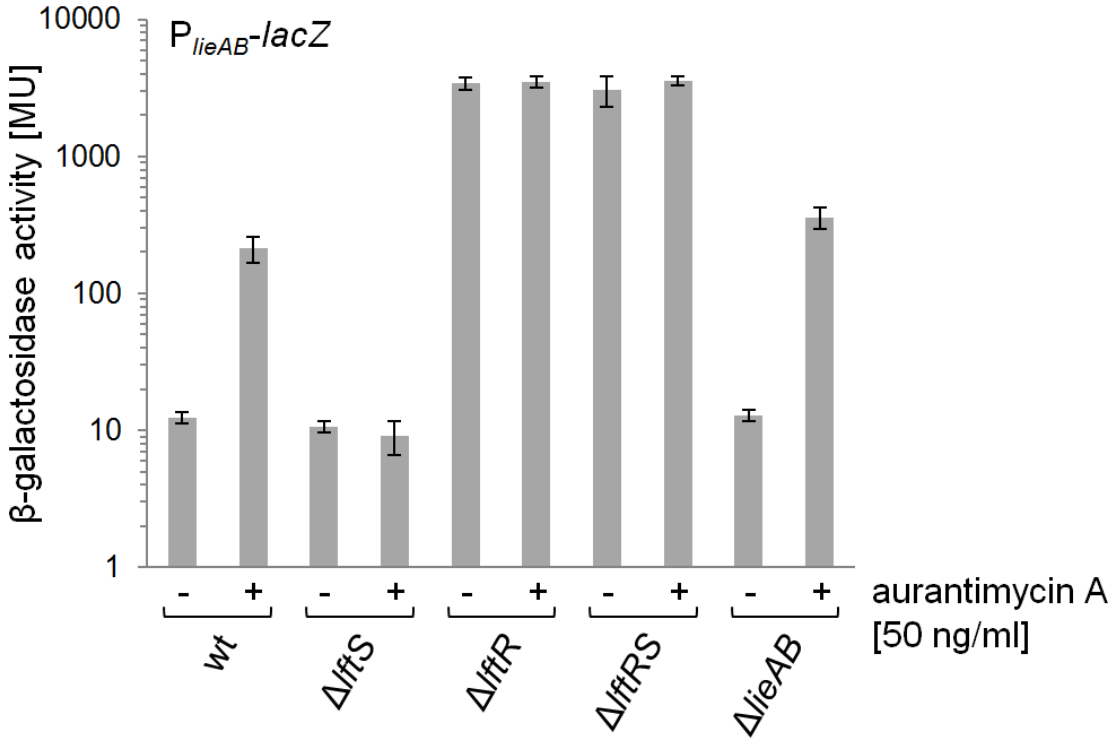

Figure 3.12: Effect of other genes in the LftR regulon on P_{lieA} induction. Aurantimycin A induced β-galactosidase activity in *lftRS* and *lieAB* mutants. Strains LMSH5 (P_{lieA}-*lacZ*), LMSH27 (Δ*lftS* P_{lieA}-*lacZ*), LMSH34 (Δ*lftR* P_{lieA}-*lacZ*), LMSH64 (Δ*lftRS* P_{lieA}-*lacZ*) and LMSH65 (Δ*lieAB* P_{lieA}-*lacZ*) were grown without antibiotic or in the presence of 50 ng/ml aurantimycin A until reaching mid-exponential phase. After cell lysis, the β-galactosidase activity was measured in the ONPG assay. The average values and standard deviation of three replicates are shown.

3.2.3 Conditions leading to the activation of LstR-controlled genes

It was previously published that the PadR-like transcription factor LstR controls the transcription of the *sigC-lstR-lmo0421* operon and that the operon is activated by heat (Zhang et al. 2005). Using a P_{sigC}-*lacZ* (LMSH12) reporter strain in the wild type, it was tried to show the induction of P_{sigC} by heat, but under the conditions used no induction could be seen (data not shown). To test whether some secondary metabolite induces expression from P_{sigC}, the DZIF natural compound collection was screened as described in the section about the LftR-controlled genes. During this screen, a slight induction of the P_{sigC}-*lacZ* reporter was observed when the strain was exposed to the macrolide antibiotics niddamycin B (producer: *Streptomyces*) and josamycin (producer: *Streptomyces*). An even weaker induction, close to the detection limit, could be seen for chromomycin A3 (producer: *Streptomyces*) and streptovaricin (producer: *Streptomyces*). Using commercially available material, it could be confirmed that josamycin is a strong inducer of the *lstR* operon (see figure 3.13). The library screen further indicated that chromomycin induces the *lstR* operon, but this result could not be reproduced with commercially available chromomycin (see figure 3.13). The other compounds were not commercially available at the time of the experiments, so the induction could not be verified.

Because the *sigC* operon was induced by two different macrolide antibiotics, it was tested if other members of this class of antibiotics also induce the expression from the *sigC* promoter. Erythromyin and tylosin are commonly used drugs (EMA 1997, Principi and Esposito 1999) that were also tested for induction of the *lstR* operon. Both compounds induced β-galactosidase activity in the P_{sigC}-*lacZ* reporter strain (see figure 3.13). The strongest induction was observed with the 16-membered macrolides josamycin and tylosin. Erythromycin repeatedly induced the reporter but the induction level was very low compared to josamycin (see figure 3.13). This indicates a targeted inactivation of LstR by macrolides or via an intra-cellular response that is triggered by the exposure to macrolides. The concentrations of the macrolide antibiotics was varied in this experiment, because of the widely differing antibacterial activites against *L. monocytogenes*.

Interestingly, longer incubation at 37°C (for example over 48 hours) increased the signal intensity significantly for all macrolides (data not shown). Macrolide antibiotics inhibit bacterial protein biosynthesis by binding to the 50S subunit of the ribosome (Champney and Burdine 1995). The antibiotics that induce the *sigC-lstR-lmo0421* operon are therefore interfering with the ability of the bacteria to synthesize new proteins. It still remains unclear why the operon should be activated under such conditions. It could be possible that conditions inhibiting cell wall synthesis (for example antibiotics targeting RodA/FtsW function) induce the production of a resistance-conferring RodA/FtsW paralog, because LstR controls expression of the RodA/FtsW paralog Lmo0421. Contrary to this idea, all of the cell wall targeting antibiotics tested (see table 3.8) did not show induction of the P_{sigC}-*lacZ* reporter (data not shown).

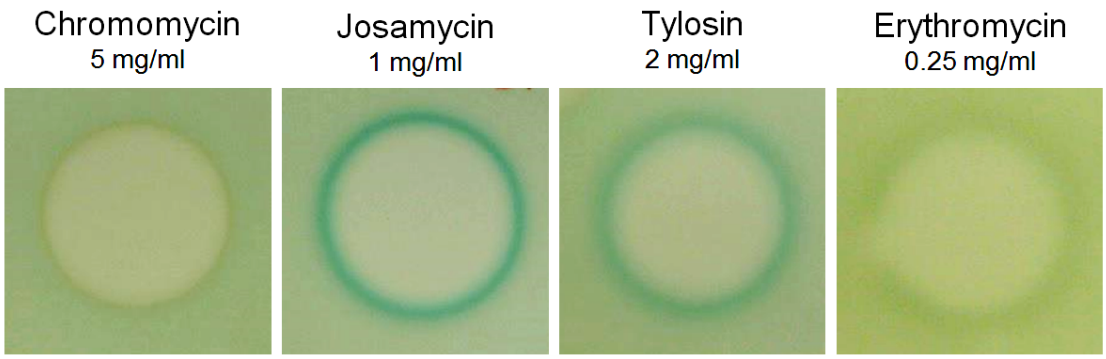

Figure 3.13: Induction of P_{sigC} by macrolide antibiotics. The P_{sigC} reporter strain LMSH12 was poured into BHI agar plates containing X-gal. Antibiotic solutions (2 μl) were spotted on top of the agar and the plates incubated over night at 37°C. The β-galactosidase activity resulting from the induction of the P_{sigC}-*lacZ* reporter construct can be seen by the blue color developing around a zone of complete growth inhibition.

3.2.4 Activity of the *lstR-sigC-lmo0421* operon depends on SigC

The *lstR-sigC-lmo0421* operon contains *sigC* and *lstR*, two proteins that are probably involved in the regulation of transcription from the *sigC* promoter (Zhang et al. 2005). In order to elucidate the role of SigC and LstR in the regulation of the *lstR-sigC-lmo0421* operon, a *sigC** mutant (LMSH89) containing a pre-mature stop condon and an *lstR** mutant (LMSH39) with amino acid exchanges in the DNA binding helix (L90A, L92A, L93A), as well as a *sigC** *lstR** double mutant (LMSH90) were constructed. Introduction of the P_{sigC}-*lacZ* reporter into these backgrounds yielded the reporter strains LMSH96 (*sigC** P_{sigC}-*lacZ*), LMSH63 (*lstR** P_{sigC}-*lacZ*), LMSH97 (*sigC** *lstR** P_{sigC}-*lacZ*), which were used together with strain LMSH12 (P_{sigC}-*lacZ*), LMSH13 (Δ*lstR* P_{sigC}-*lacZ*) and LMSH16 (*lacZ*) as controls for the following experiments. All strains were inoculated into BHI at an OD_{600} of 0.05 and grown at 37°C until reaching mid-exponential phase, harvested and lysed by sonification.

Quantification of the β-galactosidase activity in the above mentioned reporter strains showed that all promoter activity was abolished in the *sigC** background (see figure 3.14, panel A). SigC therefore seems to be essential for transcription from the *sigC* promoter. This is in agreement with results from Zhang et al. who observed that the expression of the *lstR* operon depends in part on SigC (Zhang et al. 2005).

SigC was also shown to be essential under inducing conditions. Induction by josamycin did not occur in the *sigC** mutant. Even in the *sigC** *lstR** double mutant the promoter was inactive, therefore promoter activity depended on an intact *sigC* gene (see figure 3.14 panel B). In the *lstR** single mutant the P_{sigC} promoter was constitutively active. This can be seen in the high β-galactosidase activity in the ONPG assay (see figure 3.14, panel A)

or the strong blue background coloration in the agar based experiment (see figure 3.14, panel B). Taken together these observations suggest that SigC is actively promoting transcription of its own operon under the conditions studied and the transcriptional control is based on negative regulation by LstR. Importantly, the Δ*lstR* and *lstR** mutants produced identical results in the β-galactosidase assay, indicating that the mutations introduced in the *lstR** mutant completely abolish the binding of the repressor to the DNA.

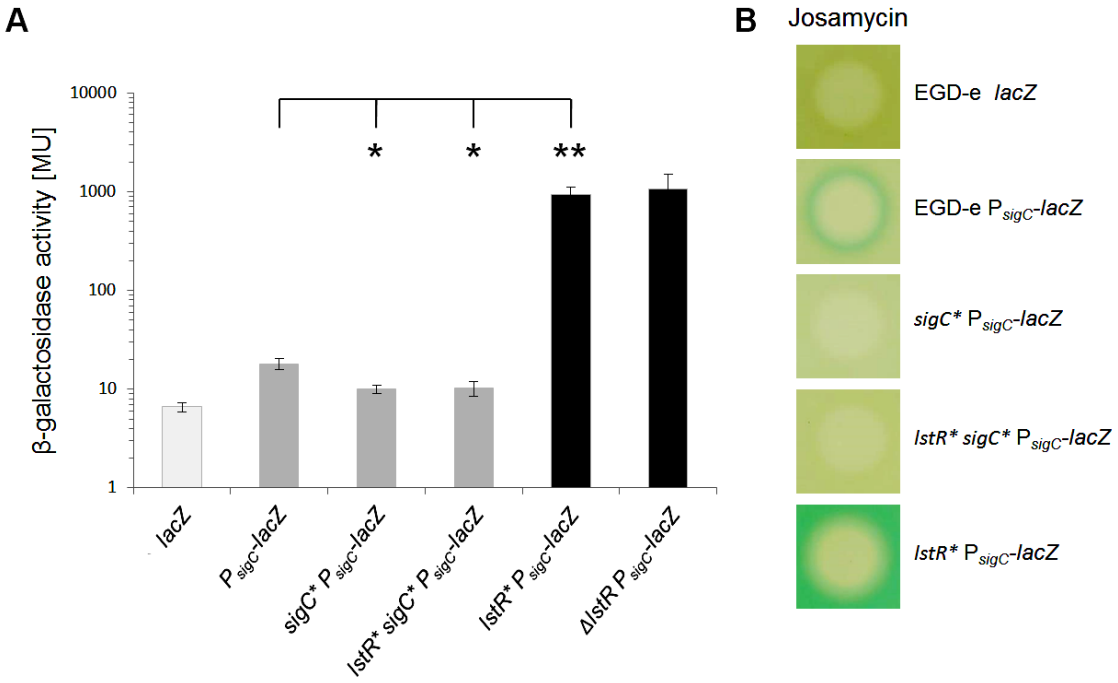

Figure 3.14: Effect of *sigC* on transcription and induction of the *sigC-lstR-lmo0421* operon. The expression from the *sigC-lstR-lmo0421* operon depends on SigC. Panel A: The strains LMSH96 (*sigC** P_{sigC}-*lacZ*), LMSH63 (*lstR** P_{sigC}-*lacZ*), LMSH97 (*sigC** *lstR** P_{sigC}-*lacZ*), together with strain LMSH12 (P_{sigC}-*lacZ*), LMSH13 (Δ*lstR* P_{sigC}-*lacZ*) and LMSH16 (promoter-less *lacZ*) as controls, were grown in BHI at 37°C until mid-exponential phase and β-galactosidase activity quantified after sonification. The average values of three independent experiments are shown with standard deviation. Asterisks indicate the statistical significance (t-test): $P<0.01$ *, $P<0.001$ **. Panel B: The same strains grown in BHI agar at 37°C over night with 2 μl of a josamycin solution (1 mg/ml) spotted on top of the agar.

3.3 The genes of the LftR regulon contribute to aurantimycin-resistance

It has been shown in the previous sections that LftR regulates the expression of the *lieAB* permease genes and of its own operon *lftRS*. These genes were expressed in the presence of rhodamine 6G (see figure 3.7), which is likely to be an artificial substrate, because it does not occur naturally (Cooksey 2016). On the other hand, the depsipeptide antibiotic aurantimycin A (Graefe et al. 1995) is a naturally occurring inducer of LftR-dependent gene expression (see figure 3.9). If the LieAB efflux pump is purposefully induced in the presence of aurantimycin, but not by rhodamine 6G, then it should convey some kind of benefit to the cell when exposed to the former substance, but not to the latter. To test if the cells become resistant, MICs were determined for the wild type and Δ*lftR*, Δ*lftS*, Δ*lieAB* and Δ*lftR*Δ*lieAB* mutants.

As can be seen from table 3.9, the Δ*lftR* mutant is 2 times as resistant against aurantimycin as the wild type or Δ*lftS* mutant. In contrast, mutants missing the *lieAB* transporter genes are much more sensitive to aurantimycin A. However, there is no such effect on resistance against rhodamine 6G (see table 3.9). This supports the hypothesis that LieAB contributes to resistance against aurantimycin A but not against rhodamine 6G. Moreover, these results are in good agreement with the hypothesis of LftR acting as a repressor of *lieAB* transcription. Thus, LftR seems to react to the same compound that is detoxified by LieAB.

Table 3.9: Aurantimycin A and rhodamine 6G MIC values. MIC values for the wild type and strains lacking genes of the *lftRS* and/or *lieAB* operons when exposed to aurantimycin A or rhodamine 6G. The strains used were LMKK26 (Δ*lftS*), LMSH26 (Δ*lftR*), LMS160 (Δ*lieAB*) and LMSH35 (Δ*lftR* Δ*lieAB*). Three independent experiments were performed and the average is shown. Deviation between the replicates was minimal to not existent (data not shown).

Genotype	**MIC aurantimycin A [μg/ml]**	**MIC rhodamine 6G [μg/ml]**
wild type	1.25	2
Δ*lftS*	1.25	2
Δ*lftR*	2.5	2
Δ*lieAB*	0.156	2
Δ*lftR* Δ*lieAB*	0.156	2

Mutants lacking the *lieAB* genes showed a strongly reduced MIC towards aurantimycin (see table 3.9). This was an indication for active transport of the antibiotic by LieAB. It was known that aurantimycin is forming pores in biological membranes (Grigoriev et

al. 1995). Pores in the membrane usually lead to rapid cell lysis and death. To observe if aurantimycin causes cell lysis, the wild type, Δ*lftR* and Δ*lftR* Δ*lieAB* mutants were incubated in buffer with or without aurantimycin. The OD of the cell suspensions was monitored during incubation at 37°C.

It can be clearly seen in figure 3.15 that all strains do significantly lyse in buffer containing aurantimycin (see figure 3.15, panel B), but not in plain buffer (see figure 3.15, panel A). Aurantimycin therefore causes cell lysis, but no differences between the wild type and the Δ*lftR* (over-producing LieAB) and Δ*lftR* Δ*lieAB* (lacking LieAB) mutants could be observed. The LieAB transporter belongs to the ABC-type (ATP binding cassette) of transporters and thus requires energy in the form of ATP to be active (Kaval et al. 2015). Therefore, the effect of glucose addition to the lysis buffer was also investigated (see figure 3.15, panel C). Under energizing conditions, the cells lacking *lftR*, and thus over-producing LieAB, are more resistant towards aurantimycin-induced lysis than the wild type or the Δ*lieAB* (lacking LieAB) mutant. This observation proves that the energy dependent transport of aurantimycin by LieAB protects the cells from lysis.

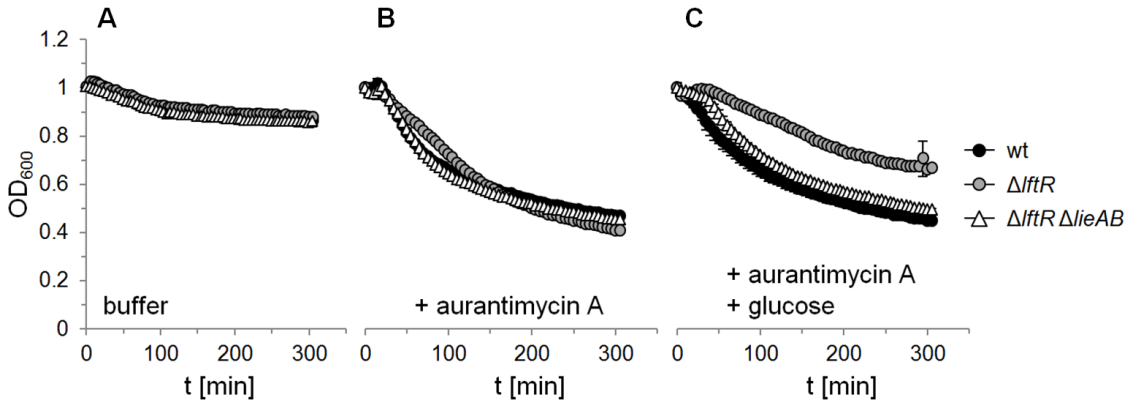

Figure 3.15: Aurantimycin A mediated lysis of *L. monocytogenes*. Wild type cells and the Δ*lftR* (LMSH26) and Δ*lftR* Δ*lieAB* (LMSH35) mutants were grown to mid-exponential phase, harvested and re-suspended in Tris-buffer. The addition of aurantimycin A to the buffer causes significant cell lysis (panel B) when compared to plain buffer (panel A). The Δ*lftR* mutant overexpressing *lieAB* is significantly more resistant to aurantimycin-induced lysis, once glucose is added as an energy source (panel C).

3.3.1 Identification of spontaneous aurantimycin-resistant suppressor mutants

It has been shown that the Δ*lftS* mutant cannot induce *lieAB* expression upon exposure to aurantimycin (see figure 3.11). Nevertheless, the Δ*lftS* mutant has the same MIC as the wild type that can induce the transcription of the resistance genes (see table 3.9). This apparent contradiction led us to examine the growth kinetics of the wild type and the Δ*lftS* (LMKK26), Δ*lieAB* (LMS160) and Δ*lftS* Δ*lieAB* (LMSH66) mutants in the presence of aurantimycin. For this purpose, the strains were initially grown to mid-exponential phase in the presence of sub-inhibitory aurantimycin concentrations (100 ng/ml). The aurantimycin-adapted cells were used to inoculate new growth curves using medium with different antibiotic concentrations. The influence differing antibiotic concentrations have on the kinetics of growth gives more detailed information than the end point determination of MIC values.

It can be seen in figure 3.16 that the stains Δ*lieAB* and Δ*lftS* Δ*lieAB* do not grow at the aurantimycin concentrations tested. The wildtype on the other hand shows a gradually increasing lag phase when exposed to increasing aurantimycin concentrations. This can be expected, when increasing concentrations of the antibiotic lead to the lysis of a successively greater part of the cells. Interestingly, the Δ*lftS* mutant did not behave like the wild type in this experiment, although it had an identical MIC. In the absence of aurantimycin, the Δ*lftS* mutant grew like all other strains tested, but in the presence of aurantimycin growth was only detectable after around 15 hours of incubation at 37°C, regardless of the antibiotic concentration applied. The growth is *lieAB*-dependent, because the Δ*lftS* Δ*lieAB* mutant completely failed to grow in the presence of aurantimycin.

The increased lag phase in medium containing aurantimycin could imply that fewer cells form the initially viable inoculum, so it takes longer until growth is detectable (Hoffmann et al. 2018). This would make sense, because aurantimycin supposedly kills the cells by disrupting their plasma membrane (see figure 3.15). Antibiotics acting by inhibiting growth would have an impact on the growth rate of bacteria (Frenkel et al. 2018). In such a case, the growth curves would have a lower slope. For the Δ*lftS* strain, growth in the presence of aurantimycin was only detected after around 15 hours of incubation, regardless of the antibiotic concentration applied. For strains missing the ABC-type transporter LieAB no growth is observable in the presence of the aurantimycin concentrations tested.

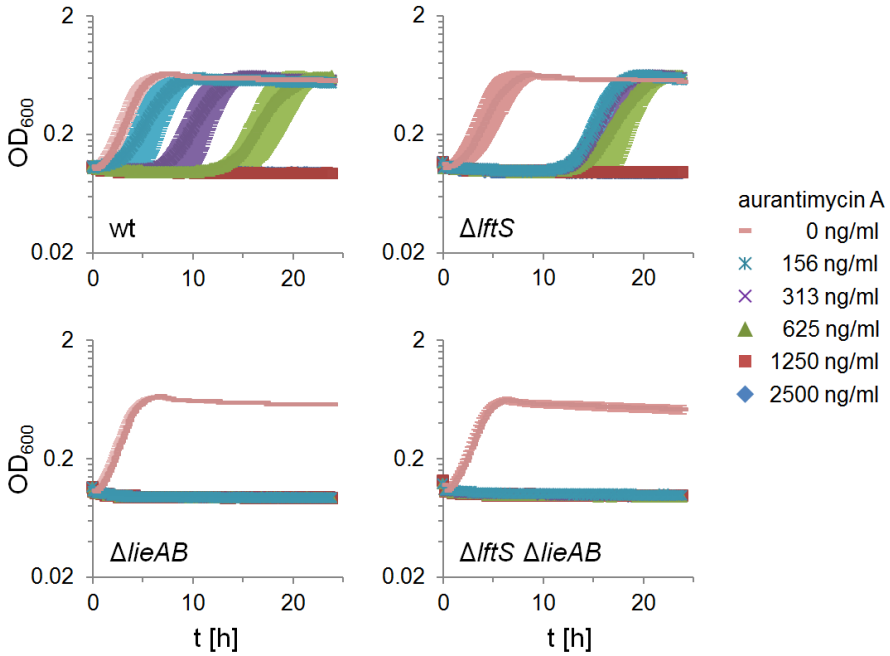

Figure 3.16: Growth at different aurantimycin A concentrations. Growth of the wild type and strains LMKK26 (Δ*lftS*), LMS160 (Δ*lieAB*) and LMSH66 (Δ*lftS* Δ*lieAB*) at 37°C in BHI with aurantimycin A concentrations as indicated. To activate *lieAB* expression, all strains were initially grown at a sub-inhibitory aurantimycin concentration of 100 ng/ml to mid-exponential phase before starting the experimental culture whose OD_{600} is shown. Average values and standard deviations of three independent experiments are depicted.

The strange growth behaviour of the Δ*lftS* mutant could imply that some cells resistant to aurantimycin have grown to a detectable OD_{600} after around 15 hours. To test this assumption, wild type and Δ*lftS* cells grown in the presence of 625 ng/ml aurantimycin were used to re-inoculate a new culture (see figure 3.17). The OD_{600} of this culture was monitored to quantify the growth behaviour. For comparison, growth of the wild type and the Δ*lftS* mutant, pre-grown at the sub-inhibitory concentration of 100 ng/ml in order to induce *lieAB* expression, were also monitored.

Figure 3.17 shows that the cultures pre-grown at sub-inhibitory concentrations of aurantimycin A showed an increased lag phase, while the cells re-inoculated from a culture containing 625 ng/ml aurantimycin (sufficient to cause lysis) did not exhibit any lag phase except at 1250 ng/ml. At this high concentration the wild type and Δ*lftS* cells pre-grown at sub-inhibitory concentrations were unable to grow. These results suggest, that the cells that have grown in the presence of 625 ng/ml aurantimycin A developed a resistance to the antibiotic.

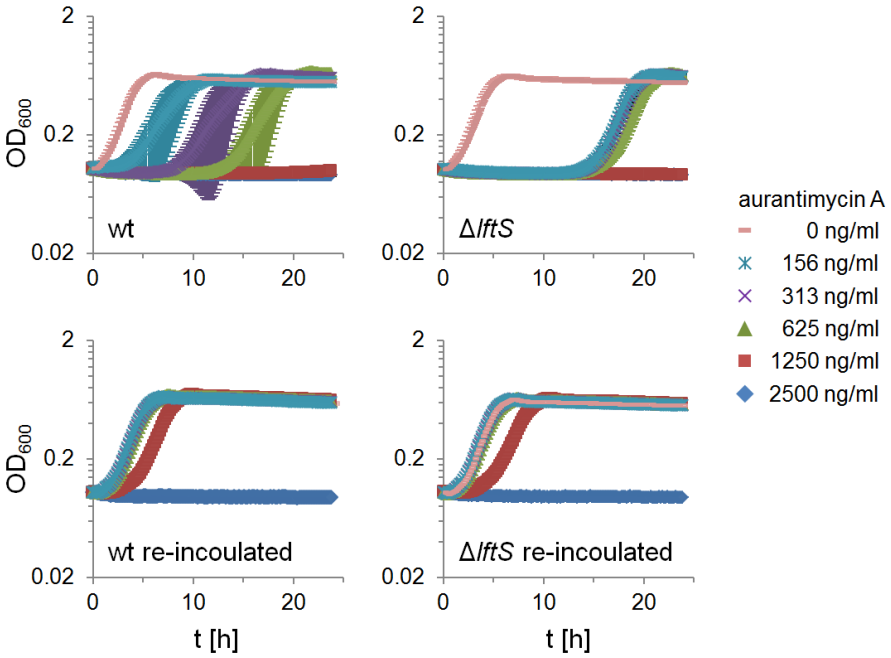

Figure 3.17: Formation of aurantimycin-resistant suppressors. Growth of wild type and Δ*lftS* (LMKK26) cells without (top) or with (bottom) previous contact to a lytic aurantimycin A concentration (625 ng/ml). The immediate growth of the re-inoculated cultures indicated the development of suppressors resistant to the antibiotic. Average values and standard deviations of three replicates are shown.

To clarify if the resistance was a transient or heritable, single wild type and Δ*lftS* colonies grown from resistant liquid cultures were isolated on BHI agar without aurantimycin. After growth on agar and in liquid medium without the antibiotic, the isolated bacteria were still resistant to aurantimycin (data not shown). It therefore seemed possible that hertiable mutations in the genome were the cause of the resistance.

It is known that inactivation of *lftR* leads to the overproduction of the LieAB transporter (Kaval et al. 2015) and that the LieAB transporter protects the cells from lysis in the presence of aurantimycin (see figure 3.15). It was therefore likely that the mutations impacted LftR. To test whether *lftR* did mutate in the resistant cells, the genomic region of *lftR* including its promoter was amplified by PCR from 20 single putative suppressors of the wild type (LMSH121-140) or the Δ*lftS* strain (LMSH141-160), grown in 20 separate cultures in the presence of 750 ng/ml aurantimycin. The PCR product was sequenced to find potential mutations.

Table 3.10: Aurantimycin suppressor mutations. Mutations found in wild type and Δ*lftS* cells grown in the presence of 750 ng/ml aurantimycin. Each suppressor was grown in a separate well of a 96-well plate. The base exchanges detected are indicated together with their position in the genome and the resulting effect they have on the LftR protein.

Strain	Background	Mutation	Effect
LMSH121	WT	G750063A	LftR: G27S
LMSH122	WT	A750155 deletion	LftR: frame shift
LMSH123	WT	G749972T	*lftR* RBS mutation
LMSH124	WT	G750063A	LftR: G27S
LMSH125	WT	A750080 deletion	LftR: frame shift
LMSH126	WT	A750155 deletion	LftR: frame shift
LMSH127	WT	A750080 deletion	LftR: frame shift
LMSH128	WT	G749973T	*lftR* RBS mutation
LMSH129	WT	C750039T	LftR: premature stop
LMSH130	WT	A750182 deletion	LftR: frame shift
LMSH131	WT	A750155 deletion	LftR: frame shift
LMSH132	WT	C750121T	LftR: T46M
LMSH133	WT	C750062A	LftR: premature stop
LMSH134	WT	A insertion afterA750155	LftR: frame shift
LMSH135	WT	A750080 deletion	LftR: frame shift
LMSH136	WT	A749939G	P_{lftR} -10 box mutation
LMSH137	WT	T750252 deletion	LftR: frame shift
LMSH138	WT	A750155 deletion	LftR: frame shift
LMSH139	WT	A750155 deletion	LftR: frame shift
LMSH140	WT	A750155 deletion	LftR: frame shift
LMSH141	Δ*lftS*	G750193A	LftR: G70D
LMSH142	Δ*lftS*	C750141T	LftR: R53C
LMSH143	Δ*lftS*	C750141T	LftR: R53C
LMSH144	Δ*lftS*	C750141T	LftR: R53C
LMSH145	Δ*lftS*	C749998T	LftR: T5I
LMSH146	Δ*lftS*	G750237T	LftR: premature stop
LMSH147	Δ*lftS*	C750141T	LftR: R53C
LMSH148	Δ*lftS*	C750141T	LftR: R53C
LMSH149	Δ*lftS*	T750252 deletion	LftR: frame shift
LMSH150	Δ*lftS*	G750253A	LftR: premature stop
LMSH151	Δ*lftS*	G750165T	LftR: premature stop
LMSH152	Δ*lftS*	T750252 deletion	LftR: frame shift
LMSH153	Δ*lftS*	T750252 deletion	LftR: frame shift
LMSH154	Δ*lftS*	G750237T	LftR: premature stop
LMSH155	Δ*lftS*	C750141T	LftR: R53C
LMSH156	Δ*lftS*	C750141T	LftR: R53C
LMSH157	Δ*lftS*	T750252 deletion	LftR: frame shift
LMSH158	Δ*lftS*	T750252 deletion	LftR: frame shift
LMSH159	Δ*lftS*	C750141T	LftR: R53C
LMSH160	Δ*lftS*	C750141T	LftR: R53C

As expected, mutations in the *lftR* gene could be found in all suppressors. A complete list of all mutations that were identified is given in table 4.2. The inactivation of the repressor in some cells led to the observation that the Δ*lftS* strain has the same MIC as the wild type. Interestingly, when the same procedure to select suppressors was done for the wild type, suppressors were also isolated. From 20 colonies grown separately at 750 ng/ml aurantimycin (highest concentration yielding growth), all 20 were suppressors with mutations in *lftR* or its promoter (see table 4.2). Besides mutations that obviously inactivate LftR, like premature stop codons or frame shifts, five single amino acid substitutions in LftR were found (G27S, T46M, G70D, R53C and T5I). These might causally link the de-repression to the structure and function of LftR (see discussion).

3.4 Identification of the LftR operator site

3.4.1 Determination of the minimal P_{lieA} promoter

To identify the region of the DNA containing the regulatory elements required for the promoter activity, the 266 bp long P_{lieA}-*lacZ* reporter (LMSH5) used in the induction screens described above was consecutively shortened to 193 bp, 152 bp, 122 bp and 97 bp upstream of the *lieAB* start codon. The resulting reporter strains were LMSH30, LMSH31, LMSH32 and LMSH33. The activity of the shortened P_{lieA}-*lacZ* reporter constructs was determined by spotting 2 μl aurantimycin (2.5 mg/ml) onto the respective reporter strains in the agar based induction assay also described above. Panel B in figure 3.18 shows that the shortest promoter retaining inducability by aurantimycin is 122 bp long. An *in silico* promoter prediction using the bprom online tool indicates that the next shortest region (97 bp in length) has lost the -35 box of the promoter (Solovyev and Salamov 2011). Without the -35 box, transcription initiation is no longer possible. This explains the observation that the 97 bp long fragment is no longer showing inducability. The 122bp long P_{lieA} promoter retained promoter activity, but was inactive unless induced by aurantimycin. This indicated that this fragment must contain all elements necessary for initiation of transcription as well as the LftR operator site.

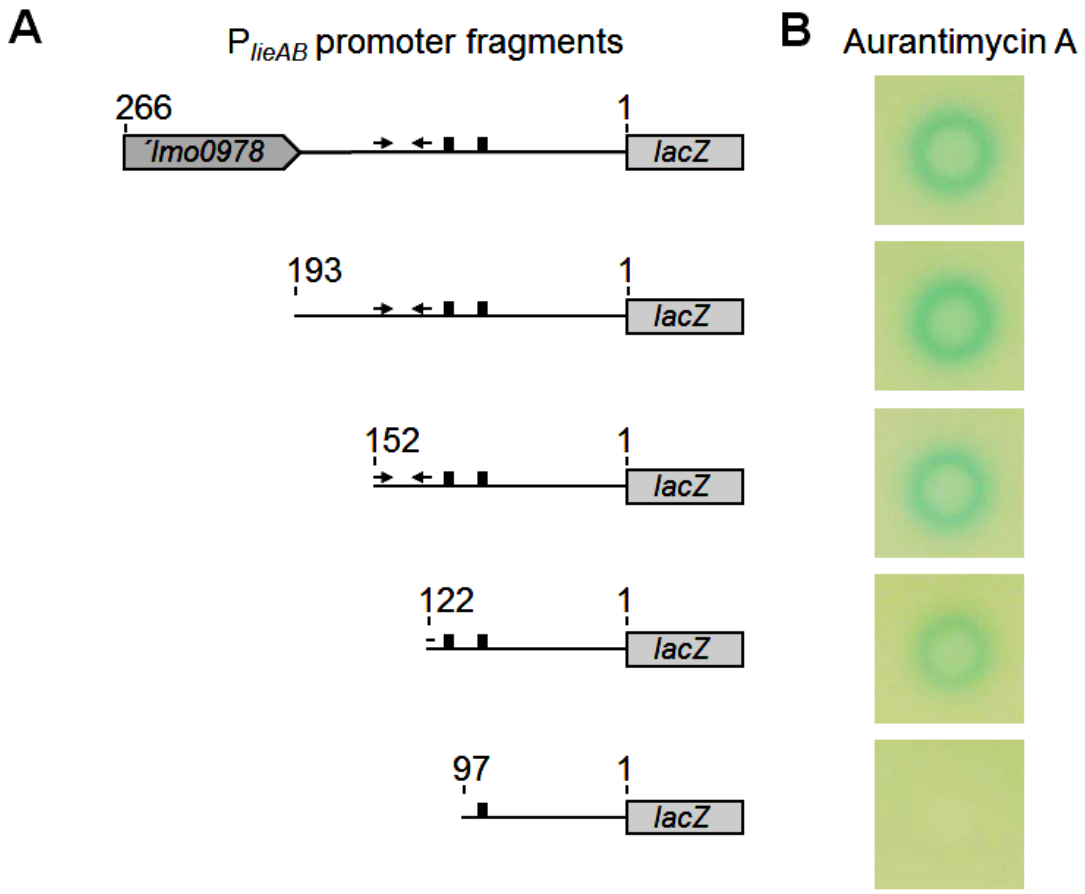

Figure 3.18: Defining the minimal P_{lieA} promoter. The initially constructed P_{lieA}-*lacZ* reporter (LMSH5) contained a 266 bp long fragment upstream of *lieA*. Shown in panel A is the consecutive shortening of this region to 193 bp (LMSH30), 152 bp (LMSH31), 122 bp (LMSH32) and 97 bp (LMSH33) upstream of *lieA*. Black boxes indicate the promoter boxes and arrows an inverted repeat present in the sequence. Panel B shows a loss of LacZ-activity for the 97 bp long fragment when induced by 2 μl aurantimycin A (2.5 mg/ml).

3.4.2 Identification of the P_{lieA} promoter region important for LftR binding

The previous results indicated that the 122 bp long promoter fragment contains the LftR operator. The next step in the identification of the LftR operator was to find DNA bases important for the binding by LftR. Based on the shortest active fragment identified, 10 bp long stretches of the promoter were mutated. Here, transversions of A to T, T to A, G to C, or C to G were made in order to prevent significant changes in DNA melting behaviour. These mutations were carried out in the region between base pair 69 and base pair 21 before the *lieA* start codon. Residues 122-69 were not mutated, because they contain the -35 and -10 box. Residues after base pair 21 were also not mutated, because they containd the ribosome binding site. The five mutants versions of the P_{lieA}-*lacZ* reporter made resulted in the strains LMSH44, LMSH45, LMSH46, LMSH47, and LMSH48. The DNA sequence of the resulting promoter fragments is shown in figure 3.19 (panel A). The ribosome binding site is also indicated in gray. When these strains were investigated for promoter activity and inducability by aurantimycin, the first two (containing mutations between the base pairs 69 and 51) showed high β-galactosidase activity (blue color) even in the absence of aurantimycin (see figure 3.19, panel B). The de-repression observed suggests that the region between base pair 69 and 51 contains the sought after LftR binding motif.

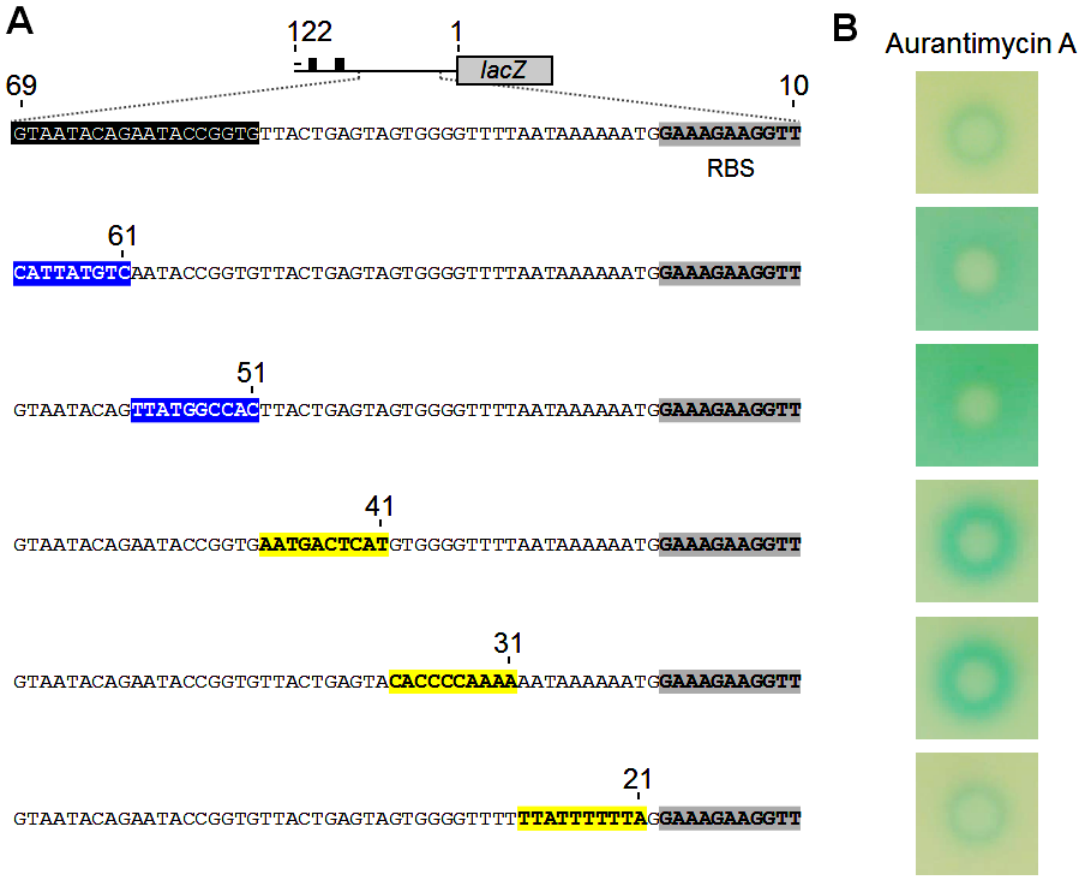

Figure 3.19: Identification of DNA regions important for LftR binding. Mutations in 10 bp long stretches of the P_{lieA}-*lacZ* reporter were made resulting in the strains LMSH44, LMSH45, LMSH46, LMSH47, and LMSH48. The resulting DNA sequences are shown with mutations having an effect on the promoter activity highlighted in blue and mutations without a visible effect highlighted in yellow. The ribosome binding site is indicated in gray (see panel A). The β-galactosidase activity, as measured in the agar-based assay, shows that mutations in the region between 69 bp and 51 bp before the *lieAB* start codon result in a visible constitutive expression from P_{lieA} as indicated by the blue background (see panel B).

3.4.3 Systematic mutagenesis of the 69-51 bp region of the P_{lieA} promoter to identify the LftR binding motif

With the information obtained, the region between base pair 69 and 51 upstream of the *lieAB* start codon should contain the putative LftR binding site. The next step was a more targeted mutational analysis of 2 base pairs at a time in this region. Like before, the mutations made were transversions (A to T, T to A, G to C, or C to G). The ten resulting strains (LMSH51 to LMSH61) were screened in the agar-based and the β-galactosidase assay for their promoter activity and inducability by aurantimycin. The wild type and Δ*lftR* mutant were used as controls. The modified promoter sequences are shown in figure 3.20, panel A, with mutations impacting LftR binding highlighted in blue and mutations without a significant impact highlighted in yellow. The results of the agar based assay indicate that starting from the duplet of base pairs 69-68 to the duplet 57-56 every second duplet has a significant effect on the strength of repression. This can be seen in the strongly blue background in the agar-based assay (figure 3.20, panel B). The promoter activity was measured by quantifying the resulting β-galactosidase activity (figure 3.20, panel C). These results confirmed the agar-based experiments and suggest that the base pairs GT-NN-TA-NN-GA-NN-AC are important for the LftR-DNA interaction.

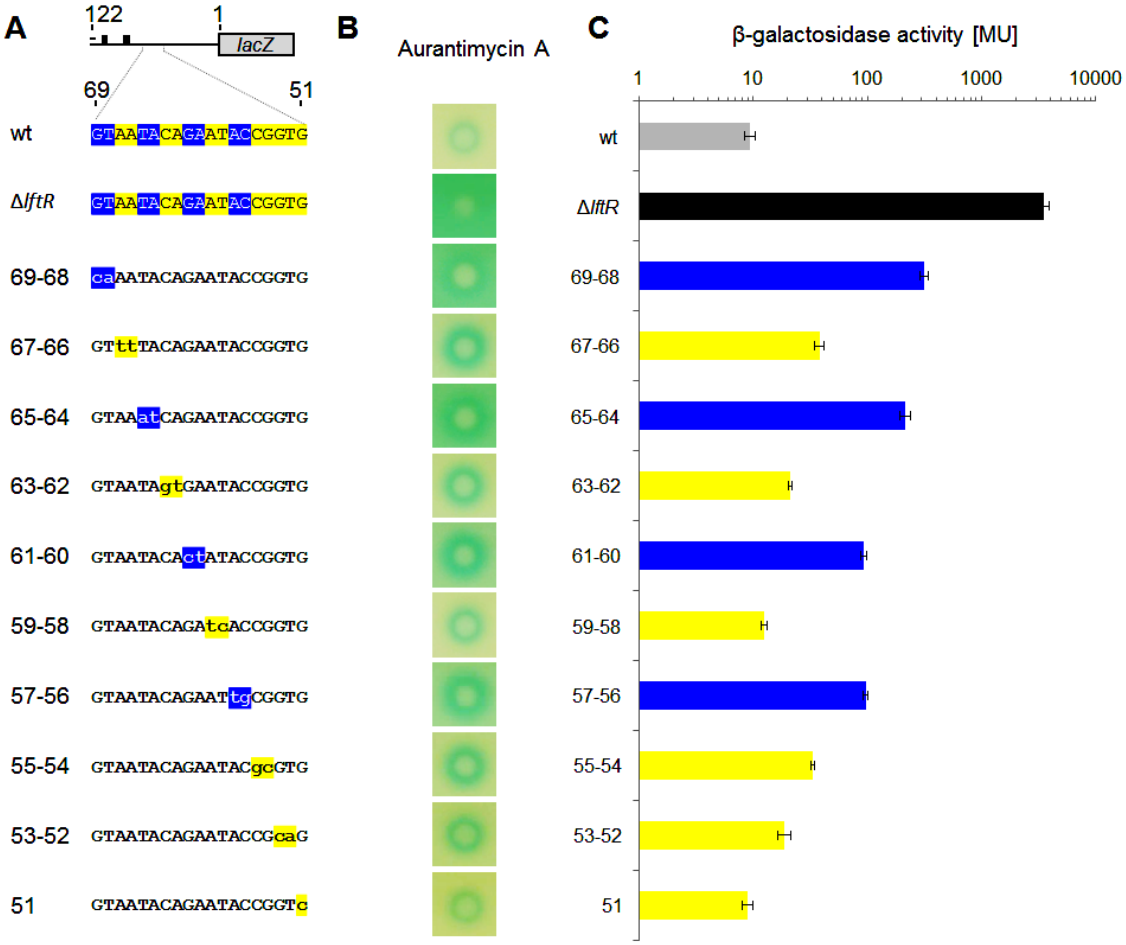

Figure 3.20: Identification of base pairs important for the LftR-DNA interaction. Mutations in 2 bp long stretches (duplets) of the 69-51 bp region were made resulting in the ten strains LMSH51 to LMSH61. The resulting DNA sequences are shown in panel A, with mutations impacting LftR binding highlighted in blue and mutations without a significant impact highlighted in yellow. Panel B: Results of the agar-based assay for P_{lieA} activity and inducability. The wild type and Δ*liftR* mutant are shown for reference. Panel C: β-galactosidase activity measurements for P_{lieA} activity of the mutated reporters. Shown are average values and standard deviations from three independent experiments.

3.4.4 Confirmation of the LftR operator in P_{lftRS}

It was shown by RNA sequencing that LftR regulates both the *lieAB* and the *lftRS* operons. Therefore, the LftR binding motif must be present in the promoter region of both genes. Comparing the 14 bp long stretch identified in the *lieA* promoter to the *lftR* promoter, a shared motif could be identified (see figure 3.21). This motif is located 13 bp downstream of the -10 box of the P_{lieA} promoter, but it overlaps with the -10 box in the P_{lftR} promoter. It should thus be impossible to modify without disrupting the promoter activity. Interestingly, a second putative binding site in the P_{lieA} promoter became obvious at this stage (underlined in red in figure 3.21). Mutations in this region did not result in altered promoter activity or inducibility, though (data not shown).

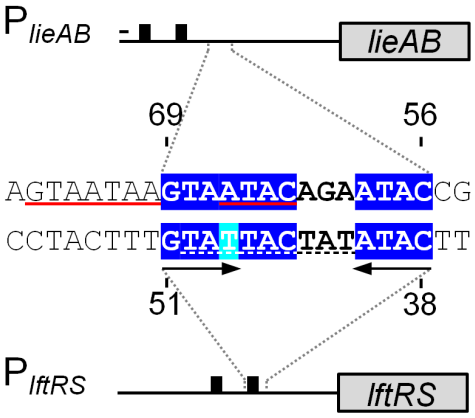

Figure 3.21: A sequence comparison of the *lieA* and *lftR* promoters. A common motif (high-lighted in blue with light blue indicating an AT wobble position) could be identified in both the *lieA* and the *lftR* promoters. Arrows further indicate the inverted repeat at the beginning and the end of the proposed binding site. Underlined in red is a second putative binding site in the *lieA* promoter. The overlapping -10 box of the *lftR* promoter is underlined by a dashed line.

Three mutants with inverted base pairs at the beginning (LMSH69 = mutant 1), end (LMSH70 = mutant 2) and middle (LMSH71 = mutant 3) of the proposed binding site in the *lftR* promoter were constructed and tested for promoter activity in the agar-based assay with the wild type promoter as a control (see figure 3.22, panel B). The promoters of mutants 1 and 3 showed no activity even in the presence of the inducer aurantimycin A, because the mutations introduced alter the -10 box (dashed underline in panel A of figure 3.22). When the end of the putative binding motif was mutated though, a strong blue background color resulted (see mutant 2 in figure 3.22, panel B). The fact that the mutation of the second part of the inverted repeat constitutively activates the P_{lftR} promoter confirmed the binding site identified in the *lieA* promoter.

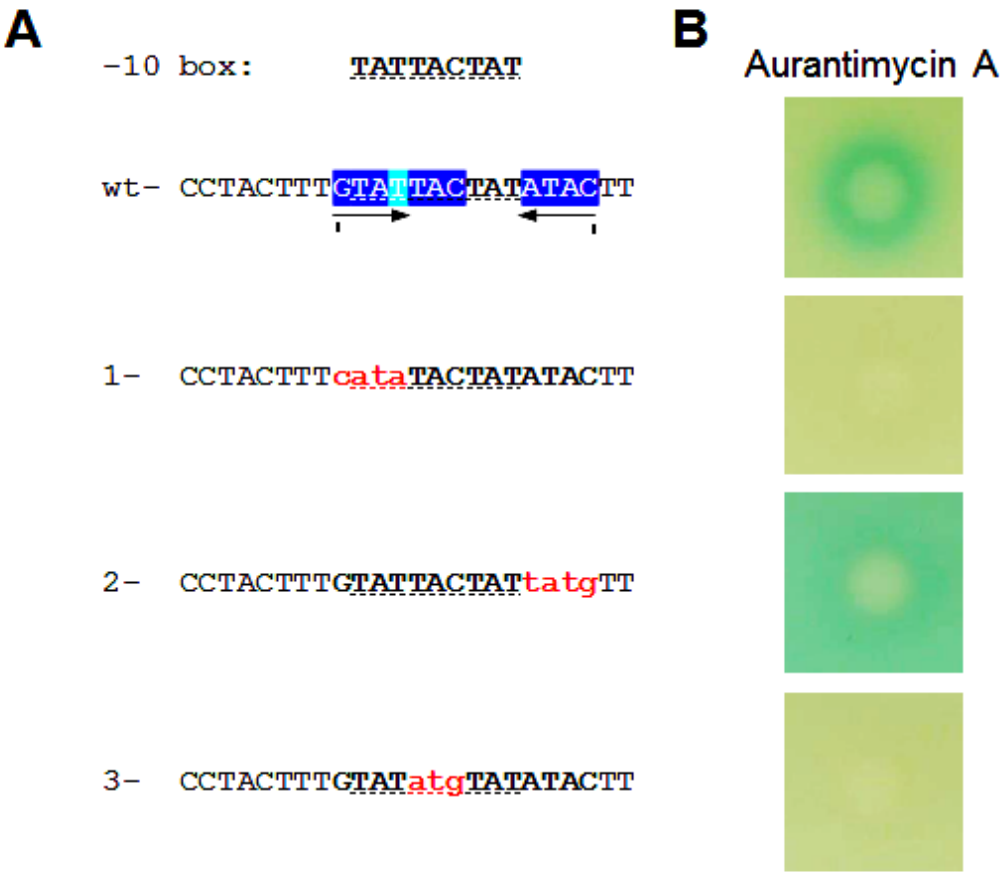

Figure 3.22: Mutations confirming the LftR binding motif in the *lftR* promoter. The reporter strains LMSH69 (mutant 1), LMSH70 (mutant 2) and LMSH71 (mutant 3) were created to confirm the putative LftR binding motif (highlighted in blue) in the *lftR* promoter. The mutations introduced in the three mutants are shown in red print (panel A). The inactivation of the downstream part of the inverted repeat (indicated by black arrows) in mutant 2 resulted in strong activity of the P_{lftR} promoter (panel B). The promoters of mutant 1 and 3, mutating the beginning or middle of the binding motif, show no activity even in the presence of the inducer aurantimycin (panel B).

3.5 Effect of the genes *sigC*, *lstR* and *lmo0421* on the resistance against the inducing macrolides josamycin and tylosin

In previous sections, it was shown that LstR mainly controls the expression of its own operon (*sigC-lstR-lmo0421*) and that expression of this operon is notably induced by the 16-membered macrolide antibiotics josamycin and tylosin. Following the results obtained with aurantimycin in the case of LftR, the MIC values of the inducing antibiotics were determined by the broth dilution method for different mutants lacking individual genes of the *sigC* operon or combinations thereof. The strains LMSH39 (*lstR**), LMSH40 (*lstR**Δ*lmo0421*), LMSH89 (*sigC**), LMMSH90 (*lstR** *sigC**) were investigated for altered resistance levels compared to the wild type. In contrast to the LftR case though, the MICs were identical for nearly all strains tested (see table 3.11). Here, the induction of *lmo0421* expression in the *lstR** mutant did not lead to detectable resistance against josamycin or tylosin, nor did the deletion of *lmo0421* affect the resistance against these antibiotics.

Table 3.11: Macrolide MIC values. MIC values of the strains LMSH39 (*lstR**), LMSH40 (*lstR**Δ*lmo0421*), LMSH89 (*sigC**), LMMSH90 (*lstR** *sigC**) exposed to the inducing macrolides josamycin and tylosin. Average values of three independent experiments are shown and the wild type MIC is listed for reference.

Genotype	**MIC josamycin [μg/ml]**	**MIC tylosin [μg/ml]**
wild type	2	4
*lstR**	2	4
*lstR** Δ*lmo0421*	1.8	4
Δ*lmo0421*	2	4
Δ*sigC*	2	4
Δ*sigC lstR**	2	4

3.6 Effect of *lstR* and *lmo0421* on the resistance against cell wall targeting antibiotics

The *sigC-lstR-lmo0421* operon consists of two genes modulating transcription (*sigC* as an activator and *lstR* as an repressor), the gene regulated in this operon should be *lmo0421*. Lmo0421 contains streches of significant sequence homology to the RodA/FtsW family of cell division proteins involved in peptidoglycan polymerization (Emami et al. 2017, Rismondo et al. 2019). *L. monocytogenes* encodes 6 proteins belonging to the FtsW/RodA family based on sequence homology (Rismondo et al. 2019). Visualizing the sequence similarity of those proteins allows conclusions on their relationships to be drawn (Gabaldón 2005). Figure 3.23 shows a phylogenetic tree visualizing the sequence similarity between the 6 proteins. Using the well described *B. subtilis* RodA and FtsW proteins as a reference, it is possible to assign an approximate function to the listerial proteins (Henriques et al. 1998, Emami et al. 2017) and most of the enzymes have recently been characterized (Rismondo et al. 2019). As shown in figure 3.23, Lmo0421 is grouped outside both groups and might thus not be a typical FtsW- or RodA-like protein. The major difference seems to be a nearly 70 amino acid long region at the N-terminus of Lmo0421 that is mainly composed of hydrophilic amino acid and absent in the other FtsW/RodA-like proteins.

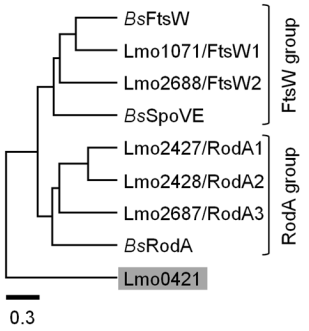

Figure 3.23: Phylogenetic tree visualizing the relationships between the 6 listerial proteins belonging to the RodA/FtsW family. The listerial proteins form two distinct clusters with the RodA/FtsW proteins *Bs*RodA, *Bs*FtsW and *Bs*SpoVE from *B. subtilis*. The *B. subtilis* proteins are shown as a reference, because their functions are well defined and seem to be identical to listerial proteins in the same cluster (Henriques et al. 1998, Emami et al. 2017, Rismondo et al. 2019).

The deletion of RodA/FtsW proteins usually leads to an alteration of the resistance to the antibiotic moenomycin that targets cell wall biosynthesis step mediated by these proteins (vanHeijenoort et al. 1987, Emami et al. 2017, Rismondo et al. 2019). In order to

determine the resistance level against moenomycin as well as other cell wall targeting antibiotics like penicillin and vancomycin, the strains *lstR** and *lstR*Δlmo0421* mutants were tested in diffusion assays. The results are shown in figure 3.24 and indicate that Lmo0421 does not act like a typical RodA/FtsW protein, because no differences in resistance could be observed for moenomycin. As none of the other cell wall targeting antibiotics causes any measurable effect, Lmo0421 also does not seem to have a role in the biosynthesis of the cell wall in general, at least under the conditions investigated.

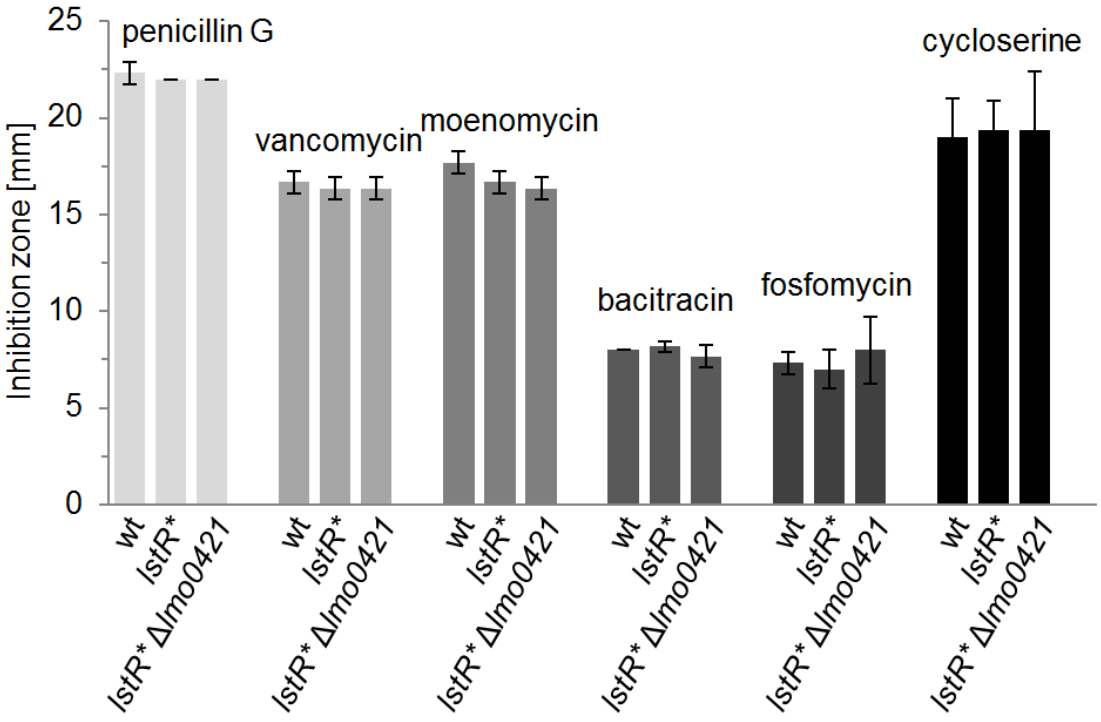

Figure 3.24: Resistance against cell wall biosynthesis inhibiting antibiotics. Disk diffusion assays were performed to determine the susceptibility of the wild type, *lstR** (LMSH39) and *lstR* Δlmo0421* (LMSH40) mutants to different antibiotics targeting the cell wall biosynthesis. Filter discs (6 mm diameter) soaked with antibiotic solution (10 μl of 1 mg/ml penicillin G, 20 mg/ml vancomycin, 1.6 mg/ml moenomycin, 40 mg/ml bacitracin, 20 mg/ml fosfomycin, or 30 mg/ml cycloserine) were placed onto a BHI plate inoculated with a lawn of one bacterial strain. Three independent experiments were performed and the average diameter of the inhibition zone resulting after over night incubation at 37°C is shown with the standard deviation.

3.7 Determining if Lmo0421 has RodA- or FtsW-like functionality

The genome of *L. monocytogenes* encodes a high numer of RodA- or FtsW-like proteins that could mask the enzymatic activity of Lmo0421. The genomic location of all the *rodA*- and *ftsW*-like genes is shown in figure 3.25, panel A. Another attempt to determine whether Lmo0421 has RodA/FtsW functionality was made. The gene *lmo0421* was strongly over-expressed in the *lstR** background (this strain was shown to have the same P_{sigC} activity as the Δ*lstR* mutant in figure 3.14). When Lmo0421 has the same function as a RodA or FtsW enzyme, it should be able to take over their role in cell wall biosynthesis.

To test this hypothesis, the unessential *lmo2427-lmo2428* operon encoding two of the RodA homologs (Rismondo et al. 2019) was deleted first. This deletion reduced the number of proteins with proven RodA-functionality to one. This last gene (*rodA3*) is essential for survival under standard conditions (Rismondo et al. 2019). It could then be tested whether Lmo0421 has RodA activity by inactivation of the *rodA3* gene in a strain expressing *lmo0421*. In the case that Lmo0421 has RodA activity, the essential *rodA3* gene should become dispensable. Similarly, inactivation of the *ftsW* genes in the *lmo0421* expressing *lstR** mutant should show whether Lmo0421 has FtsW activity.

Using the wild type, the *lstR** (LMSH39), Δ*rodA1-rodA2* (LMSH67) and the Δ*rodA1-rodA2 lstR** (LMSH68) mutants, we attempted to inactivate the remaining RodA- or FtsW-like proteins by insertion of a plasmid that disrupts the genes. To do so, pMAD derivatives containing an internal part of the genes *lmo1071* (*ftsW1*), *lmo2688* (*ftsW2*) and *lmo2687* (*rodA3*) followed by a TAA stop codon were constructed. These plasmids can be integrated into the genome at 42°C, because they possess an temperature-sensitive origin of replication. Integration of the plasmid into the target gene would result in two disrupted gene fragments, thereby inactivating the gene product (see figure 3.25, panel B).

The results of the inactivation experiments are shown in figure 3.25, panel C. In the wild type and *lstR** background only *ftsW1* was essential. When *rodA1* and *rodA2* have been deleted, *rodA3* and *ftsW2* also become essential. This observation is in agreement with other results on the function of these genes (Rismondo et al. 2019). The *lmo0421* overexpressing strains (*lstR**) are unable to compensate for the loss of the *rodA* or *ftsW* genes. When over-produced, Lmo0421 should have been able substitute for the loss of the other genes. As this is not the case, Lmo0421 does not exhibit a RodA/FtsW functionality under the conditions tested.

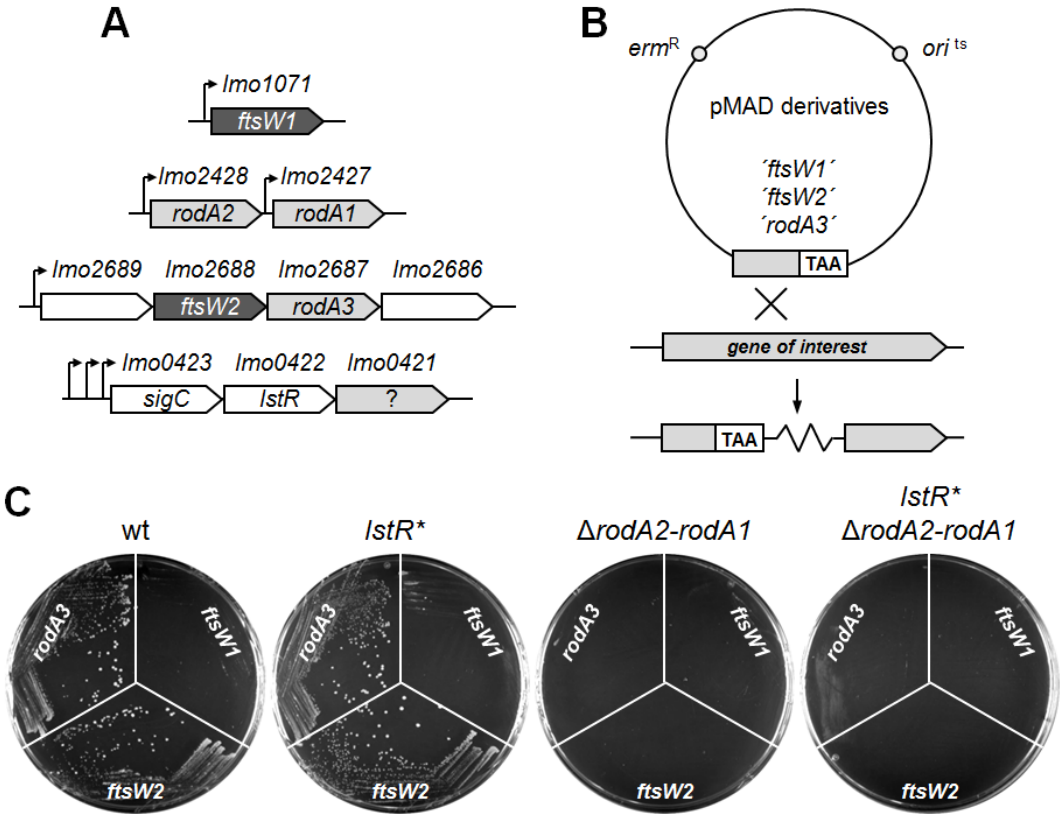

Figure 3.25: Disruption of the *rodA*- and *ftsW*-like genes. Panel A: Genomic location of the *rodA* and *ftsW* homologous genes of *L. monocytogenes*. Panel B: Plasmids constructed to inactivate the RodA/FtsW homologs *lmo1071* (*ftsW1*), *lmo2688* (*ftsW2*) and *lmo2687* (*rodA3*) contained an internal fragment of the respective genes followed by a stop codon, as well as an erythromycin resistance marker (erm^R) and a heat-sensitive origin of replication (ori^{ts}). Panel C: Results of the inactivation experiments in the wild type, *lstR** (LMSH39), Δ*lmo2427-2428* (LMSH67) and Δ*lmo2427-2428 lstR** (LMSH68) backgrounds.

3.8 Cold-sensitive growth phenotype of the *lltR** mutant

The genes of the *lltR-lmo0600-lmo0601* operon have not been characterized in the scientific literature. Our screen of the natural compound collection performed here to identify conditions leading to gene expression also failed to identify substances that induce the *lltR-lmo0600-lmo0601* operon, which therefore remains enigmatic. In order to identify phenotypes that might be associated with the PadR-like repressor LltR, standard experiments to phenotypically describe listerial strains were performed. These included growth in BHI at 30, 37 and 42°C, lysozyme induced lysis and intra-cellular replication in murine macrophages, but non yielded significant differences (data not shown). Interestingly, when the *lltR** mutant was kept on agar plates at 6°C for prolonged periods of time, the colonies did not seem to grow larger. The ability of *L. monocytogenes* to grow at low temperature was used in the past to enrich cultures for *Listeria* (Lewis and Corry 1991). To test if the growth of the *lltR** mutant is impaired at refrigeration temperatures, liquid cultures were inoculated and incubated statically at 6°C. A clear growth inhibition could be observed at 6°C, while the mutant behaves like the wild type at 37°C (see figure 3.26). The *ladR* and *lstR* mutants are shown for reference, but do not exhibit any difference to the wild type at both temperatures.

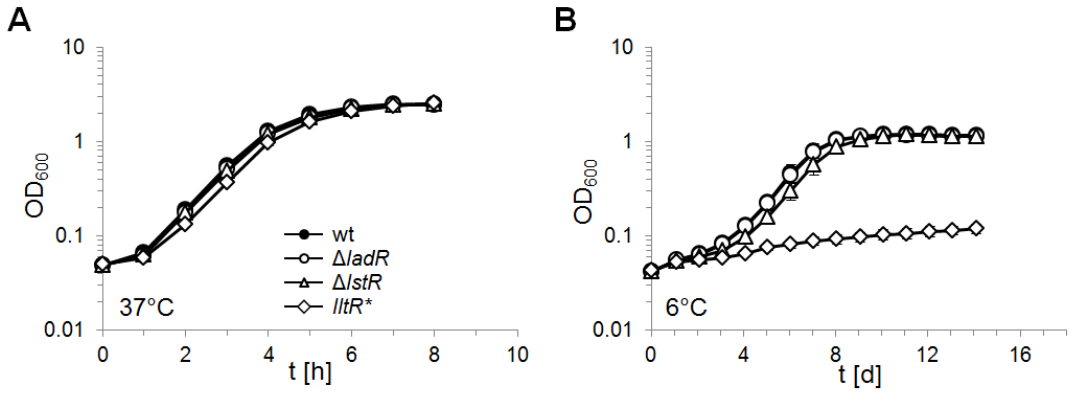

Figure 3.26: Cold-sensitive growth phenotype of the *lltR mutant.** Strains LMSH1 (Δ*ladR*), LMSH2 (Δ*lstR*) and LMSH3 (*lltR**) behave like the wild type when grown in BHI at 37°C (panel A). When the same strains are grown at 6°C though, the *lltR** mutant shows a pronounced growth deficit (panel B).

To confirm that the growth defect at low temperature is caused by the inactivation of LltR in the *lltR** mutant, a plasmid carrying a copy of the original gene under the control of an IPTG-inducible promoter was constructed. This plasmid was introduced into the *lltR** mutant and the growth of the resulting strain (LMSH42) was monitored on BHI plates with and without IPTG at 6°C. In the presence of an intact copy of the *lltR* gene, the *lltR** mutant was again able to grow at refrigeration temperature (see figure 3.27). The presence or absence of the inducer IPTG was not important, presumably because a very low transcription level is sufficient for the strong repressor LltR to fulfil its function. These observations are in accordance with the low expression level and autoregulatory nature of the *lltR* gene that have been shown in the RNA sequencing experiments. It can thus be concluded, that active LltR is important for the growth of *L. monocytogenes* on BHI at low temperatures.

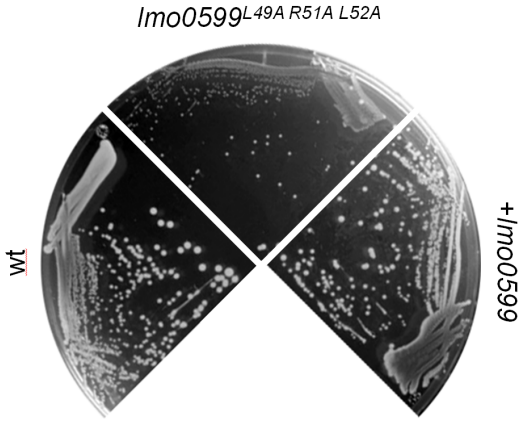

Figure 3.27: Complementation of the cold-sensitive phenotype. After 6 weeks of incubation at 6°C on BHI agar containing 1 mM IPTG, the wild type grew into big colonies (left), while the strain LMSH3 (*lltR**) formed only small colonies (top). The introduction of a plasmid carrying an intact copy of *lltR* into the *lltR** mutant (strain LMSH42) complements the growth defect.

3.9 Effect of the genes *lmo0600* and *lmo0601* on growth at refrigeration temperature

According to the RNA sequencing results, the two genes *lmo0600* and *lmo0601* are strongly up-regulated in the *lltR** mutant when compared to the wild type. To determine if the growth deficit of the *lltR** mutant is caused by the over-expression of one of those genes, *lmo0600* and *lmo0601* were deleted in the *lltR** background resulting in the strains LMSH50 (*lltR** Δ*lmo0600*) and LMSH51 (*lltR** Δ*lmo0601*). The deletion of *lmo0600* restored the growth of the *lltR** mutant at 6°C. The *lltR** Δ*lmo0601* strain on the other hand, did not grow at refrigeration termperature (see figure 3.28).

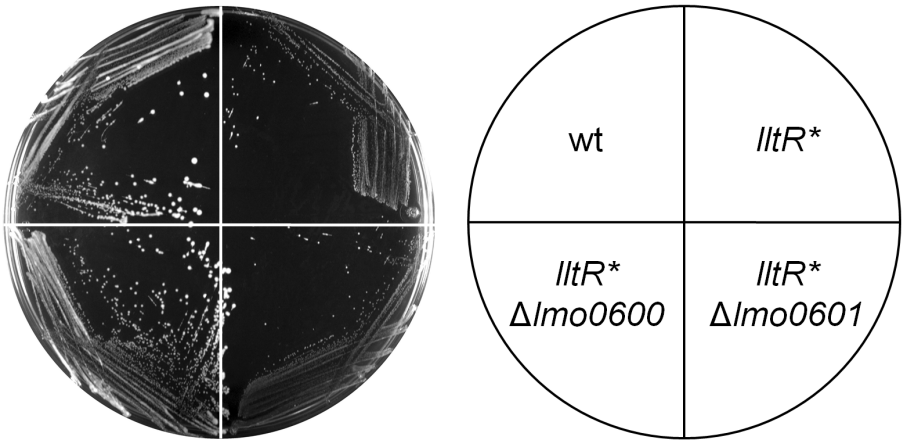

Figure 3.28: *lmo0600* is responsible for the growth defect 6°C. The over-expression of *lmo0600* causes the growth deficit of the *lltR** mutant at 6°C. The strains LMSH3 (*lltR**), LMSH50 (*lltR** Δ*lmo0600*) and LMSH51 (*lltR** Δ*lmo0601*) were grown for 6 weeks at 6°C on BHI agar with the wild type as a reference.

The deletion of *lmo0601* in the *lmo0599* mutant background seemed to change the colony morphology when grown at 6°C (data not shown). It appeared as though the colonies became translucent or started to lyse when compared to the parental *lltR** mutant. If this impression was true and lysis actually occured, then it should become more apparent after longer incubation times. To investigate this hypothesis, the plate shown in figure 3.28 was incubated for another 6 months at 6°C. After this long incubation period, it became obvious that the mutant *lltR**Δ*lmo0601* did indeed lyse (see figure 3.29).

The fact that the deletion of *lmo0600* in the *lltR** background re-enables growth at low temperatures, while the deletion of *lmo0601* aggravates the phenotype by leading to lysis suggests that both proteins are important for growth at low temperatures and might be

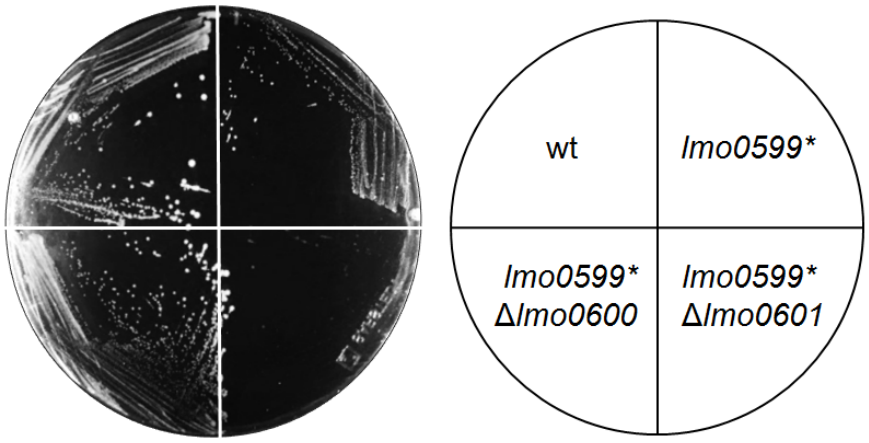

Figure 3.29: The gene *lmo0601* seems to protect the cells from lysis at low termperature. The same plate as shown in figure 3.28 after an incubation period totalling 7.5 months at 6°C. The *lltR*Δlmo0601* mutant (LMSH51 in the bottom right section) did lyse nearly completely.

functionally related. The exact biological function of the *lltR-lmo0600-lmo0601* operon and conditions leading to its expression still need to be clarified in future experiments.

3.10 Characterization of *lltR** suppressor mutants that are able to grow at 6°C

When the *lltR** mutant LMSH3 was grown on BHI agar plates at 6°C for prolonged periods of time, some colonies grew much larger in size than all the rest (data not shown). To determine if the bacteria in these colonies had regained the ability to grow under refrigeration, they were streaked to single cells and grown over night at 37°C. A single colony was then transferred into liquid medium and after incubation at 37°C the resulting culture was stored at -80°C. Material from these cultures was again streaked onto BHI and incubated at 6°C for 6 weeks to confirm the ability to grow at low temperature. The parental strain LMSH3 (showing only weak growth) and the wild type (showing growth) were used as controls. The results (not shown) confirmed that all the isolated suppressor grew like the wild type. The same procedure was repeated for the *lltR* Δlmo0601* mutant (LMSH51), which was also unable to grow at 6°C. Suppressors could be easily isolated in this mutant as well.

The overexpression of *lmo0600* caused the inability of the *lltR** and the *lltR* Δlmo0601* mutants to grow at low temperatures (see figure 3.28). The possibility that the suppressors that were again able to grow had acquired mutations in *lmo0600* was investigated next.

The genomic region of *lltR-lmo0600* and the P_{lltR} promoter were amplified by PCR and sequenced. The results confirmed that most mutants did indeed inactivate *lmo0600* (see Table 3.12). A disruption of Lmo0600 by insertion of a premature stop codon or a frame shift was most commonly observed. There were also three single amino acid exchanges in Lmo0600 that could have occurred at positions important for the protein function. Interestingly, one mutation seemed to affect the repressor LltR instead of Lmo0600. The exchange C16F at the beginning of LltR affected a cysteine residue in the α-1 helix. This position is not conserved among the PadR-like transcriptions factors (see figure 1.4) and the role of this position is so far unclear. One possible explanation why this exchange leads to growth at 6°C could be that LltR* with the C16F exchange is again able to repress its operon.

Table 3.12: Suppressor mutations of the cold-sensitive phenotype. Mutations found in suppressors isolated from the *lltR** (LMSH3) and the *lltR** Δ*lmo0601* mutants grown at 6°C. The base exchanges detected are indicated together with their position in the genome and the resulting effect they have on the Lmo0600 protein or on LltR.

Strain	Background	Mutation	Effect
LMSH104	*lltR**	A640221G	P_{lltR} -35 box mutation
LMSH105	*lltR**	A640869 deletion	Lmo0600: frame shift
LMSH106	*lltR**	A640758C	Lmo0600: Q45P
LMSH107	*lltR**	A640221G	P_{lltR} -35 box mutation
LMSH108	*lltR**	A640869 deletion	Lmo0600: frame shift
LMSH109	*lltR**	G640611T	Lmo0600: RBS mutated, LltR: E104D
LMSH110	*lltR** Δ*lmo0601*	C640782A	Lmo0600: P53Q
LMSH111	*lltR** Δ*lmo0601*	C640871T	Lmo0600: Q83 stop
LMSH112	*lltR** Δ*lmo0601*	C640757T	Lmo0600: Q45 stop
LMSH113	*lltR** Δ*lmo0601*	G640346T	LltR: C16F
LMSH114	*lltR** Δ*lmo0601*	insertion after T641002	Lmo0600: frame shift
LMSH115	*lltR** Δ*lmo0601*	C640757T	Lmo0600: Q45 stop
LMSH116	*lltR** Δ*lmo0601*	insertion after A640656	Lmo0600: frame shift
LMSH117	*lltR** Δ*lmo0601*	G640731A	Lmo0600: G36E

Chapter 4

Discussion

4.1 PadR-like repressors strongly regulate a small set of genes

The RNA sequencing data obtained for the Δ*lftR* mutant fit well to the previous knowledge of tight regulation of the *lieAB* operon. The strong overproduction of LieAB in a Δ*lftR* mutant was first shown using crude protein extracts (Kaval et al. 2015). The high amount of *lieAB* mRNA detected using RNA sequencing (nearly 500-fold more in the Δ*lftR* mutant than in the wild type) supports this observation. Besides confirming existing knowledge, RNA sequencing also revealed the autoregulation of the *lftRS* operon (see table 3.2). Northern blotting to detect *lftS* mRNA (see figure 3.6) and LacZ-assays (see figure 3.5) verified the autoregulation and lend overall confidence to the results.

The two genes *lmo0981* and *lmo0982* located immediately downstream of *lieAB* are also up-regulated significantly in the Δ*lftR* mutant. A closer look at how the sequencing reads map to this region of the genome revealed that transcription is not properly terminated after *lieB*, so that longer transcripts spanning the entire region form *lmo0979* to *lmo0982* are formed. This effect is probably due to the complete absence of LftR, a constellation unlikely to occur under natural conditions. Under natural conditions, LftR will be gradually inactivated at contact with the inducer, allowing expression of *lieAB* and *lftRS* operons. New repressor molecules will be produced together with the LieAB transporter and these additional LftR molecules can then repress transcription as soon as the antibiotic concentration drops due to the activity of the LieAB transporter. The auto-regulatory nature of LftR (the more LftR is inactivated, the more new LftR will be synthesized) thus prevents constantly high transcription levels and the induction rate is rather determined by the dynamic equilibrium between the concentration of the repressor LftR and its effector.

Smaller regulatory effects were also observed in the RNA sequencing data for the Δ*lftR* mutant. The data revealed the down-regulation of SigB-controlled genes (see table 3.3). The down-regulation ranged from around 2.4-fold to around 30-fold. An explanation for all of the down-regulated genes was found in a second mutation that abolished RsbT activity (see figure 3.3). Mutations in *rsbT* are known to lead to a *sigB* null phenotype (Chaturongakul and Boor 2004), so the *rsbT*^{C10T} mutation probably caused the inactivation of SigB in the strain LMKK42. Overall, the data for the Δ*lftR* mutant is in accordance with existing knowledge, as well as extending the regulon of LftR by the *lftRS* operon.

In the case of LadR, the regulation of the multi-drug-efflux pump encoding gene *mdrL* is well known (Huillet et al. 2006). Also, the induction of *mdrL* expression in a *ladR* mutant was measured as being around 30-fold in a previous study (Crimmins et al. 2008). This latter study also showed a three-fold induction of the multi-drug-transporter gene *mdrM* in the Δ*ladR* mutant background (Crimmins et al. 2008). In perfect agreement with these results, RNA sequencing data showed a more than 150-fold induction of *mdrL*. The two other genes significantly regulated in the Δ*ladR* mutant were the 3-fold up-regulated efflux pump *lmo1617* (*mdrM*) and its transcriptional regulator *lmo1618* (*marR*). These genes are transcribed together as one operon (Toledo-Arana et al. 2009) and *mdrM* is known to be LadR-regulated (Crimmins et al. 2008). Thus, even the relatively weak three-fold induction of *mdrM* and *marR* expression was reliably detected using RNA sequencing and confirmed the previous result. A Δ*marR* mutant induced *mdrM* around 70-fold (Crimmins et al. 2008). It thus seems like *mdrM* is not a primary target of LadR, but is regulated due to weak interaction effects.

The lineage-specific thermal regulator LstR showed a more complex regulatory behavior than LadR. In total there were six up- and four down-regulated genes (see table 3.5 and 3.6). Of these genes, the most strongly regulated were *lmo0421* and *lmo0423* (*sigC*). Both are located in the same operon as *lstR* (Toledo-Arana et al. 2009). Other up-regulated genes (*lmo0420* and *lmo0419*) are located directly downstream of the *sigC-lstR-lmo0421* operon. The function of *lmo0419* and *lmo0420* remains unclear. In the absence of LstR, the strong transcription from the *sigC* promoter might not be properly terminated. This leads to the production of transcripts from genes located downstream of this operon, for example *lmo0420*. In the case of *lmo0420*, these transcripts are in anti-sense orientation and might interfere with the expression and regulation of this gene (Thomason and Storz 2010). The gene *lmo0419* has the same orientation as the *sigC* operon and is therefore up-regulated by incomplete termination of *sigC-lstR-lmo0421* transcripts. This is a similar situation as was observed with up-regulated *lieAB* transcripts in the Δ*lftR* mutant, where incomplete termination of transcription after lieAB lead to transcription of the down-stream genes *lmo0981* and *lmo0982*. Similar effects occur in the Δ*lstR* mutant, but are most likely irrelevant under natural conditions.

The genes up-regulated in the *lltR** (*lmo0599*) mutant show the same general pattern as observed for other PadR-like repressors. The *lltR-0600-0601* operon is strongly repressed by LltR. The next most strongly regulated gene *lmo0602* is located immediately down-

stream and in the same orientation. It is annotated as a transcriptional regulator and might be responsible for the weak up-regulation observed for a small number of other genes. It could also be the case that LltR itself has small effects on their expression. This behavior could be similar to the weak regulation of the *marR-mdrM* operon by LadR.

In conclusion it can be said, that the PadR-like repressors investigated strongly regulate a small set of genes and most of them are auto-regulatory. Strongly repressed genes are up-regulated around 150-fold in the mutants lacking the cognate repressor. The auto-regulation could not be shown for *ladR*, as a Δ*ladR* mutant was used. Still, the *ladR* and *mdrL* genes are transcribed from promoters located in the same intergenic region (see figure 1.5). Therefore, the control of both promoters by one LadR-binding operator seems possible.

Smaller regulatory effects on a limited number of genes could also be observed in the RNA sequencing data. Incomplete termination of transcription (in the case of *lftR*, *lstR* and *lltR*) or weak recognition of other operators (as is likely for *ladR*) could be factors resulting in minor up-regulation of secondary genes. Such effects are unlikely to manifest under natural circumstances, because the induction of auto-regulatory systems can never lead to the same expression level as the deletion of the repressor. The negative feedback loop integrated in the regulation will prevent constantly high expression levels and might serve to limit gene expression to the lowest level still resulting in an efficient response.

Over all, the RNA sequencing results proved to be very reliable, because they could be confirmed using LacZ assays and Northern blotting. Further, previously published results could be confirmed as well. However, it was impossible to draw conclusions on the biological function of the PadR-like repressors from the pattern of deregulated genes observed by RNA-Seq. The conditions leading to induction of PadR-dependent genes as well as their function need to be determined in separate experiments.

4.2 Conditions leading to the activation of PadR-dependent promoters

It was shown by RNA sequencing that the genes controlled by PadR-like repressors are not significantly expressed in *L. monocytogenes* EGD-e under standard conditions. Such tight regulation indicates that the target genes are beneficial only under very specific circumstances. The expression is normally switched off by the PadR-like repressors, because it would result in a waste of energy and could also be detrimental to growth and survival of *L. monocytogenes*. This becomes especially clear in the case of LltR where the over-expression of its target gene *lmo0600* prevents growth at refrigeration temperature (see figure 3.28). The same could be the case with LadR-controlled *mdrL* expression under infection conditions, because the inactivation of the repressor leads to an increased interferon response (Crimmins et al. 2008). An increased interferon response on the other hand has been shown to decrease the capacity of the bacteria to grow *in vivo* (Crimmins et al. 2008). LftR also switches of the production of the ABC-type transporter LieAB that could import toxic substances like ethidium bromide (Kaval et al. 2015).

Knowledge of conditions leading to the induction of normally silent genes could help to identify the function of those genes. In literature, several conditions and substances have been described to induce expression of genes controlled by PadR-like transcription factors (Ahmed et al. 1994, Morita et al. 2003, Zhang et al. 2005, Huillet et al. 2006, Tran et al. 2008). An initial screen of these conditions identified rhodamine 6G and rhodamine B as inducers of LftR-controlled gene expression (see figure 3.7). Rhodamine dyes do not occur in nature (Cooksey 2016), so they are unlikely to be natural effectors of LftR. Still, even artificial substrates allow the study of the underlying mechanisms regulating gene expression. For example, it was possible to identify the essentiality of LftS for *lieAB* induction using the rhodamine dyes (see figure 3.10).

For the repressor LadR, no inducing conditions could be found, despite previous studies indicating that it reacts to rhodamine 6G in a different *L. monocytogenes* strain (Huillet et al. 2006, Crimmins et al. 2008). The RNA sequencing data showed that the absolute expression of *lmo1409* (*mdrL*) in the Δ*ladR* mutant is relatively low, when compared to the other PadR-type repressors (see figure 3.1 or figure 3.5). The expression from the LadR-controlled *mdrL* promoter was also low in the β-galactosidase assay, compared to the promoters controlled by LftR, LstR and LltR (see figure 3.5). It could therefore be the case that the expression level under inducing conditions is not high enough to be detected in the agar based screen. The induction by rhodamine 6G has not been quantified in this work. The quantification could be used as a control to confirm whether in the EGD-e background there is a weak induction or no induction at all.

The tight repression of *mdrL* might be essential under some conditions, for example dur-

ing infection so as to not induce host defenses. This makes sense in the light of the fact that *lmo1409* influences the interferon response in eukaryotic host cells (Crimmins et al. 2008). Using qPCR it has been shown that in the presence of rhodamine 6G *mdrL* is up-regulated, but expression remains at a fairly low absolute level (Crimmins et al. 2008). Under the same conditions, the expression levels observed for other pumps (*mdrT* and *mdrM*) reached much higher levels than for *mdrL* (Crimmins et al. 2008). This corroborates the hypothesis that the low absolute expression is the reason why the agar based assay failed to detect induction. In the case of *lieAB*, induction by aurantimycin A was easily detectable due to the very strong activity of the *lieAB* promoter (see figure 3.1 or figure 3.5). When *L. monocytogenes* comes into contact with this compound, a high expression level is absolutely essential for survival, because without quick production of the LieAB transporter the cell would lyse and die. If MdrL is transporting a less toxic substance, a low absolute expression level under inducing conditions might be sufficient. A very high transport efficiency or low membrane permeability of the target compound could also compensate for low expression levels.

Even if rhodamine 6G is an effector of LadR, it is of synthetic origin (Cooksey 2016) and therefore unlikely to be the original target molecule of the naturally evolved LadR-MdrL system. A natural effector might give a much clearer induction signal no matter if measured by qPCR or the agar based screen. Taken together, the data suggest that the natural effector of LadR and the substrate of MdrL have not yet been identified. The LacZ-based reporter assay may also not have been suitable to detect induction of the P_{sigC} promoter by heat, because of LacZ stability or expression issues at elevated temperatures (Schrögel and Allmansberger 1997).

An unbiased screen of a natural compound collection was performed, because the initial testing of conditions and substrates mentioned in the literature only identified rhodamine dyes as artificial substrates. The screen of the DZIF natural compound library containing 681 secondary metabolites from streptomycetes, myxobacteria and fungi revealed one substance that induced LftR-controlled genes and two substances that induced LstR-controlled genes. Transcription of the LftR-controlled *lieAB* genes encoding an ABC-type transporter was induced by the depsipeptide antibiotic aurantimycin A and the *lstR* operon was induced by the 16-membered macrolide antibiotics niddamycin and josamycin. No substances that induce expression of the *lltR* operon or of the *mdrL* gene were found. This suggests that the observed induction of *lieAB* by aurantimycin and the *lstR* operon by josamycin and niddamycin is specific for the respective repressor-effector combinations.

4.3 LftR-controlled aurantimycin-resistance genes might be important for the survival of *L. monocytogenes* in the environment

When antibiotics specifically induce gene expression, the regulated genes often confer some kind of resistance to the antibiotic (Ohki et al. 2003, Lai et al. 2007, Chancey et al. 2011, Nawrocki et al. 2014). This was also the case for LftR, which controlled the production of the ABC-type transporter LieAB. The exposure *L. monocytogenes* to aurantimycin induced *lieAB* expression and the LieAB transporter conferred resistance to aurantimycin-induced lysis (see figure 3.15).

Aurantimycin A is a secondary metabolite synthesized by the soil bacterium *Streptomyces aurantiacus* (Graefe et al. 1995). The antibiotic is very toxic to Gram-positive bacteria with MICs below 0.01-0.1 μg/ml reported for *B. subtilis*, *Staphylococcus aureus* and streptococci. Gram-negative bacteria are intrinsically resistant to aurantimycins (Graefe et al. 1995). The biosynthetic gene cluster needed for aurantimycin synthesis contains 36 open reading frames encoding different enzymes involved in the synthesis and tailoring of the antibiotic as well as an ABC transporter (Zhao et al. 2016). This particular ABC transporter, ArtJK, shows around 50 % similarity to LieAB from *L. monocytogenes* and could be responsible for the export aurantimycin from *S. aurantiacus* cells. Based on the similarity between ArtJK and LieAB the hypothesis that LieAB exports aurantimycin A becomes more likely.

The importance of LieAB for the resistance of *L. monocytogenes* against aurantimycin was shown by determining the MIC of aurantimycin against *lftRS* and/or *lieAB* mutants (see Table 2.8). Compared to other Gram-positive bacteria (Graefe et al. 1995), the *L. monocytogenes* EGD-e wild type is highly resistant against aurantimycin. The Δ*lftR* mutant overexpressing LieAB had a MIC even higher than the wild type. Mutants lacking *lieAB* on the other hand were very sensitive to the antibiotic, even at low concentrations (see table 3.9). The MIC values of the Δ*lieAB* mutants were in the same range as the values observed for other Gram-positive bacteria (Graefe et al. 1995). Putting everything together, the data suggest that the LftR-controlled *lieAB* operon becomes active in the presence of aurantimycin and the LieAB transporter exports the antibiotic from the cell (an/or the cell membrane).

Taking all results into consideration, the working model of LftR-controlled aurantimycin-resistance looks as depicted in figure 4.1. In the absence of an effector, basal amounts (light color) of LftR and LftS are produced due to background activity of P_{lftRS}. This basal activity results from incomplete repression of P_{lftRS} by LftR (see the higher activity of P_{lftR} compared to P_{lieA} in figure 3.8). The presence of basal amounts of the two proteins allows for efficient repression of *lieAB* (no expression implied by gray color in figure 4.1),

as well as effector recognition.

In the presence of aurantimycin, LftR is no longer able to bind to the DNA. The P_{lieAB} and P_{lftRS} promoters are now accessible to RNA polymerase and become active (saturated color). The high activity of the de-repressed P_{lieAB} promoter allows the cell to synthesize large amounts of LieAB (Kaval et al. 2015). This is necessary in order to protect the cell from death by lysis (see figure 3.15).

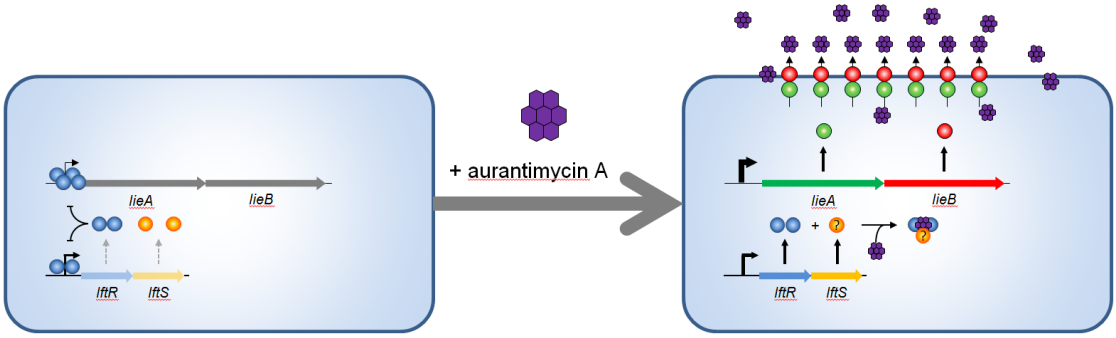

Figure 4.1: Working model of the LftR-controlled resistance to aurantimycin. In the absence of the antibiotic (left), the *lieAB* operon is strongly repressed, while a basal amount of LftR and LftS are being produced from a leaky *lftR* promoter. In the presence of aurantimycin, LftR is unable to bind the promoters and large amounts of LieAB are produced to protect the cell from lysis. The role of LftS in the induction process is still unclear.

The role of LftR clearly is the repression of the *lieAB* operon in the absence of effector molecules like aurantimycin A. The role of LftS in this scheme is not yet understood. LftS is essential for the induction by aurantimycin (see figures 3.10 and 3.11), but whether it is involved in sensing or binding of the antibiotic or in the removal of LftR from the operator under inducing conditions remains to be determined.

It is also unclear if aurantimycin interacts with LftR or LftS. In the PadR-like repressor LmrR, a hydrophobic cavity was suggested to bind planar polycyclic compounds (Madoori et al. 2009). The binding of effector could in turn cause structural rearrangements that prevent binding of the repressor to the DNA. A similar cavity exists in the structure of LftR (Lee et al. 2019). Binding of aurantimycin to this pore could result in structural rearrangements that regulate the LftR-DNA interaction. This needs to be proven in further experiments, for example by co-crystallization or in EMSA studies using purified protein and effector. Unfortunately, such a regulatory mechanism would not explain the essentiality of LftS for the induction process, so the true mechanism might be more complex. LftS could for example bind the effector and then interact with LftR to prevent repression. Other regulatory modes like complex formation between LftR and LftS are also possible. LftS contains the domain of unknown function DUF1048. To-

date no protein with such a domain has been described in the scientific literature. The function of LftS in LftR-mediated gene regulation has been identified in this work. This might offer the chance to assign a biological role to a whole class of proteins, if the same regulatory pattern could be confirmed in other proteins containing DUF1048.

The presence of aurantimycin-resistance genes in the genome of *L. monocytogenes* suggests that under natural conditions an interaction between aurantimycin producing bacteria and *L. monocytogenes* could take place. Additionally, the high sensitivity of Gram-positiv bacteria that do not carry aurantimycin-resistance genes (Graefe et al. 1995) suggests that *L. monocytogenes* is better able to survive in environments where the antibiotic is present. Both, *L. monocytogenes* and aurantimycin-producing *S. aurantiacus* have been isolated from soil (Vijayabharathi et al. 2011, Linke et al. 2014), supporting the hypothesis that the two species might somehow interact or compete with each other in this habitat. Another open question is, whether the LftRS-LieAB system is specific for aurantimycin or whether other depsipeptides will also be detoxified. If the latter is true, LieAB might be a more broadly relevant resistance mechanism against depsipeptides.

4.4 Mutations found in aurantimycin-resistant suppressors

In liquid culture, aurantimycin-resistant suppressors could be readily selected when the wild type or the Δ*lftS* mutant were grown in the presence of toxic aurantimycin concentrations. Both of these strains do not express the *lieAB* transporter genes under normal conditions. When induced, the wild type will produce the transporter, but the Δ*lftS* mutant is unable to do so (see figures 3.10 and 3.11). Nevertheless, both strains grew in over night cultures containing aurantimycin at concentrations that were toxic to Δ*lieAB* mutants (see figure 3.16).

When single cells were isolated from these over night cultures, sequencing of the *lftRS* operon and its promoter revealed that all cells had acquired mutations in *lftR* or its promoter (see table 3.10). The promoter mutations effected the -10 box or the RBS of *lftR*, most likely leading to the inactivation of the *lftRS* operon. Mutations in *lftR*, which result in a non-functional *lftR* gene, lead to constitutive expression of the *lieAB* transporter genes and to aurantimycin-resistance as an end result. The observation that strains lacking the *lieAB* genes did not develop resistance is in good agreement with this hypothesis, because the resistance determinant is absent these strains (see figure 3.16). The Δ*lftR* strain on the other hand is always resistant.

The formation of aurantimycin-resistant suppressors is the reason that both the wild type

and the Δ*lftS* mutant showed identical MICs (see table 3.9). MIC values are usually determined after over night incubation, but this time was long enough for the resistant mutants to over-grow the culture. It must therefore be concluded that the mutations inactivating LftR could form very easily or could already be present in a sub-population of the inoculum.

Most suppressor mutations found in aurantimycin-resistant mutants inactivated LftR by disrupting the *lftR* gene or its promoter via frame shifts and premature stop codons (see table 3.10). The few single amino acid substitutions identified could be a valuable tool for the characterization of the function and DNA interaction of LftR. The crystal structure of LftR has been published recently (Lee et al. 2019). Based on this information, it is possible to link the suppressor mutations to the structure of the protein (see figure 4.2).

Figure 4.2 shows the single amino acid exchanges found in the wild type and the Δ*lftS* mutant. At the bottom of the figure, the secondary structural elements of LftR according to its crystal structure are shown (Lee et al. 2019). The two mutations T46M and R53C map in the putative DNA binding helix and could therefore prevent binding or recognition of the operator by LftR. The arginine in position 53 belongs to a positively charged patch (K9, R53, K56, K64, K66, R73, and K74) that was identified in the structure of LftR (Lee et al. 2019). This patch could facilitate interactions with the negatively charged phosphate backbone of the DNA helix (Lee et al. 2019). Although the threonine in position 46 is not highly conserved, this position might be an important determinant of the sequence specificity of LftR. The mutation T5I is located in the first helix $\alpha 0$ that together with helix $\alpha 4$ is involved in LftR dimer formation (Lee et al. 2019). This mutation could prevent the formation of a functional LftR dimer and thereby prevent LftR-mediated *lieAB* repression. The two glycine replacements G27S and G70D are located at the beginning of the α-helix 2 and beta-sheet 2. Glycine is known to be important for the formation of secondary structures (Imai and Mitaku 2005). For example, it might work as a helix breaker creating helices of a defined length. In LftR, nearly all secondary structural elements are flanked by glycine residues (see figure 4.2). The protein could adopt a different secondary structure when these residues are mutated, thereby disrupting its function.

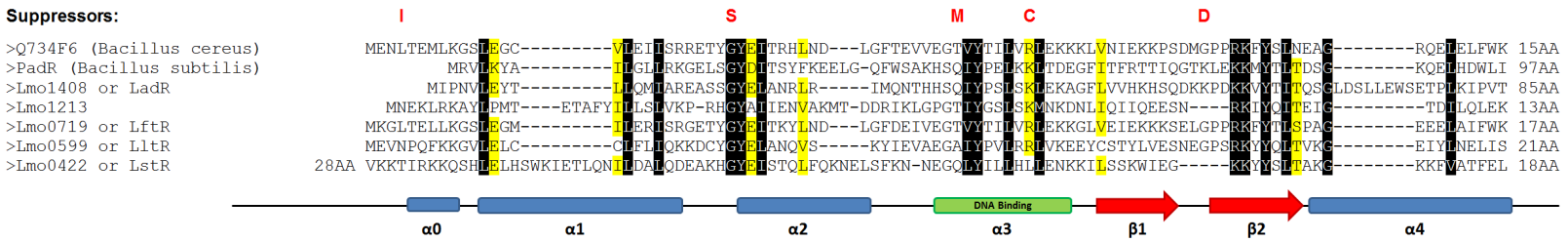

Figure 4.2: Location of the mutations found in aurantimycin-resistant suppressors. The mutations found are shown in red above an alignment of the listerial PadR-like protein sequences with the sequence of PadR from *B. subtilis* and the PadR-like protein Q734F6 from *B. cereus*. Conserved amino acid positions are highlighted in black (highly conserved) and yellow (conserved). The schematic at the bottom indicates the secondary structural elements of LftR, based on the results from Lee et al. 2019.

Localizing the amino acid exchanges found in aurantimycin-resistant suppressors in the 3D-structure of LftR gives a more detailed impression of the impact they might have (see figure 4.3). The superposition of the LftR dimer with a DNA double helix shown in figure 4.3 revealed that all the exchanges (colored in red) occurred in parts of LftR that are in close contact with the DNA. Additionally, the glycine exchanges affect areas that are in close contact with the phosphate backbone of the DNA (see figure 4.3 or 4.4). Exchange of the small glycine residues for bulkier amino acids might therefore lead to steric clashes that prevent LftR from binding to the DNA. The exchange of glycine for negatively charged glutamate at position 70 will also lead to repelling electrostatic effects between the negatively charged phosphate backbone and the protein. This position is also part of the loop structure in the beta-wing of LftR. It has been shown that the beta-wing is essential for binding of PadR and LftR (Park et al. 2017, Lee et al. 2019). Mutations that impact the structure in this part of LftR should therefore also impact the binding to the DNA.

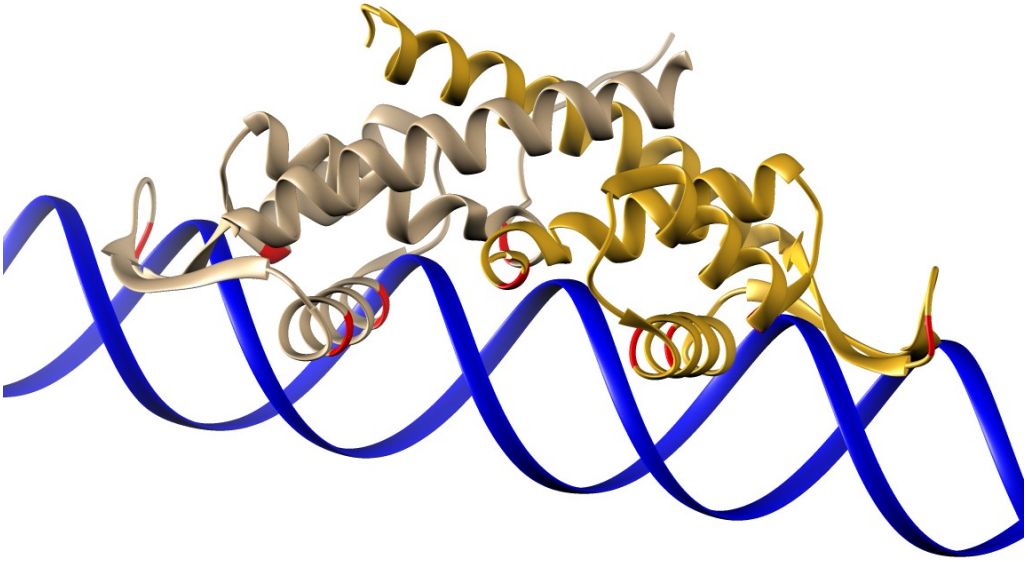

Figure 4.3: Location of the suppressor mutations in the 3 dimensional structure of LftR. A superposition of the crystal structure of LftR (PDB: 6ABQ) with a DNA double helix (blue) shows how all single amino acid mutations found in aurantimycin-resistant suppressors (colored in red) are located at the interface with the DNA.

The other amino acid exchanges that did not affect glycine residues changed positions that might be directly involved in interactions of LftR with DNA bases. Threonine at position 46 and arginine at position 53 are part of the DNA-binding helix and might interact with base pairs in the major groove, while the threonine at position 5 could interact with the DNA in the minor groove (see figure 4.4). It is interesting to note, that the R53C mutation was found in 9 independent Δ*lftS* suppressors, but not a single time among 20 wild type suppressors (see table 3.10). Besides being part of a positively charged patch that could

stabilize protein-DNA interactions (Lee et al. 2019), this position might somehow be important for the interaction of LftR and LftS, because the mutation was only found in the Δ*lftS* background. It could for example play a role in the LftS-dependent induction of gene expression upon exposure to effector molecules. Isolation and sequencing of more suppressor mutants could yield more mutations that allow for further characterization of the LftR protein.

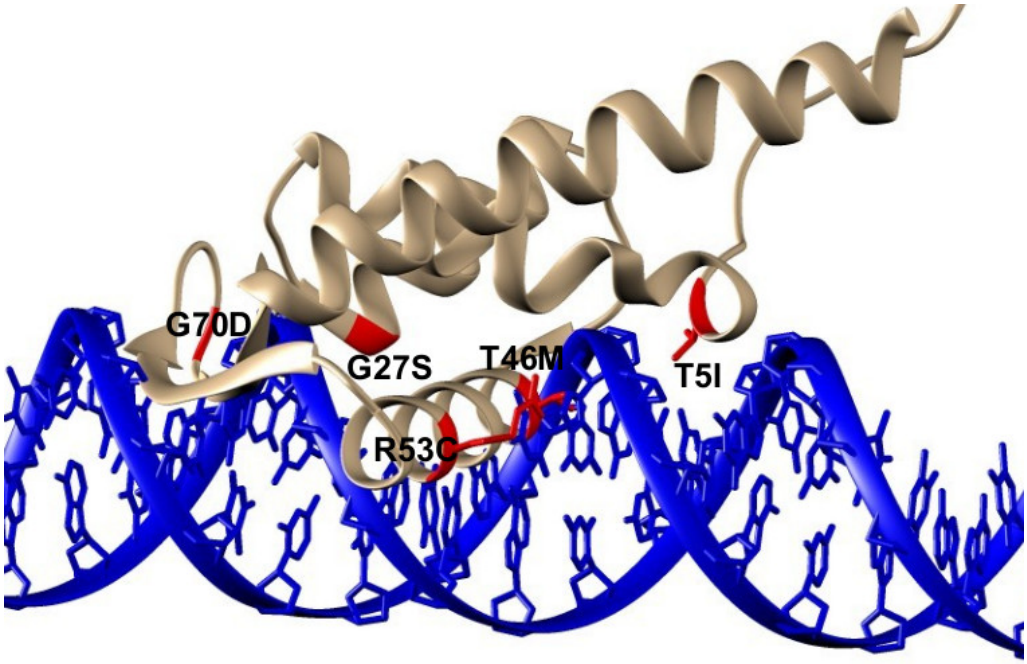

Figure 4.4: Close-up look at the suppressor mutations in chain A of the LftR dimer. The superposition of chain A of LftR (PDB: 6ABQ) with a DNA double helix shows that the mutations T5I, T46M and R53C alter amino acids that could directly interact with specific DNA bases, while the glycine exchanges G27S and G70D are located in areas that are close to the phosphate backbone of the DNA.

4.5 The LftR operator sequence

In accordance with the RNA sequencing results which showed that only the genes *lftRS* and *lieAB* are strongly regulated by LftR (see table 3.2), the putative LftR operator motif GTAW-TACNNN-ATAC (see figure 3.21) can only be found twice in the genome of *L. monocytogenes* EGD-e. It consists of an imperfect inverted repeat separated by a 6 nucleotide spacer region (GTAW-N6-ATAC). The inverted repeat alone can be found 192

times in the genome of *L. monocytogenes* EGD-e. This shows that the conserved bases in the spacer region must also be important for the recognition of the motif. The repeat identified also differs from the suggested canonical PadR ATGT/ACAT repeat (Fibriansah et al. 2012), but is of the same length.

The fact that the inverted repeat is imperfect in the *lieA* promoter while a perfect repeat can be found in the *lftR* promoter is somewhat surprising, especially when considering that the *lieA* promoter is strongly repressed, while the *lftR* promoter shows a detectable background activity in Northern blots (see figure 3.6). A potential reason for this observation could be that there are other motifs, beside the primary operator, that play a role in the total repression of the respective promoters. The *lieA* promoter with the 69-68 exchange is the *lieA* promoter variant with the highest activity *in vivo* (see figure 3.20), but its activity only reached between 10 or 20 % of the maximal promoter activity measured in the absence of LftR. The result that the maximum de-repression obtained by mutation of the proposed binding site did not reach the same level as in the Δ*lftR* mutant indicates residual binding of LftR outside of its core operator region.

Another possible explanation for residual binding could be that LftR is able to bind DNA as a monomer. In the experiments performed, a defined set of bases was mutated at any one time. Inactivation of both ends of the operator has yet to be tested. Therefore, it is possible that one LftR monomer could bind one side of the operator and partially repress transcription. Full repression is achieved by another monomer also binding to the other side of the operator or by binding of the dimerized protein. Further, it can not be excluded that elements further upstream of the investigated region are also important for LftR binding. DNAse protection assays could help clarify this point.

LmrR, which like LftR is a PadR-type transcription factor of subfamily-2 (Park et al. 2017), has been shown to protect two sites in promoter of its target gene *lmrCD* from DNase digestion experiments (Agustiandari et al. 2008). Of the two sites protected from DNase degradation only one contains the inverted repeat motif that is thought to be the primary binding site of LmrR (Agustiandari et al. 2008). LmrR thus seems to also bind to DNA sequences that do not contain a classical operator sequence including an inverted repeat. The classical operator has therefore been proposed to act as a nucleation site for repressor molecules that enables bigger DNA-protein complexes to form (Agustiandari et al. 2011).

Another model of LmrR-dependent regulation suggests that LmrR exhibits non-specific DNA absorption and specific operator interaction states (Takeuchi et al. 2017). Effector binding to LmrR is believed to shift this equilibrium towards the non-specifically DNA-bound state leading to relief of repression (Takeuchi et al. 2017). It would be much more difficult to determine the exact role of the operator, when the proteins exhibits unspecific-DNA interaction as proposed by this model. However, such a model could explain why complete de-repression was not achieved by the introduction of mutations in the LftR operator.

A motif very similar, but less conserved than the original LftR binding site is present in the *lieAB* promoter. This motif (GTAATAA-N3-ATAC, underlined in figure 3.21) overlaps with the consensus LftR operator. To test if this secondary motif is also involved in the repression of the *lieA* promoter, it was mutated in addition to the 69-68 exchange, but no additional de-repression was observed (data not shown). We were able to identify the sequence GTAW-TACNNN-ATAC as the main DNA binding motif recognized by LftR using base permutations and promoter-*lacZ* reporter constructs. Still, the exact regulatory mechanism on which the *lieAB* repression by LftR is based remains to be determined.

4.6 The function of LstR remains unclear

The *sigC-lstR-lmo0421* operon is not present in all strains of *L. monocytogenes*. Only strains belonging to lineage II (serotypes: 1/2a, 1/2c, 3a) carry these genes (Zhang et al. 2003). Members of lineage II are commonly isolated from foods, but are found less frequently in human clinical cases than lineage I strains (Gray et al. 2004). Natural selection seems to have favored the presences of these genes in lineage II, while it was favorable for lineage I strains to lose them. The specific conditions that underlie the selection pressure will probably be understood once the biological function of the operon has been determined.

The results obtained in this study allow the generation of a simple regulatory model of the *sigC-lstR-lmo0421* operon as shown in figure 4.5. Expression from the LstR operon is regulated by two proteins: SigC and LstR. The data suggest that SigC is essential for the transcription from P_{sigC} (see figure 3.14). While SigC has an activating effect, LstR negatively controls the expression of the operon (see figure 3.14). The function of Lmo0421 is still unclear, but it does not seem to perform the same function as the homologous RodA/FtsW proteins (see figure 3.25).

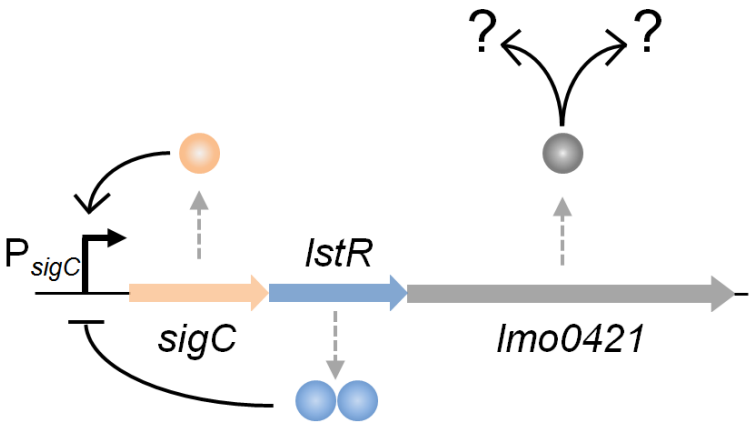

Figure 4.5: Model of the regulation of the *sigC-lstR-lmo0421* operon. SigC is needed for the activity of the P_{sigC} promoter, while LstR negatively controls the expression of the operon. The role of Lmo0421 still needs to be determined.

The natural compound screen revealed that the LstR-controlled genes were induced by the 16-membered macrolide antibiotics niddamycin and josamycin. The induction by josamycin and other macrolide antibiotics (tylosin and erythromycin) was confirmed using commercially available preparations of both compounds (see figure 3.13). Surprisingly, no effect on the resistance against these antibiotics could be detected in mutant strains lacking *lmo0421*, the effector gene of this operon (see table 3.11).

There are several possible explanations for this observation. First, the induction by the macrolides could be unrelated to the biological function as was the case for LftR and rhodamine 6G. Second, it could be the case that under the investigated conditions insufficient amounts of protein accumulated to show a measurable effect. Induction has only been shown on the level of RNA, so the actual protein overproduction needs to be proven in future experiments. Third, the effect of Lmo0421 could be masked by other proteins; for example by the other RodA/FtsW proteins.

Having Lmo0421, a protein showing homology to RodA or FtsW proteins involved in cell wall synthesis, under the control of a PadR-like repressor and an alternative sigma factor is a unique constellation. The sigma factor and the repressor could integrate different signals so that *lmo0421* will only be transcribed when the two signals are registered at the same time. The RodA/FtsW paralog Lmo0421 might thus only be activated under very specific conditions. The negative and positive feedback loops enmeshed in the regulation of the *sigC-lstR-lmo0421* could also result in a variety of different expression patterns depending on the strength of the feedback loops involved (Rodrigo et al. 2016). The regulation could be important for the quick production of protein upon induction or could

result in behaviors such as bistability or oscillation (Rodrigo et al. 2016). It might be helpful to monitor the response of the operon after addition of an inducer like josamycin using a fluorescent reporter to determine what behavior actually occurs.

4.7 LltR-controlled genes are associated with the ability of *L. monocytogenes* to grow at low temperature

In contrast to many other bacteria, *L. monocytogenes* is able to grow at very low temperatures (Junttila et al. 1988, Walker et al. 1990). This capacity is a major determinant in its ability to infect humans and cause disease as shown by a risk assessment model developed by the Food and Agriculture Organization of the United Nations (FAO 2004). In this report the Food and Agriculture Organization of the United Nations suggested that "nearly all cases of listeriosis result from the consumption of high numbers of the pathogen. (FAO 2004)" Ready-to-eat and other foods stored in the fridge for prolonged periods of time are especially prone to be infection sources, because long storage periods allow the pathogen to grow to high densities necessary for infections to occur (FAO 2004).

Japan is a highly developed country, but to-date only a single outbreak of *L. monocytogenes* has been described in Japan (Makino et al. 2005). In this outbreak, the infection vehicle was cheese, a food not part of a traditional Japanese diet. Interestingly, there is also no mandatory notification system for listeriosis in Japan (Miya et al. 2016). For enterohemorrhagic *E. coli* (EHEC) a nationwide surveillance was established after a series of outbreaks in 1996 involving more than 7,500 cases, while in more recent years around 3,000 cases, or roughly 24 EHEC cases/million person, are reported every year (Terajima et al. 2014). It might be possible that without major outbreaks and only sporadic cases, there has not been enough incentive to justify the establishment of an mandatory surveillance system in Japan.

Estimations of the annual rate of listeriosis in Japan range from 83 up to 200 cases a year, with a resulting rate of up to 1.4 cases/million persons (Okutani et al. 2004, Miya et al. 2016). This rate is indeed much below the 4 cases/million persons common in Europe (Goulet et al. 2008), but without extensive national data from Japan a sound comparison is impossible. An MLST-based analysis of some Japanese isolates came to the conclusion that they came from sporadic cases (Miya et al. 2016).

Many of the milk or meat based ready-to-eat foods that are often sources of infection in the west (Swaminathan and Gerner-Smidt 2007) are not part of a traditional Japanese diet. The traditional Japanese diet could thus be a factor limiting the incidence of listeriosis by reducing exposure to foods frequently associated with listeriosis in the west. On the other

hand, raw seafood is often consumed in Japan and some products have been shown to be frequently contaminated with low levels of *L. monocytogenes* (Miya et al. 2010). It is tempting to speculate that the Japanese food culture focused on fresh foods is preventing infections with *L. monocytogenes*, even when the food is consumed raw, because high contamination levels are necessary for infections to occur (FAO 2004). The absence of processed milk and meat products in the traditional diet and the focus on fresh food could prevent *L. monocytogenes* from growing to the densities required for infections to occur, because the products are not stored for extended periods of time under refrigeration.

The *lltR* gene is strongly expressed during growth at 10°C when compared to 37°C (Liu et al. 2002). This supports the assumption that the regulator LltR is essential for growth at low temperatures. The results obtained here show that the presence of an intact copy of the *lltR* gene is indeed essential under refrigeration conditions (see figure 3.27). When the repressor is inactivated, the genes *lmo0600* and *lmo0601* are over-expressed (see table 3.7) and the over-expression of *lmo0600* prevents *L. monocytogenes* from growing efficiently at 6°C (see figure 3.28).

Studying the molecular mechanisms of how the *lltR* operon impacts growth at refrigeration temperature might significantly enhance the understanding of growth of *L. monocytogenes* at low temperature. In order to gain a full understanding of the underlying mechanisms, it is important that the functions of LltR-controlled genes *lmo0600* and *lmo0601* will be determined. Based on sequence similarity, Lmo0600 might be an integral membrane protein and Lmo0601 and internalin-like protein. Several potential functions of the genes are suggested in figure 4.6. These could serve as an inspiration for future experiments.

According to the *in silico* function prediction, both of the proteins might be associated with the membrane. The fact that the *lltr** Δ*lmo0601* mutant lysed at 6°C, while the *lltr** mutant did not (see figure 3.29), suggests a functional link between *lmo0600* and *lmo0601*. The repression of *lmo0600* is necessary for efficient growth at low temperatures. One valid conclusion is that induction of *lmo0600* is unlikely to occur at 6°C, because it would be detrimental for growth. It is therefore essential to find other phenotypes associated with the *lltR* operon in order to characterize its function. It would be especially interesting to find natural conditions or substances that induce the expression of *lmo0600*. Adding an inducer to *L. monocytogenes* cultures at low temperature should prevent growth, possibly providing a novel strategy to control *L. monocytogenes* contamination of refrigerated food.

Figure 4.6: Guesses about the function of Lmo0600 and Lmo0601. Potential functions of the hypothetical proteins Lmo0600 and Lmo0601 are suggested here. The suggestions are based on the *in silico* notion of Lmo0600 being an integral membrane protein and Lmo0600 showing similarity to bacterial adhesins.

Abbreviations

BHI	-	brain heart infusion medium
cDNA	-	copy deoxyribonucleic acid (DNA sequences of all annotated/predicted RNA transcripts in an organism)
ddH_2O	-	double distilled water
DNA	-	deoxyribonucleic acid
DUF	-	domain of unknown function
EDTA	-	ethylenediaminetetraacetic acid
MIC	-	minimal inhibitory concentration
min	-	minutes
MLST	-	multilocus sequence typing
MOPS	-	3-(N-morpholino)propanesulfonic acid
OD	-	optical density
OE-PCR	-	overlap extension PCR
ONPG	-	*o*-nitrophenyl-β-galactoside
PMSF	-	phenylmethanesulfonyl fluoride
PVDF	-	polyvinylidene difluoride
PBP	-	penicillin binding protein
RBS	-	ribosome binding site
RKI	-	Robert Koch-Institute
RNA	-	ribonucleic acid
rRNA	-	ribosomal RNA
sRNA	-	small RNA
TPM	-	transcripts per million (RNA molecules sequenced)

Acknowledgements

I want to thank everyone who supported me during the research and writing of this thesis:

- My supervisor PD Dr. Sven Halbedel for guidance and his invaluable advice and support in scientific questions.
- Prof. Dr. Antje Flieger for the time, support and effort invested in this work and the evaluation of my thesis.
- Prof. Dr. Susanne Engelmann for a very enlightening discussion and the willingness to take on the duty to review my work.
- Apl. Prof. Dr. Michael Hust for sharing his scientific perspective and being prepared to evaluate the thesis as a member of my thesis committee.
- Dr. Stephan Fuchs for his advice in bioinformatics and assay based questions.
- Dr. Philipp Aurass, Dr. Christina Lang and Dr. Sangeeta Banerji for discussions and support in and outside of the laboratory.
- The other lab members of the *Listeria* group with special thanks to Simone Dumschat and Birgitt Hahn for invaluable expertise and support in screening or infection experiments.
- Dr. Martin Fischer and especially Sabrina Wamp for all the interesting, frustrating and funny days in the lab.
- Ute Strutz, Christian Galisch, Wiebke Michel, Miriam Hiller as well as all other colleagues for the characteristic atmosphere at the RKI Wernigerode.
- Finally and without many words, my family for the wonderful time we could spend in Wernigerode. Thank you for your support.

Without the contributions from everyone this work would certainly have been very different.

Bibliography

Aeschlimann, J. R. (2012). "The role of multidrug efflux pumps in the antibiotic resistance of *Pseudomonas aeruginosa* and other gram-negative bacteria. Insights from the Society of Infectious Diseases Pharmacists". In: *Pharmacotherapy* 23 (7), pp. 916–924. DOI: 10.1592/phco.23.7.916.32722.

Agustiandari, H., Lubelski, J., Berg van Saparoea, H. B. van den, Kuipers, O. P., and Driessen, A. J. M. (2008). "LmrR Is a Transcriptional Repressor of Expression of the Multidrug ABC Transporter LmrCD in *Lactococcus lactis*". In: *J Bacteriol* 190 (2), pp. 759–63. DOI: 10.1128/JB.01151-07.

Agustiandari, H., Peeters, E., Wit, J. G. de, Charlier, D., and Driessen, A. J. M. (2011). "LmrR-mediated gene regulation of multidrug resistance in *Lactococcus lactis*". In: *Microbiology* 157 (Pt 5), pp. 1519–1530. DOI: 10.1099/mic.0.048025-0.

Ahmed, M., Borsch, C., Taylor, S., Vázquez-Laslop, N., and Neyfakh, A. (1994). "A protein that activates expression of a multidrug efflux transporter upon binding the transporter substrates". In: *J Biol Chem* 269 (45), pp. 28506–13.

Aldred, K. J., Kerns, R. J., and Osheroff, N. (2014). "Mechanism of quinolone action and resistance". In: *Biochemistry* 53 (10), pp. 1565–1574. DOI: 10.1021/bi5000564.

Alifano, P., Palumbo, C., Pasanisi, D., and Talà, A. (2015). "Rifampicin-resistance, rpoB polymorphism and RNA polymerase genetic engineering". In: *J Biotechnol* 202:60-77. DOI: 10.1016/j.jbiotec.2014.11.024.

Alvarez-Ortega, C., Olivares, J., and Martínez, J. L. (2013). "RND multidrug efflux pumps: what are they good for?" In: *Front Microbiol* 4:7. DOI: 10.3389/fmicb.2013.00007.

Ambrose, K. D., Nisbet, R., and Stephens, D. S. (2005). "Macrolide Efflux in *Streptococcus pneumoniae* Is Mediated by a Dual Efflux Pump (*mel* and *mef*) and Is Erythromycin Inducible". In: *Antimicrob Agents Chemother* 49 (10), pp. 4203–4209. DOI: 10.1128/AAC.49.10.4203-4209.2005.

Angelo, K. M., Conrad, A. R., Saupe, A., Dragoo, H., West, N., Sorenson, A., Barnes, A., Doyle, M., Beal, J., Jackson, K. A., Stroika, S., Tarr, C., Kucerova, Z., Lance, S., Gould, L. H., Wise, M., and Jackson, B. R. (2017). "Multistate outbreak of *Listeria monocytogenes* infections linked to whole apples used in commercially produced, prepackaged caramel apples: United States, 2014-2015". In: *Epidemiol Infect* 145 (5), pp. 848–856. DOI: 10.1017/S0950268816003083.

Annous, B. A., Becker, L. A., Bayles, D. O., Labeda, D. P., and Wilkinson, B. J. (1997). "Critical Role of Anteiso-$C_{15:0}$ Fatty Acid in the Growth of *Listeria monocytogenes* at Low Temperatures". In: *Appl Environ Microbiol* 63 (10), pp. 3887–94.

Aravind, L., Anantharaman, V., Balaji, S., Babu, M. M., and Iyer, L. M. (2005). "The many faces of the helix-turn-helix domain: Transcription regulation and beyond". In: *FEMS Microbiol Rev* 29 (2), pp. 231–262. DOI: 10.1016/j.fmrre.2004.12.008.

Arnaud, M., Chastanet, A., and Débarbouillé, M. (2004). "New Vector for Efficient Allelic Replacement in Naturally Nontransformable, Low-GC-Content, Gram-Positive Bacteria". In: *Appl Environ Microbiol* 70 (11), pp. 6887–91. DOI: 10.1128/AEM.70.11.6887-6891.2004.

Barthelmebs, L., Divies, C., and Cavin, J.-F. (2000a). "Knockout of the p-Coumarate Decarboxylase Gene from *Lactobacillus plantarum* Reveals the Existence of Two Other Inducible Enzymatic Activities Involved in Phenolic Acid Metabolism". In: *Appl Environ Microbiol* 66 (8), pp. 3368–3375. DOI: 10.1128/aem.66.8.3368-3375.2000.

Barthelmebs, L., Lecomte, B., Divies, C., and Cavin, J.-F. (2000b). "Inducible Metabolism of Phenolic Acids in *Pediococcus pentosaceus* Is Encoded by an Autoregulated Operon Which Involves a New Class of Negative Transcriptional Regulator". In: *J Bacteriol* 182 (23), pp. 6724–31. DOI: 10.1128/JB.182.23.6724-6731.2000.

Beigelman, P. and Rantz, L. (1950). "The clinical importance of coagulase-positive, penicillin-resistant *Staphylococcus aureus*". In: *N Engl J Med* 242 (10), pp. 353–358. DOI: 10.1056/NEJM195003092421002.

Berche, P. (1995). "Bacteremia is required for invasion of the murine central nervous system by *Listeria monocytogenes*". In: *Microb Pathog* 18 (5), pp. 323–336. DOI: 10.1006/mpat.1995.0029.

Bernard, R., Guiseppi, A., Chippaux, M., Foglino, M., and Denizot, F. (2007). "Resistance to Bacitracin in *Bacillus subtilis*: Unexpected Requirement of the BceAB ABC Transporter in the Control of Expression of Its Own Structural Genes". In: *J Bacteriol* 189 (23), pp. 8636–8642. DOI: 10.1128/JB.01132-07.

Best, M., Kennedy, M. E., and Coates, F. (1990). "Efficacy of a variety of disinfectants against *Listeria* spp." In: *Appl Environ Microbiol* 56 (2), pp. 377–380. URL: https://www.ncbi.nlm.nih.gov/pmc/articles/PMC183348/.

Blanco, P., Hernando-Amado, S., Reales-Calderon, J. A., Corona, F., Lira, F., Alcalde-Rico, M., Bernardini, A., Sanchez, M. B., and Martinez, J. L. (2016). "Bacterial Multidrug Efflux Pumps: Much More Than Antibiotic Resistance Determinants". In: *Microorganisms* 4(1): 14. DOI: 10.3390/microorganisms4010014.

Bucur, F. I., Grigore-Gurgu, L., Crauwels, P., Riedel, C. U., and Nicolau, A. I. (2018). "Resistance of *Listeria monocytogenes* to Stress Conditions Encountered in Food and Food Processing Environments". In: *Front Microbiol* 9:2700. DOI: 10.3389/fmicb.2018.02700.

Burn, C. G. (1936). "Clinical and Pathological Features of an Infection Caused by a New Pathogen of the Genus Listerella". In: *Am J Pathol* 12 (3), pp. 341–8. URL: https://www.ncbi.nlm.nih.gov/pmc/articles/PMC1911083/.

Campbell, E. A., Korzheva, N., Mustaev, A., Murakami, K., Nair, S., Goldfarb, A., and Darst, S. A. (2001). "Structural mechanism for rifampicin inhibition of bacterial RNA polymerase". In: *Cell* 104 (6), pp. 901–912. DOI: 10.1016/S0092-8674(01)00286-0.

Campos, M. A., Vargas, M. A., Regueiro, V., Llompart, C. M., Albertí, S., and Bengoechea, J. A. (2004). "Capsule polysaccharide mediates bacterial resistance to antimicrobial peptides". In: *Infect Immun* 72 (12), pp. 7107–7114. DOI: 10.1128/IAI.72.12.7107-7114.2004.

Champney, W. S. and Burdine, R. (1995). "Macrolide antibiotics inhibit 50S ribosomal subunit assembly in *Bacillus subtilis* and *Staphylococcus aureus*". In: *Antimicrob Agents Chemother* 39 (9), pp. 2141–2144. DOI: 10.1128/aac.39.9.2141.

Chancey, S. T., Zhou, X., Zähner, D., and Stephens, D. S. (2011). "Induction of efflux-mediated macrolide resistance in *Streptococcus pneumoniae*". In: *Antimicrob Agents Chemother* 55 (7), pp. 3413–22. DOI: 10.1128/AAC.00060-11.

Charlier, C., Perrodeau, É., Leclercq, A., Cazenave, B., Pilmis, B., Henry, B., Lopes, A., Maury, M., Moura, A., Goffinet, F., Dieye, H., Thouvenot, P., Ungeheuer, M., Tourdjman, M., Goulet, V., deValk, H., Lortholary, O., Ravaud, P., Lecuit, M., and group, M. study (2017). "Clinical features and prognostic factors of listeriosis: the MONALISA national prospective cohort study". In: *Lancet Infect Dis* 17 (5), pp. 510–519. DOI: 10.1016/S1473-3099(16)30521-7.

Chaturongakul, S. and Boor, K. J. (2004). "RsbT and RsbV Contribute to σ^B-Dependent Survival under Environmental, Energy, and Intracellular Stress Conditions in *Listeria monocytogenes*". In: *Appl Environ Microbiol* 70 (9), pp. 5349–56. DOI: 10.1128/AEM.70.9.5349-5356.2004.

Chaturongakul, S., Raengpradub, S., Palmer, M. E., Bergholz, T. M., Orsi, R. H., Hu, Y., Ollinger, J., Wiedmann, M., and Boor, K. J. (2011). "Transcriptomic and Phenotypic Analyses Identify Coregulated, Overlapping Regulons among PrfA, CtsR, HrcA, and the Alternative Sigma Factors σ^B, σ^C, σ^H, and σ^L in *Listeria monocytogenes*". In: *Appl Environ Microbiol* 77 (1), pp. 187–200. DOI: 10.1128/AEM.00952-10.

Chico-Calero, I., Suárez, M., González-Zorn, B., Scortti, M., Slaghuis, J., Goebel, W., The European Listeria Genome Consortium, and Vázquez-Boland, J. A. (2002). "Hpt, a bacterial homolog of the microsomal glucose- 6-phosphate translocase, mediates rapid intracellular proliferation in *Listeria*". In: *PNAS* 99 (1), pp. 431–436. DOI: 10.1073/pnas.012363899.

Clardy, J., Fischbach, M., and Currie, C. (2009). "The natural history of antibiotics". In: *Curr Biol* 19 (11), R437–441. DOI: 10.1016/j.cub.2009.04.001.

Cole, M. B., Jones, M. V., and Holyoak, C. (1990). "The effect of pH, salt concentration and temperature on the survival and growth of *Listeria monocytogenes*". In: *J Appl Bacteriol* 69 (1), pp. 63–72. DOI: 10.1111/j.1365-2672.1990.tb02912.x.

Cooksey, C. J. (2016). "Quirks of dye nomenclature. 5. Rhodamines". In: *Biotech Histochem* 91 (1), pp. 71–76. DOI: 10.3109/10520295.2015.1074287.

Cossart, P., Vicente, M. F., Mengaud, J., Baquero, F., Perez-Diaz, J. C., and Berche, P. (1989). "Listeriolysin O is essential for virulence of *Listeria monocytogenes*: direct

evidence obtained by gene complementation". In: *Infect Immun* 57 (11), pp. 3629–3636. URL: https://www.ncbi.nlm.nih.gov/pmc/articles/PMC259877/.

Crimmins, G. T., Herskovits, A. A., Rehder, K., Sivick, K. E., Lauer, P., Jr., T. W. D., and Portnoy, D. A. (2008). "*Listeria monocytogenes* multidrug resistance transporters activate a cytosolic surveillance pathway of innate immunity". In: *PNAS* 105 (29), pp. 10191–6. DOI: 10.1073/pnas.0804170105.

Cui, L., Iwamoto, A., Lian, J.-Q., Neoh, H.-m., Maruyama, T., Horikawa, Y., and Hiramatsu, K. (2006). "Novel Mechanism of Antibiotic Resistance Originating in Vancomycin-Intermediate *Staphylococcus aureus*". In: *Antimicrob Agents Chemother* 50 (2), pp. 428–438. DOI: 10.1128/AAC.50.2.428-438.2006.

Dalton, C. B., Austin, C. C., Sobel, J., Hayes, P. S., Bibb, W. F., Graves, L. M., Swaminathan, B., Proctor, M. E., and Griffin, P. M. (1997). "An Outbreak of Gastroenteritis and Fever Due to *Listeria monocytogenes* in Milk". In: *N Engl J Med* 336, pp. 100–105. DOI: 10.1056/NEJM199701093360204.

Domann, E., Wehland, J., Rohde, M., Pistor, S., Hartl, M., Goebel, W., Leimeister-Wächter, M., Wuenscher, M., and Chakraborty, T. (1992). "A novel bacterial virulence gene in *Listeria monocytogenes* required for host cell microfilament interaction with homology to the proline-rich region of vinculin". In: *EMBO J* 11 (5), pp. 1981–1990.

Donald, A., Fenlon, D., and Seddon, B. (1995). "The relationship between ecophysiology, indigenous microflora and growth of *Listeria monocytogenes* in grass silage". In: *J Appl Bacteriol* 79 (2), pp. 141–148. DOI: 10.1111/j.1365-2672.1995.tb00927.x.

Du, D., Wang-Kan, X., Neuberger, A., Veen, H. W. van, Pos, K. M., Piddock, L. J. V., and Luisi, B. F. (2018). "Multidrug efflux pumps: structure, function and regulation". In: *Nat Rev Microbiol* 16 (9), pp. 523–539. DOI: 10.1038/s41579-018-0048-6.

Duval, M., Dar, D., Carvalho, F., Rocha, E. P. C., Sorek, R., and Cossart, P. (2018). "HflXr, a homolog of a ribosome-splitting factor, mediates antibiotic resistance". In: *Proc Natl Acad Sci U S A* 115 (52), pp. 13359–13364. DOI: 10.1073/pnas.1810555115.

EMA (1997). *Tylosin*. Summary report. Version EMEA/MRL/205/97-FINAL. The European Agency for the Evaluation of Medicinal Products. URL: https://www.ema.europa.eu/en/documents/mrl-report/tylosin-summary-report-3-committee-veterinary-medicinal-products_en.pdf.

Emami, K., Guyet, A., Kawai, Y., Devi, J., Wu, L. J., Allenby, N., Daniel, R. A., and Errington, J. (2017). "RodA as the missing glycosyltransferase in *Bacillus subtilis* and antibiotic discovery for the peptidoglycan polymerase pathway". In: *Nat Microbiol* 2: 16253. DOI: 10.1038/nmicrobiol.2016.253.

EMBL-EBI (2018). *Listeria monocytogenes cDNA*. URL: ftp://ftp.ensemblgenomes.org/pub/bacteria/release-38/fasta/bacteria_0_collection/listeria_monocytogenes_egd_e/cdna/.

FAO (2004). *Risk assessment of Listeria monocytogenes in ready-to-eat foods*. Technical Report. World Health Organization, Food and Agriculture Organization of the United Nations.

Faralla, C., Bastounis, E. E., Ortega, F. E., Light, S. H., Rizzuto, G., Gao, L., Marciano, D. K., Nocadello, S., Anderson, W. F., Robbins, J. R., Theriot, J. A., and Bakard-

jiev, A. I. (2018). "*Listeria monocytogenes* InlP interacts with afadin and facilitates basement membrane crossing". In: *PLoS Pathog* 14(5):e1007094. DOI: 10.1371/journal.ppat.1007094.

Farber, J. M. and Peterkin, P. I. (1991). "*Listeria monocytogenes*, a food-borne pathogen". In: *Microbiol Rev* 55 (3), pp. 476–511.

Fenlon, D. A. (1999). *Listeria, listeriosis, and food safety*. *Listeria monocytogenes in the natural environment*. 2nd. Marcel Dekker, New York, N.Y. ISBN: 0-8247-0235-2.

Fibriansah, G., Kovács, Á. T., Pool, T. J., Boonstra, M., Kuipers, O. P., and Thunnissen, A.-M. W. H. (2012). "Crystal structures of two transcriptional regulators from *Bacillus cereus* define the conserved structural features of a PadR subfamily". In: *PLoS One* 7(11):e48015. DOI: 10.1371/journal.pone.0048015.

Fleming, A. (1929). "On the Antibacterial Action of Cultures of a *Penicillium*, with Special Reference to their Use in the Isolation of *B. influenzae*". In: *Br J Exp Pathol* 10 (3), pp. 226–236.

Freitag, N. E., Port, G. C., and Miner, M. D. (2009). "*Listeria monocytogenes* - from saprophyte to intracellular pathogen". In: *Nat Rev Microbiol* 7 (9), pp. 623–8. DOI: 10.1038/nrmicro2171.

Frenkel, N., Dover, R. S., Titon, E., Shai, Y., and Rom-Kedar, V. (2018). "Bistable bacterial growth dynamics in the presence of antimicrobial agents". In: *bioRxiv*. DOI: 10.1101/330035.

Frère, J. M., Nguyen-Distèche, M., Coyette, J., and Joris, B. (1992). *The Chemistry of β-Lactams*. *Mode of action: interaction with the penicillin binding proteins*. Ed. by M. I. Page. Springer, Dordrecht. DOI: 10.1007/978-94-011-2928-2_5.

Gabaldón, T. (2005). "Evolution of proteins and proteomes: a phylogenetics approach". In: *Evol Bioinform Online* 1: 51-61, PMC2658874.

George, S. M., Lund, B. M., and Brocklehurst, T. (1988). "The effect of pH and temperature on initiation of growth of *Listeria monocytogenes*". In: *Lett Appl Microbiol* 6 (6), pp. 153–6. DOI: 10.1111/j.1472-765X.1988.tb01237.x.

Ghosh, P., Halvorsen, E. M., Ammendolia, D. A., Mor-Vaknin, N., O'Riordan, M. X. D., Brumell, J. H., Markovitz, D. M., and Higgins, D. E. (2018). "Invasion of the Brain by *Listeria monocytogenes* Is Mediated by InlF and Host Cell Vimentin". In: *MBio* 9(1). pii: e00160-18. DOI: 10.1128/mBio.00160-18.

Gill, D. A. (1933). "Circling disease: A meningoencephalitis of sheep in New Zealand". In: *Vet J* 89 (6), pp. 258–70. DOI: 10.1016/S0372-5545(17)39206-4.

Glaser, P., Frangeul, L., Buchrieser, C., Rusniok, C., Amend, A., Baquero, F., Berche, P., Bloecker, H., Brandt, P., Chakraborty, T., Charbit, A., Chetouani, F., Couvé, E., Daruvar, A. de, Dehoux, P., Domann, E., Dominguez-Bernal, G., Duchaud, E., Durant, L., Dussurget, O., Entian, K.-D., Fsihi, H., Portillo, F. G.-D., Garrido, P., Gautier, L., Goebel, W., Gómez-López, N., Hain, T., Hauf, J., Jackson, D., Jones, L.-M., Kaerst, U., Kreft, J., Kuhn, M., Kunst, F., Kurapkat, G., Madueño, E., Maitournam, A., Vicente, J. M., Ng, E., Nedjari, H., Nordsiek, G., Novella, S., Pablos, B. de, Pérez-Diaz, J.-C., Purcell, R., Remmel, B., Rose, M., Schlueter, T., Simoes, N., Tierrez, A., Vázquez-

Boland, J.-A., Voss, H., Wehland, J., and Cossart, P. (2001). "Comparative Genomics of *Listeria* Species". In: *Science* 294, pp. 849–852. DOI: 10.1126/science.1063447.

Goulet, V., Hedberg, C., Monnier, A. L., and deValk, H. (2008). "Increasing Incidence of Listeriosis in France and Other European Countries". In: *Emerg Infect Dis* 15 (5), pp. 734–740. DOI: 10.3201/eid1405.071395.

Graefe, U., Schlegel, R., Ritzau, M., Ihn, W., Dornberger, K., Stengel, C., Fleck, W., Gutsche, W., Haertl, A., and Paulus, E. (1995). "Aurantimycins, new depsipeptide antibiotics from *Streptomyces aurantiacus* IMET 43917. Production, isolation, structure elucidation, and biological activity." In: *J Antibiot (Tokyo)* 48 (2), pp. 119–25. DOI: 10.7164/antibiotics.48.119.

Gray, M. J., Freitag, N. E., and Boor, K. J. (2006). "How the Bacterial Pathogen *Listeria monocytogenes* Mediates the Switch from Environmental Dr. Jekyll to Pathogenic Mr. Hyde". In: *Infect Immun* 74 (5), pp. 2505–2512. DOI: 10.1128/IAI.74.5.2505-2512.2006.

Gray, M. J., Zadoks, R. N., Fortes, E. D., Dogan, B., Cai, S., Chen, Y., Scott, V. N., Gombas, D. E., Boor, K. J., and Wiedmann, M. (2004). "*Listeria monocytogenes* Isolates from Foods and Humans Form Distinct but Overlapping Populations". In: *Appl Environ Microbiol* 70 (10), pp. 5833–41. DOI: 10.1128/AEM.70.10.5833-5841.2004.

Gray, M. L. and Killinger, A. H. (1966). "*Listeria monocytogenes* and listeric infections." In: *Bacteriol Rev* 30 (2), pp. 309–82. URL: https://www.ncbi.nlm.nih.gov/pmc/articles/PMC440999/.

Grigoriev, P., Schlegel, R., Dornberger, K., and Graefe, U. (1995). "Formation of membrane pores by aurantimycins A and B, new lipopeptide antibiotics from *Streptomyces aurantiacus*". In: *Bioelectrochem Bioenerg* 36 (1), pp. 57–9. DOI: 10.1016/0302-4598(94)01721-C.

Gründling, A., Burrack, L. S., Bouwer, H. G. A., and Higgins, D. E. (2004). "*Listeria monocytogenes* regulates flagellar motility gene expression through MogR, a transcriptional repressor required for virulence". In: *PNAS* 101 (33), pp. 12318–12323. DOI: 10.1073/pnas.0404924101.

Guérin, F., Galimand, M., Tuambilangana, F., Courvalin, P., and Cattoir, V. (2014). "Overexpression of the Novel MATE Fluoroquinolone Efflux Pump FepA in *Listeria monocytogenes* Is Driven by Inactivation of Its Local Repressor FepR". In: *PLoS One* 9 (9), e106340. DOI: 10.1371/journal.pone.0106340.

Guillet, C., Join-Lambert, O., Monnier, A. L., Leclercq, A., Mechaï, F., Mamzer-Bruneel, M.-F., Bielecka, M. K., Scortti, M., Disson, O., Berche, P., Vazquez-Boland, J., Lortholary, O., and Lecuit, M. (2010). "Human Listeriosis Caused by *Listeria ivanovii*". In: *Emerg Infect Dis* 16 (1), pp. 136–138. DOI: 10.3201/eid1601.091155.

Gury, J., Barthelmebs, L., Tran, N. P., Diviès, C., and Cavin, J.-F. (2004). "Cloning, Deletion, and Characterization of PadR, the Transcriptional Repressor of the Phenolic Acid Decarboxylase-Encoding padA Gene of *Lactobacillus plantarum*". In: *Appl Environ Microbiol* 70 (4), pp. 2146–53. DOI: 10.1128/AEM.70.4.2146-2153.2004.

Hain, T., Hossain, H., Chatterjee, S. S., Machata, S., Volk, U., Wagner, S., Brors, B., Haas, S., Kuenne, C. T., Billion, A., Otten, S., Pane-Farre, J., Engelmann, S., and

Chakraborty, T. (2008). "Temporal transcriptomic analysis of the *Listeria monocytogenes* EGD-e sigmaB regulon". In: *BMC Genomics* 8:20. DOI: 10.1186/1471-2180-8-20.

Halbedel, S., Prager, R., Banerji, S., Kleta, S., Trost, E., Nishanth, G., Alles, G., Hölzel, C., Schlesiger, F., Pietzka, A., Schlüter, D., and Flieger, A. (2019). "A *Listeria monocytogenes* ST2 clone lacking chitinase ChiB from an outbreak of non-invasive gastroenteritis". In: *Epidemiol Infect* 8 (1), pp. 17–28. DOI: 10.1080/22221751.2018.1558960.

Hauf, S., Herrmann, J., Miethke, M., Gibhardt, J., Commichau, F. M., Müller, R., Fuchs, S., and Halbedel, S. (2019a). "Aurantimycin resistance genes contribute to survival of *Listeria monocytogenes* during life in the environment". In: *Mol Microbiol* 111 (4), pp. 1009–1024. DOI: 10.1111/mmi.14205.

Hauf, S., Möller, L., Fuchs, S., and Halbedel, S. (2019b). "PadR-type repressors controlling production of a non-canonical FtsW/RodA homologue and other trans-membrane proteins". In: *Sci Rep* 9: 10023. DOI: 10.1038/s41598-019-46347-w.

Henriques, A. O., Glaser, P., Piggot, P. J., and Moran, C. P. J. (1998). "Control of cell shape and elongation by the rodA gene in *Bacillus subtilis*". In: *Mol Microbiol* 28 (2), pp. 235–247. DOI: 10.1046/j.1365-2958.1998.00766.x.

Heravi, K. M., Lange, J., Watzlawick, H., Kalinowski, J., and Altenbuchner, J. (2015). "Transcriptional Regulation of the Vanillate Utilization Genes (vanABK Operon) of *Corynebacterium glutamicum* by VanR, a PadR-Like Repressor". In: *J Bacteriol* 197 (5), pp. 959–972. DOI: 10.1128/JB.02431-14.

Herrmann, J., JanRybniker, and RolfMüller (2017). "Novel and revisited approaches in antituberculosis drug discovery". In: *Curr Opin Biotechnol* 48:94-101. DOI: 10.1016/j.copbio.2017.03.023.

Hoffmann, S., Walter, S., Blume, A.-K., Fuchs, S., Schmidt, C., Scholz, A., and Gerlach, R. G. (2018). "High-Throughput Quantification of Bacterial-Cell Interactions Using Virtual Colony Counts". In: *Front Cell Infect Microbiol* 8: 43. DOI: 10.3389/fcimb.2018.00043.

Høibya, N., Bjarnsholt, T., Givskov, M., Molin, S., and Ciofu, O. (2010). "Antibiotic resistance of bacterial biofilms". In: *Int J Antimicrob Agents* 35 (4), pp. 322–332. DOI: 10.1016/j.ijantimicag.2009.12.011.

Huillet, E., Larpin, S., Pardon, P., and Berche, P. (1999). "Identification of a new locus in *Listeria monocytogenes* involved in cellobiose-dependent repression of *hly expression*". In: *FEMS Microbiol Lett* 174 (2), pp. 265–72. DOI: 10.1111/j.1574-6968.1999.tb13578.x.

Huillet, E., Velge, P., Vallaeys, T., and Pardon, P. (2006). "LadR, a new PadR-related transcriptional regulator from *Listeria monocytogenes*, negatively regulates the expression of the multidrug efflux pump MdrL". In: *FEMS Microbiol Lett* 254 (1), pp. 87–94. DOI: 10.1111/j.1574-6968.2005.00014.x.

Imai, K. and Mitaku, S. (2005). "Mechanisms of secondary structure breakers in soluble proteins". In: *Biophysics (Nagoya-shi)* 1, pp. 55–65. DOI: 10.2142/biophysics.1.55.

Jandhyala, S. M., Talukdar, R., Subramanyam, C., Vuyyuru, H., Sasikala, M., and Reddy, D. N. (2015). "Role of the normal gut microbiota". In: *World J Gastroenterol* 21 (29), pp. 8787–8803. DOI: 10.3748/wjg.v21.i29.8787.

Jiang, X., Yu, T., Xu, Y., Wang, H., Korkeala, H., and Shi, L. (2018). "MdrL, a major facilitator superfamily efflux pump of *Listeria monocytogenes* involved in tolerance to benzalkonium chloride". In: *Appl Microbiol Biotechnol* Epub, pp. 1–12. DOI: 10.1007/s00253-018-9551-y.

Jones, E. M. and MacGowan, A. P. (1995). "Antimicrobial chemotherapy of human infection due to *Listeria monocytogenes*". In: *Eur J Clin Microbiol Infect Dis* 14 (3), pp. 165–075. DOI: 10.1007/BF02310351.

Joseph, B. and Goebel, W. (2007). "Life of *Listeria monocytogenes* in the host cells' cytosol". In: *Microbes Infect* 9 (10), pp. 1188–1195. DOI: 10.1016/j.micinf.2007.05.006.

Junttila, J. R., Niemelä, S., and Hirn, J. (1988). "Minimum growth temperatures of *Listeria monocytogenes* and non-haemolytic listeria". In: *J Appl Bacteriol* 65 (4), pp. 321–7. DOI: 10.1111/j.1365-2672.1988.tb01898.x.

Kanki, M., Naruse, H., and Kawatsu, K. (2018). "Comparison of listeriolysin O and phospholipases PlcA and PlcB activities, and initial intracellular growth capability among food and clinical strains of *Listeria monocytogenes*". In: *J Appl Microbiol* 124 (3), pp. 899–909. DOI: 10.1111/jam.13692.

Kannan, K., Kanabar, P., Schryer, D., Florin, T., Oh, E., Bahroos, N., Tenson, T., Weissman, J. S., and Mankin, A. S. (2014). "The general mode of translation inhibition by macrolide antibiotics". In: *PNAS* 111 (45), pp. 15958–63. DOI: 10.1073/pnas.1417334111.

Kapoor, G., Saigal, S., and Elongavan, A. (2017). "Action and resistance mechanisms of antibiotics: A guide for clinicians". In: *J Anaesthesiol Clin Pharmacol* 33 (3), pp. 300–305. DOI: 10.4103/joacp.JOACP_349_15.

Kaval, K. G., Hahn, B., Tusamda, N., Albrecht, D., and Halbedel, S. (2015). "The PadR-like transcriptional regulator LftR ensures efficient invasion of *Listeria monocytogenes* into human host cells". In: *Front Microbiol* 6. DOI: 10.3389/fmicb.2015.00772.

Kazmierczak, M. J., Mithoe, S. C., Boor, K. J., and Wiedmann, M. (2003). "*Listeria monocytogenes* σ^B regulates stress response and virulence functions". In: *J Bacteriol* 185 (19), pp. 5722–5734. DOI: 10.1128/jb.185.19.5722-5734.2003.

Kersey, P. J., Allen, J. E., Allot, A., Barba, M., Boddu, S., Bolt, B. J., Carvalho-Silva, D., Christensen, M., Davis, P., Grabmueller, C., Kumar, N., Liu, Z., Maurel, T., Moore, B., McDowall, M. D., Maheswari, U., Naamati, G., Newman, V., Ong, C. K., Paulini, M., Pedro, H., Perry, E., Russell, M., Sparrow, H., Tapanari, E., Taylor, K., Vullo, A., Williams, G., Zadissia, A., Olson, A., Stein, J., Wei, S., Tello-Ruiz, M., Ware, D., Luciani, A., Potter, S., Finn, R. D., Urban, M., Hammond-Kosack, K. E., Bolser, D. M., Silva, N. D., Howe, K. L., Langridge, N., Maslen, G., Staines, D. M., and Yates, A. (2018). "Ensembl Genomes 2018: an integrated omics infrastructure for non-vertebrate species." In: *Nucleic Acids Res* 46 (D1), pp. D802–8. DOI: 10.1093/nar/gkx1011.

Kocks, C., Hellio, R., Gounon, P., Ohayon, H., and Cossart, P. (1993). "Polarized distribution of *Listeria monocytogenes* surface protein ActA at the site of directional actin assembly". In: *J Cell Sci* 105 (Pt3):699-710.

Kohanski, M. A., Dwyer, D. J., and Collins, J. J. (2010). "How antibiotics kill bacteria: From targets to networks". In: *Nat Rev Microbiol* 8 (6), pp. 423–435. DOI: 10.1038/nrmicro2333.

Korzybski, T., Kowszyk-Gindifer, Z., and Kurylowicz, W. (1967). *Antibiotics: Origin, Nature and Properties*. Trans. by E. Paryski.

Kovacikova, G., Lin, W., and Skorupski, K. (2003). "The virulence activator AphA links quorum sensing to pathogenesis and physiology in *Vibrio cholerae* by repressing the expression of a penicillin amidase gene on the small chromosome". In: *J Bacteriol* 185 (16), pp. 4825–4836. DOI: 10.1128/JB.185.16.4825-4836.2003.

Łabaj, P. P. and Kreil, D. P. (2016). "Sensitivity, specificity, and reproducibility of RNA-Seq differential expression calls". In: *Biol Direct* 11: 66. DOI: 10.1186/s13062-016-0169-7.

Lai, Y., Villaruz, A. E., Li, M., Cha, D. J., Sturdevant, D. E., and Otto, M. (2007). "The human anionic antimicrobial peptide dermcidin induces proteolytic defence mechanisms in staphylococci". In: *Mol Microbiol* 63 (2), pp. 497–506. DOI: 10.1111/j.1365-2958.2006.05540.x.

Larsen, M. H., Leisner, J. J., and Ingmer, H. (2010). "The Chitinolytic Activity of *Listeria monocytogenes* EGD Is Regulated by Carbohydrates but Also by the Virulence Regulator PrfA". In: *Appl Environ Microbiol* 76 (19), pp. 6470–6476. DOI: 10.1128/AEM.00297-10.

Lecuit, M., Vandormael-Pournin, S., Lefort, J., Huerre, M., Gounon, P., Dupuy, C., Babinet, C., and Cossart, P. (2001). "A transgenic model for listeriosis: role of internalin in crossing the intestinal barrier". In: *Science* 292 (5522), pp. 1722–1725. DOI: 10.1126/science.1059852.

Lee, C., Kim, M. I., Park, J., and Hong, M. (2019). "Structure-based molecular characterization and regulatory mechanism of the LftR transcription factor from *Listeria monocytogenes*: Conformational flexibilities and a ligand-induced regulatory mechanism". In: *PLoS One* 14(4):e0215017. DOI: 10.1371/journal.pone.0215017.

Leisner, J. J., Larsen, M. H., Jørgensen, R. L., Brøndsted, L., Thomsen, L. E., and Ingmer, H. (2008). "Chitin Hydrolysis by *Listeria* spp., Including *L. monocytogenes*". In: *Appl Environ Microbiol* 74 (12), pp. 3823–3830. DOI: 10.1128/AEM.02701-07.

Lewin, G. R., Carlos, C., Chevrette, M. G., Horn, H. A., McDonald, B. R., Stankey, R. J., Fox, B. G., and Currie, C. R. (2016). "Evolution and Ecology of *Actinobacteria* and Their Bioenergy Applications". In: *Annu Rev Microbiol* 70:235-54. DOI: 10.1146/annurev-micro-102215-095748.

Lewis, K. (2012). *Antibiotic Resistance. Handbook of Experimental Pharmacology, vol 211. Persister Cells: Molecular Mechanisms Related to Antibiotic Tolerance.* Ed. by A. Coates. Springer, Berlin, Heidelberg. DOI: 10.1007/978-3-642-28951-4_8.

Lewis, S. J. and Corry, J. E. L. (1991). "Comparison of a cold enrichment and the FDA method for isolating *Listeria monocytogenes* and other *Listeria* spp. from ready-to-eat

food on retail sale in the U.K". In: *Int J Food Microbiol* 12 (2-3), pp. 281–286. DOI: 10.1016/0168-1605(91)90080-9.

Linke, K., Rückerl, I., Brugger, K., Karpiskova, R., Walland, J., Muri-Klinger, S., Tichy, A., Wagner, M., and Stessl, B. (2014). "Reservoirs of *Listeria* Species in Three Environmental Ecosystems". In: *Appl Environ Microbiol* 80 (18), pp. 5583–5592. DOI: 10.1128/AEM.01018-14.

Liu, S., Graham, J. E., Bigelow, L., II, P. D. M., and Wilkinson, B. J. (2002). "Identification of *Listeria monocytogenes* Genes Expressed in Response to Growth at Low Temperature". In: *Appl Environ Microbiol* 68 (4), pp. 1697–1705. DOI: 10.1128/AEM.68.4.1697-1705.2002.

Mackey, B. and Bratchell, N. (1989). "The heat resistance of *Listeria monocytogenes*". In: *Lett Appl Microbiol* 9, pp. 89–94. DOI: 10.1111/j.1472-765X.1989.tb00298.x.

Madoori, P. K., Agustiandari, H., Driessen, A. J. M., and Thunnissen, A.-M. W. H. (2009). "Structure of the transcriptional regulator LmrR and its mechanism of multidrug recognition". In: *EMBO J* 28 (2), pp. 156–166. DOI: 10.1038/emboj.2008.263.

Makino, S.-I., Kawamoto, K., Takeshi, K., Okada, Y., Yamasaki, M., S.Yamamoto, and S.Igimi (2005). "An outbreak of food-borne listeriosis due to cheese in Japan, during 2001". In: *Int J Food Microbiol* 104 (2), pp. 189–196. DOI: 10.1016/j.ijfoodmicro.2005.02.009.

Mao, S., Zhang, M., and Zhu, J. L. andWeiyun (2015). "Characterising the bacterial microbiota across the gastrointestinal tracts of dairy cattle: membership and potential function". In: *Sci Rep* 5:16116. DOI: 10.1038/srep16116.

Mateus, T., Silva, J., Maia, R. L., and Teixeira, P. (2013). "Listeriosis during Pregnancy: A Public Health Concern". In: *ISRN Obstet Gynecol* 2013: 851712. DOI: 10.1155/2013/851712.

Mattila, M., Somervuo, P., Rattei, T., Korkeala, H., Stephan, R., and Tasara, T. (2012). "Phenotypic and transcriptomic analyses of Sigma L-dependent characteristics in *Listeria monocytogenes* EGD-e". In: *Food Microbiol* 32 (1), pp. 152–164. DOI: 10.1016/j.fm.2012.05.005.

Mazzei, T., Mini, E., Novelli, A., and Periti, P. (1993). "Chemistry and mode of action of macrolides". In: *J Antimicrob Chemother* 31 Suppl C:1-9. DOI: 10.1093/jac/31.suppl_c.1.

McCollum, J. T., Cronquist, A. B., Silk, B. J., Jackson, K. A., O'Connor, K. A., Cosgrove, S., Gossack, J. P., Parachini, S. S., Jain, N. S., Ettestad, P., Ibraheem, M., Cantu, V., Joshi, M., DuVernoy, T., Fogg, N. W. J., Gorny, J. R., Mogen, K. M., Spires, C., Teitell, P., Joseph, L. A., Tarr, C. L., Imanishi, M., Neil, K. P., and Mahon, R. V. T. B. E. (2013). "Multistate outbreak of listeriosis associated with cantaloupe". In: *N Engl J Med* 369, pp. 944–953. DOI: 10.1056/NEJMoa1215837.

McCoy, L. S., Xie, Y., and Tor, Y. (2011). "Antibiotics that target protein synthesis". In: *Wiley Interdiscip Rev RNA* 2 (2), pp. 209–232. DOI: 10.1002/wrna.60.

Meeske, A. J., Riley, E. P., Robins, W. P., Uehara, T., Mekelanos, J. J., Kahne, D., Walker, S., Kruse, A. C., Bernhardt, T. G., and Rudner, D. Z. (2016). "SEDS proteins are a

widespread family of bacterial cell wall polymerases". In: *Nature* 537 (7622), pp. 634–638. DOI: 10.1038/nature19331.

Mengaud, J., Ohayon, H., Gounon, P., Mège, R.-M., and Cossart, P. (1996). "E-Cadherin Is the Receptor for Internalin, a Surface Protein Required for Entry of *Listeria monocytogenes* into Epithelial Cells". In: *Cell* 84 (6), pp. 923–932. DOI: 10.1016/S0092-8674(00)81070-3.

Milenbachs, A. A., Brown, D. P., Moors, M., and Youngman, P. (2003). "Carbon-source regulation of virulence gene expression in *Listeria monocytogenes*". In: *Mol Microbiol* 23 (5), pp. 1075–1085. DOI: 10.1046/j.1365-2958.1997.2711634.x.

Miya, S., Takahashi, H., Ishikawa, T., Fujii, T., and Kimura, B. (2010). "Risk of *Listeria monocytogenes* Contamination of Raw Ready-To-Eat Seafood Products Available at Retail Outlets in Japan". In: *Appl Environ Microbiol* 76 (10), pp. 3383–3386. DOI: 10.1128/AEM.01456-09.

Miya, S., Takahashi, H., Nakagawa, M., Kuda, T., Igimi, S., and Kimura, B. (2016). "Genetic Characteristics of Japanese Clinical *Listeria monocytogenes* Isolates". In: *PLoS One* 10(3):e0122902. DOI: 10.1371/journal.pone.0122902.

Moellering, R. J. (1981). "Essential characteristics of antibiotics for the treatment of seriously ill patients". In: *Clin Ther* 4 Suppl A:1-7.

Monk, I. R., Gahan, C. G. M., and Hill, C. (2008). "Tools for Functional Postgenomic Analysis of *Listeria monocytogenes*". In: *Appl Environ Microbiol* 74 (13), pp. 3921–3934. DOI: 10.1128/AEM.00314-08.

Morita, Y., Murata, T., Mima, T., Shiota, S., Kuroda, T., Mizushima, T., Gotoh, N., Nishino, T., and Tsuchiya, T. (2003). "Induction of mexCD-oprJ operon for a multidrug efflux pump by disinfectants in wild-type *Pseudomonas aeruginosa* PAO1". In: *J Antimicrob Chemother* 51 (4), pp. 991–4. DOI: 10.1093/jac/dkg173.

Morvan, A., Moubareck, C., Leclercq, A., Hervé-Bazin, M., Bremont, S., Lecuit, M., Courvalin, P., and Monnier, A. L. (2010). "Antimicrobial resistance of *Listeria monocytogenes* strains isolated from humans in France". In: *Antimicrob Agents Chemother* 54 (6), pp. 2728–2731. DOI: 10.1128/AAC.01557-09.

Mujahid, S., Orsi, R. H., Vangay, P., Boor, K. J., and Wiedmann, M. (2013a). "Protein level identification of the *Listeria monocytogenes* Sigma H, Sigma L, and Sigma C regulons". In: *BMC Microbiol* 13: 156. DOI: 10.1186/1471-2180-13-156.

Mujahid, S., Orsi, R., Vangay, P., Boor, K., and Wiedmann, M. (2013b). "Refinement of the *Listeria monocytogenes* σ^B regulon through quantitative proteomic analysis". In: *Microbiology* 159 (Pt 6), pp. 1109–19. DOI: 10.1099/mic.0.066001-0.

Munita, J. M. and Arias, C. A. (2016). "Mechanisms of antibiotic resistance". In: *Microbiol Spectr* 4 (2). DOI: 10.1128/microbiolspec.VMBF-0016-2015.

Murray, E., Webb, R., and Swann, M. (1926). "A disease of rabbits characterised by a large mononuclear leucocytosis, caused by a hitherto undescribed bacillus *Bacterium monocytogenes* (n.sp.)" In: *J Pathol* 29 (4), pp. 407–39. DOI: 10.1002/path.1700290409.

Nawrocki, K. L., Crispell, E. K., and McBride, S. M. (2014). "Antimicrobial Peptide Resistance Mechanisms of Gram-Positive Bacteria". In: *Antibiotics (Basel)* 3 (4), pp. 416–92. DOI: 10.3390/antibiotics3040461.

Nguyen, T. K. C., Tran, N. P., and Cavin, J.-F. (2011). "Genetic and Biochemical Analysis of PadR-padC Promoter Interactions during the Phenolic Acid Stress Response in *Bacillus subtilis* 168". In: *J Bacteriol* 193 (16), pp. 4180–4191. DOI: 10.1128/JB.00385-11.

Nyfeldt, A. (1929). "Etiologie de la mononucleose infectieuse". In: *Comptes Rendus des Seances de la Societe de Biologie* 101, pp. 590–591.

Ohki, R., Giyanto, Tateno, K., Masuyama, W., Moriya, S., Kobayashi, K., and Ogasawara, N. (2003). "The BceRS two-component regulatory system induces expression of the bacitracin transporter, BceAB, in B*acillus subtilis*". In: *Mol Microbiol* 49 (4), pp. 1135–44. DOI: 10.1046/j.1365-2958.2003.03653.x.

Okutani, A., Okada, Y., Yamamoto, S., and Igimi, S. (2004). "Nationwide survey of human *Listeria monocytogenes* infection in Japan". In: *Epidemiol Infect* 132 (4), pp. 769–772. DOI: 10.1017/s0950268804001967.

Oliver, H. F., Orsi, R. H., Ponnala, L., Keich, U., Wang, W., Sun, Q., Cartinhour, S. W., Filiatrault, M. J., Wiedmann, M., and Boor, K. J. (2009). "Deep RNA sequencing of *L. monocytogenes* reveals overlapping and extensive stationary phase and sigma B-dependent transcriptomes, including multiple highly transcribed noncoding RNAs". In: *BMC Genomics* 10:641. DOI: 10.1186/1471-2164-10-641.

Ooi, S. T. and Lorber, B. (2005). "Gastroenteritis Due to *Listeria monocytogenes*". In: *Clin Infect Dis* 40 (9), pp. 1327–32. DOI: 10.1086/429324.

Ortega, F. E., Rengarajan, M., Chavez, N., Radhakrishnan, P., Gloerich, M., Bianchini, J., Siemers, K., Luckett, W. S., Lauer, P., Nelson, W. J., and Theriot, J. A. (2017). "Adhesion to the host cell surface is sufficient to mediate *Listeria monocytogenes* entry into epithelial cells". In: *Mol Biol Cell* 28(22):2945-2957. DOI: 10.1091/mbc.E16-12-0851.

Pan, Y., Breidt, F. J., and Kathariou, S. (2006). "Resistance of *Listeria monocytogenes* biofilms to sanitizing agents in a simulated food processing environment". In: *Appl Environ Microbiol* 72 (12), pp. 7711–7717. DOI: 10.1128/AEM.01065-06.

Park, S. C., Kwak, Y. M., Song, W. S., Hong, M., and Yoon, S.-i. (2017). "Structural basis of effector and operator recognition by the phenolic acid-responsive transcriptional regulator PadR". In: *Nucleic Acids Res* 45 (22), pp. 13080–13093. DOI: 10.1093/nar/gkx1055.

Paspaliari, D. K., Loose, J. S. M., Larsen, M. H., and Vaaje-Kolstad, G. (2015). "*Listeria monocytogenes* has a functional chitinolytic system and an active lytic polysaccharide monooxygenase". In: *FEBS J* 282 (5), pp. 921–936. DOI: 10.1111/febs.13191.

Patro, R., Duggal, G., Love, M. I., Irizarry, R. A., and Kingsford, C. (2017). "Salmon provides fast and bias-aware quantification of transcript expression". In: *Nat Methods* 14 (4), pp. 417–9. DOI: 10.1038/nmeth.4197.

Pentecost, M., Otto, G., Theriot, J. A., and Amieva, M. R. (2006). "*Listeria monocytogenes* Invades the Epithelial Junctions at Sites of Cell Extrusion". In: *PLoS Pathog* 2(1): e3. DOI: 10.1371/journal.ppat.0020003.

Perrin, M., Bemer, M., and Delamare, C. (2003). "Fatal Case of *Listeria innocua* Bacteremia". In: *J Clin Microbiol* 41 (11), pp. 5308–5309. DOI: 10.1128/JCM.41.11.5308-5309.2003.

Pfam, E. M. B. L. (2019). *Family: PadR (PF03551), Species distribution*. URL: https://pfam.xfam.org/family/PadR#tabview=tab7.

Pine, L., Malcolm, G. B., Brooks, J. B., and Daneshvar, M. I. (1989). "Physiological studies on the growth and utilization of sugars by *Listeria* species". In: *Can J Microbiol* 35 (2), pp. 245–254. DOI: 10.1139/m89-037.

Pizarro-Cerdá, J., Kühbacher, A., and Cossart, P. (2012). "Entry of *Listeria monocytogenes* in Mammalian Epithelial Cells: An Updated View". In: *Cold Spring Harb Perspect Med* 2(11):a010009. DOI: 10.1101/cshperspect.a010009.

Poole, K. (2007). "Efflux pumps as antimicrobial resistance mechanisms". In: *Ann Med* 39 (3), pp. 162–176. DOI: 10.1080/07853890701195262.

Poteete, A. R., Rennell, D., and Bouvier, S. E. (1992). "Functional significance of conserved amino acid residues". In: *Proteins* 13 (1), pp. 38–40. DOI: 10.1002/prot.340130104.

Pouillot, R., Klontz, K. C., Chen, Y., Burall, L. S., Macarisin, D., Doyle, M., Bally, K. M., Strain, E., Datta, A. R., Hammack, T. S., and Doren, J. M. V. (2016). "Infectious Dose of *Listeria monocytogenes* in Outbreak Linked to Ice Cream, United States, 2015". In: *Emerg Infect Dis* 22 (12), pp. 2113–2119. DOI: 10.3201/eid2212.160165.

Principi, N. and Esposito, S. (1999). "Comparative Tolerability of Erythromycin and Newer Macrolide Antibacterials in Paediatric Patients". In: *Drug Saf* 20 (1), pp. 25–41. DOI: 10.2165/00002018-199920010-00004.

Quereda, J. J., Pucciarelli, M. G., Botello-Morte, L., Calvo, E., Carvalho, F., Bouchier, C., Vieira, A., Mariscotti, J. F., Chakraborty, T., Cossart, P., Hain, T., Cabanes, D., and Portillo, F. G.-d. (2013). "Occurrence of mutations impairing sigma factor B (SigB) function upon inactivation of *Listeria monocytogenes* genes encoding surface proteins". In: *Microbiology* 157 (Pt 7), pp. 1328–39. DOI: 10.1099/mic.0.067744-0.

Rieke, E. L., Soupir, M. L., Moorman, T. B., Yang, F., and Howe, A. C. (2018). "Temporal Dynamics of Bacterial Communities in Soil and Leachate Water After Swine Manure Application". In: *Front Microbiol* 9: 3197. DOI: 10.3389/fmicb.2018.03197.

Rismondo, J., Halbedel, S., and Gründling, A. (2019). "Cell shape and antibiotic resistance is maintained by the activity of multiple FtsW and RodA enzymes in *Listeria monocytogenes*". In: *bioRxiv* 589911. DOI: 10.1101/589911.

Roberts, M. C. (2005). "Update on acquired tetracycline resistance genes". In: *FEMS Microbiol Lett* 245 (2), pp. 195–203. DOI: 10.1016/j.femsle.2005.02.034.

Rocourt, J., Hof, H., Schrettenbrunner, A., Malinverni, R., and Bille, J. (1986). "Acute purulent *Listeria seelingeri* meningitis in an immunocompetent adult". In: *Schweiz Med Wochenschr* 116 (8), pp. 248–251.

Rocourt, J. (1999). *Listeria, listeriosis, and food safety. The Genus Listeria and Listeria monocytogenes: Phylogenetic Position, Taxonomy, and Identification*. Ed. by E. T. Ryser. Ed. by E. H. Marth. 2nd. Marcel Dekker, New York, N.Y. ISBN: 0-8247-0235-2.

Rodrigo, G., Bajic, D., Elola, I., and Poyatos, J. F. (2016). "Antagonistic autoregulation speeds up a homogeneous response in *Escherichia coli*". In: *Sci Rep* 6:36196. DOI: 10.1038/srep36196.

Romanova, N. A., Wolffs, P. F., Brovko, L. Y., and Griffiths, M. W. (2006). "Role of efflux pumps in adaptation and resistance of *Listeria monocytogenes* to benzalkonium chloride". In: *Appl Environ Microbiol* 72, pp. 3498–503. DOI: 10.1128/AEM.72.5.3498-3503.2006.

Romeroa, V. M. and Morikawa, K. (2016). "*Listeria monocytogenes* σ^H Contributes to Expression of Competence Genes and Intracellular Growth". In: *J Bacteriol* 198 (8), pp. 1207–1217. DOI: 10.1128/JB.00718-15.

Schrögel, O. and Allmansberger, R. (1997). "Optimisation of the BgaB reporter system: determination of transcriptional regulation of stress responsive genes in *Bacillus subtilis*". In: *FEMS Microbiol Lett* 153 (1), pp. 237–243. DOI: 10.1111/j.1574-6968.1997.tb10488.x.

Schuchat, A., Deaver, K. A., Wenger, J. D., Plikaytis, B. D., Mascola, L., Pinner, R. W., Reingold, A. L., Broome, C. V., Swaminathan, B., Hayes, P. S., Graves, L., Pierce, R., Przybyszewski, V., Ransom, R., Reeves, M., Weaver, R., Anderson, G., Stone, E., Krauss, K., Castillon, M., Harvey, C., Stull, T., Stephens, D., Farley, M., Archer, P., Strack, J., Istre, G., Rados, M., Taylor, J., and Lefkowitz, L. (1992). "Role of foods in sporadic listeriosis. I. Case-control study of dietary risk factors. The Listeria Study Group." In: *JAMA* 267 (15), pp. 2041–5. DOI: 10.1001/jama.1992.03480150047035.

Shen, Y., Naujokas, M., Park, M., and Ireton, K. (2000). "InlB-Dependent Internalization of *Listeria* Is Mediated by the Met Receptor Tyrosine Kinase". In: *Cell* 103 (3), pp. 501–510. DOI: 10.1016/S0092-8674(00)00141-0.

Silk, B. J., Mahon, B. E., Griffin, P. M., Gould, L. H., Tauxe, R. V., Crim, S. M., Jackson, K. A., Gerner-Smidt, P., Herman, K. M., and Henao, O. L. (2013). "Vital Signs: Listeria Illnesses, Deaths, and Outbreaks — United States, 2009–2011". In: *MMWR Morb Mortal Wkly Rep* 62 (22), pp. 448–452. DOI: 10.1016/j.annemergmed.2013.08.006.

Silva, R. S. D., Kovacikova, G., Lin, W., Taylor, R. K., Skorupski, K., and Kull, F. J. (2005). "Crystal Structure of the Virulence Gene Activator AphA from *Vibrio cholerae* Reveals It Is a Novel Member of the Winged Helix Transcription Factor Superfamily". In: *J Biol Chem* 280 (14), pp. 13779–13783. DOI: 10.1074/jbc.M413781200.

Slutsker, L. and Schuchat, A. (1999). *Listeria, listeriosis, and food safety*. *Listeriosis in Humans*. Ed. by E. T. Ryser. Ed. by E. H. Marth. 2nd. Marcel Dekker, New York, N.Y. ISBN: 0-8247-0235-2.

Smith, G. A., Marquis, H., Jones, S., Johnston, N. C., Portnoy, D. A., and Goldfine, H. (1995). "The two distinct phospholipases C of L*isteria monocytogenes* have overlapping roles in escape from a vacuole and cell-to-cell spread". In: *Infect Immun* 63 (11), pp. 4231–4237.

Solovyev, V. and Salamov, A. (2011). *Metagenomics and its Applications in Agriculture, Biomedicine and Environmental Studies*. *Automatic Annotation of Microbial Genomes and Metagenomic Sequences*. Ed. by R. Li. Nova Science Publishers.

Southwick, F. S. (2006). *Phagocytosis of bacteria and bacterial pathogenicity. Listeria invasion and spread in non-professional phagocytes*. Ed. by J. D. Ernst. Ed. by O. Stendahl.

Stephan, R., Althaus, D., Kiefer, S., Lehner, A., Hatz, C., Schmutz, C., Jost, M., Gerber, N., Baumgartner, A., Hächler, H., and Mäusezahl-Feuz, M. (2015). "Foodborne transmission of *Listeria monocytogenes* via ready-to-eat salad: A nationwide outbreak in Switzerland, 2013–2014". In: *Lancet Infect Dis* 57, pp. 14–17. DOI: 10.1016/j.foodcont.2015.03.034.

Stewart, P. S. (2002). "Mechanisms of antibiotic resistance in bacterial biofilms". In: *Int J Med Microbiol* 292 (2), pp. 107–113. DOI: 10.1078/1438-4221-00196.

Studer, P., Borisova, M., Schneider, A., Ayala, J. A., Mayer, C., Schuppler, M., Loessner, M. J., and Briers, Y. (2016). "The Absence of a Mature Cell Wall Sacculus in Stable *Listeria monocytogenes* L-Form Cells Is Independent of Peptidoglycan Synthesis". In: *PLoS One* 11 (5), eCollection. DOI: 10.1371/journal.pone.0154925.

Sugiyama, M., Mochizuki, H., and Osamu Nimi, R. N. (1981). "Mechanism of protection of protein synthesis against streptomycin inhibition in a producing strain". In: *J Antibiot (Tokyo)* 34 (9), pp. 1183–1188. DOI: 10.7164/antibiotics.34.1183.

Swaminathan, B. and Gerner-Smidt, P. (2007). "The epidemiology of human listeriosis". In: *Microbes Infect* 9 (10), pp. 1236–1243. DOI: 10.1016/j.micinf.2007.05.011.

Takai, N., Ikeuchi, S., Manabe, K., and Kutsuna, S. (2006). "Expression of the circadian clock-related gene pex in cyanobacteria increases in darkness and is required to delay the clock". In: *J Biol Rhythms* 21 (4), pp. 235–244. DOI: 10.1177/0748730406289400.

Takeuchi, K., Imai, M., and Shimada, I. (2017). "Dynamic equilibrium on DNA defines transcriptional regulation of a multidrug binding transcriptional repressor, LmrR". In: *Sci Rep* 7(1):267. DOI: 10.1038/s41598-017-00257-x.

Tamburro, M., Ripabelli, G., Vitullo, M., Dallman, T. J., Pontello, M., Amar, C. F. L., and Sammarco, M. L. (2015). "Gene expression in *Listeria monocytogenes* exposed to sublethal concentration of benzalkonium chloride." In: *Comp Immunol Microbiol Infect Dis* 40, pp. 31–9. DOI: 10.1016/j.cimid.2015.03.004.

Terajima, J., Iyoda, S., Ohnishi, M., and Watanabe, H. (2014). "Shiga Toxin (Verotoxin)-Producing *Escherichia coli* in Japan". In: *Microbiol Spectr* 2 (5). DOI: 10.1128/microbiolspec.EHEC-0011-2013.

Tetz, G. and Tetz, V. (2017). "Introducing the sporobiota and sporobiome". In: *Gut Pathog* 9: 38. DOI: 10.1186/s13099-017-0187-8.

Thomason, M. K. and Storz, G. (2010). "Bacterial antisense RNAs: How many are there and what are they doing?" In: *Annu Rev Genet* 44: 167-188. DOI: 10.1146/annurev-genet-102209-163523.

Tiensuu, T., Andersson, C., Rydén, P., and Johansson, J. (2013). "Cycles of light and dark co-ordinate reversible colony differentiation in *Listeria monocytogenes*". In: *Mol Microbiol* 87 (4), pp. 909–924. DOI: 10.1111/mmi.12140.

Toledo-Arana, A., Dussurget, O., Nikitas, G., Sesto, N., Guet-Revillet, H., Balestrino, D., Loh, E., Gripenland, J., Tiensuu, T., Vaitkevicius, K., Barthelemy, M., Vergassola, M., Nahori, M.-A., Soubigou, G., Régnault, B., Coppée, J.-Y., Lecuit, M., Johansson, J.,

and Cossart, P. (2009). "The *Listeria* transcriptional landscape from saprophytism to virulence". In: *Nature* 459 (7249), pp. 950–6. DOI: 10.1038/nature08080.

Tran, N. P., Gury, J., Dartois, V., Nguyen, T. K. C., Seraut, H., Barthelmebs, L., Gervais, P., and Cavin, J.-F. (2008). "Phenolic Acid-Mediated Regulation of the padC Gene, Encoding the Phenolic Acid Decarboxylase of *Bacillus subtilis*". In: *J Bacteriol* 190 (9), pp. 3213–24. DOI: 10.1128/JB.01936-07.

Trimble, M. J., Mlynárčik, P., Kolář, M., and Hancock, R. E. (2016). "Polymyxin: Alternative Mechanisms of Action and Resistance". In: *Cold Spring Harb Perspect Med* 6(10):a025288. DOI: 10.1101/cshperspect.a025288.

Trivedi, P., Delgado-Baquerizo, M., Anderson, I. C., and Singh, B. K. (2016). "Response of Soil Properties and Microbial Communities to Agriculture: Implications for Primary Productivity and Soil Health Indicators". In: *Front Plant Sci* 7: 990. DOI: 10.3389/fpls.2016.00990.

Valk, H. de, Jacquet, C., Goulet, V., Vaillant, V., Perra, A., Simon, F., Desenclos, J., and Martin, P. (2005). "Surveillance of listeria infections in Europe". In: *Euro Surveill* 10 (10), pp. 251–255. DOI: 10.2807/esm.10.10.00572-en.

vanHeijenoort, Y., Leduc, M., Singer, H., and vanHeijenoort, J. (1987). "Effects of moenomycin on *Escherichia coli*". In: *J Gen Microbiol* 133 (3), pp. 667–674. DOI: 10.1099/00221287-133-3-667.

Vasseur, C., Baverel, L., Hébraud, M., and Labadie, J. (1999). "Effect of osmotic, alkaline, acid or thermal stresses on the growth and inhibition of *Listeria monocytogenes*". In: *J Appl Microbiol* 86 (3), pp. 469–76. DOI: 10.1046/j.1365-2672.1999.00686.x.

Vijayabharathi, R., Bruheim, P., Andreassen, T., Raja, D. S., Devi, P. B., Sathyabama, S., and Priyadarisini, V. B. (2011). "Assessment of resistomycin, as an anticancer compound isolated and characterized from *Streptomyces aurantiacus* AAA5". In: *J Microbiol* 49 (6), pp. 920–926. DOI: 10.1007/s12275-011-1260-5.

Vivant, A.-L., Garmyn, D., and Piveteau, P. (2019). "*Listeria monocytogenes*, a down-to-earth pathogen". In: *Front Cell Infect Microbiol* 3:87. DOI: 10.3389/fcimb.2013.00087.

Völker, U., Engelmann, S., Maul, B., Riethdorf, S., Völker, A., Schmid, R., Mach, H., and Hecker, M. (1994). "Analysis of the induction of general stress proteins of *Bacillus subtilis*." In: *Microbiology* 140 (Pt 4), pp. 741–52. DOI: 10.1099/00221287-140-4-741.

Walker, S., Archer, P., and Banks, J. (1990). "Growth of *Listeria monocytogenes* at refrigeration temperatures". In: *J Appl Bacteriol* 68 (2), pp. 157–62. DOI: 10.1111/j.1365-2672.1990.tb02561.x.

Weisblum, B. (1995). "Erythromycin resistance by ribosome modification". In: *Antimicrob Agents Chemother* 39 (3), pp. 577–585. DOI: 10.1128/aac.39.3.577.

Wood, T. K., Knabel, S. J., and Kwan, B. W. (2013). "Bacterial Persister Cell Formation and Dormancy". In: *Appl Environ Microbiol* 79 (23), pp. 7116–7121. DOI: 10.1128/AEM.02636-13.

Wright, G. D. (2005). "Bacterial resistance to antibiotics: Enzymatic degradation and modification". In: *Adv Drug Deliv Rev* 57 (10), pp. 1451–1470. DOI: 10.1016/j.addr.2005.04.002.

Wu, S. W., Lencastre, H. de, and Tomasz, A. (2001). "Recruitment of the *mecA* Gene Homologue of *Staphylococcus sciuri* into a Resistance Determinant and Expression of the Resistant Phenotype in *Staphylococcus aureus*". In: *J Bacteriol* 183 (8), pp. 2417–2424. DOI: 10.1128/JB.183.8.2417-2424.2001.

Zhang, C., Nietfeldt, J., Zhang, M., and Benson, A. K. (2005). "Functional Consequences of Genome Evolution in *Listeria monocytogenes*: the *lmo0423* and *lmo0422* Genes Encode σ^c and LstR, a Lineage II-Specific Heat Shock System". In: *J Bacteriol* 187 (21), pp. 7243–53. DOI: 10.1128/JB.187.21.7243-7253.2005.

Zhang, C., Zhang, M., Ju, J., Nietfeldt, J., Wise, J., Terry, P. M., Olson, M., Kachman, S. D., Wiedmann, M., Samadpour, M., and Benson, A. K. (2003). "Genome diversification in phylogenetic lineages I and II of *Listeria monocytogenes*: identification of segments unique to lineage II populations". In: *J Bacteriol* 185 (18), pp. 5573–84. DOI: 10.1128/JB.185.18.5573-5584.2003.

Zhao, H., Wang, L., Wan, D., Qi, J., Gong, R., Deng, Z., and Chen, W. (2016). "Characterization of the aurantimycin biosynthetic gene cluster and enhancing its production by manipulating two pathway-specific activators in *Streptomyces aurantiacus* JA 4570". In: *Microb Cell Fact* 15: 160. DOI: 10.1186/s12934-016-0559-7.

Zwiener, I., Frisch, B., and Binder, H. (2014). "Transforming RNA-Seq Data to Improve the Performance of Prognostic Gene Signatures". In: *PLoS One* 9(1): e85150. DOI: 10.1371/journal.pone.0085150.